

¹

Doctoral Thesis

²

Microbiota in Human Diseases

³

Jaewoong Lee

⁴

Department of Biomedical Engineering

⁵

Ulsan National Institute of Science and Technology

⁶

2025

⁷

Microbiota in Human Diseases

⁸

Jaewoong Lee

⁹

Department of Biomedical Engineering

¹⁰

Ulsan National Institute of Science and Technology

Microbiota in Human Diseases

A thesis/dissertation submitted to
Ulsan National Institute of Science and Technology
in partial fulfillment of the
requirements for the degree of
Doctor of Philosophy

Jaewoong Lee

04.16.2025 of submission

Approved by

Advisor

Semin Lee

Microbiota in Human Diseases

Jaewoong Lee

This certifies that the thesis/dissertation of Jaewoong Lee is approved.

04.16.2025 of submission

Signature

Advisor: Semin Lee

Signature

Taejoon Kwon

Signature

Eunhee Kim

Signature

Kyemyung Park

Signature

Min Hyuk Lim

13

Abstract

14 (Microbiome)

15 (PTB) Section 2 introduces...

16 (Periodontitis) Section 3 describes...

17 (Colon) Setion 4...

18 (Conclusion)

19

20 **This doctoral dissertation is an addition based on the following papers that the author has already
21 published:**

- 22 • Hong, Y. M., **Lee, Jaewoong**, Cho, D. H., Jeon, J. H., Kang, J., Kim, M. G., ... & Kim, J. K. (2023).
23 Predicting preterm birth using machine learning techniques in oral microbiome. *Scientific Reports*,
24 13(1), 21105.

Contents

26	1	Introduction	1
27	2	Predicting preterm birth using random forest classifier in salivary microbiome	8
28	2.1	Introduction	8
29	2.2	Materials and methods	10
30	2.2.1	Study design and study participants	10
31	2.2.2	Clinical data collection and grouping	10
32	2.2.3	Salivary microbiome sample collection	10
33	2.2.4	16s rRNA gene sequencing	10
34	2.2.5	Bioinformatics analysis	11
35	2.2.6	Data and code availability	11
36	2.3	Results	12
37	2.3.1	Overview of clinical information	12
38	2.3.2	Comparison of salivary microbiomes composition	12
39	2.3.3	Random forest classification to predict PTB risk	12
40	2.4	Discussion	20
41	3	Random forest prediction model for periodontitis statuses based on the salivary microbiomes	22
42	3.1	Introduction	22
43	3.2	Materials and methods	24
44	3.2.1	Study participants enrollment	24
45	3.2.2	Periodontal clinical parameter diagnosis	24
46	3.2.3	Saliva sampling and DNA extraction procedure	26
47	3.2.4	Bioinformatics analysis	26
48	3.2.5	Data and code availability	27
49	3.3	Results	29

50	3.3.1	Summary of clinical information and sequencing data	29
51	3.3.2	Diversity indices reveal differences among the periodontitis severities .	29
52	3.3.3	DAT among multiple periodontitis severities and their correlation . .	29
53	3.3.4	Classification of periodontitis severities by random forest models . .	30
54	3.4	Discussion	51
55	4	Metagenomic signature analysis of Korean colorectal cancer	55
56	4.1	Introduction	55
57	4.2	Materials and methods	57
58	4.2.1	Study participants enrollment	57
59	4.2.2	DNA extraction procedure	57
60	4.2.3	Bioinformatics analysis	57
61	4.2.4	Data and code availability	59
62	4.3	Results	60
63	4.3.1	Summary of clinical characteristics	60
64	4.3.2	Gut microbiome compositions	60
65	4.3.3	Diversity indices	61
66	4.3.4	DAT selection	62
67	4.3.5	Random forest prediction	64
68	4.4	Discussion	82
69	5	Conclusion	83
70	References		84
71	Acknowledgments		100

72

List of Figures

73	1	DAT volcano plot for PTB prediction	14
74	2	Salivary microbiome compositions over DAT for PTB prediction	15
75	3	Random forest-based PTB prediction model	16
76	4	Diversity indices	17
77	5	PROM-related DAT between FTB and PTB	18
78	6	Validation of random forest-based PTB prediction model	19
79	7	Diversity indices for periodontitis	37
80	8	DAT for periodontitis	38
81	9	Correlation heatmap between periodontitis DAT	39
82	10	Random forest classification metrics for periodontitis prediction	40
83	11	Random forest classification metrics from external datasets	41
84	12	Rarefaction curves for alpha-diversity indices	42
85	13	Salivary microbiome compositions in the different periodontal statuses	43
86	14	Correlation plots for periodontitis DAT	44
87	15	Clinical measurements by the periodontitis statuses	45
88	16	Number of read counts by the periodontitis statuses	46
89	17	Proportions of periodontitis DAT	47

90	18	Random forest classification metrics with the full microbiome compositions and ANCOM-selected DAT compositions	48
91			
92	19	Alpha-diversity indices account for evenness	49
93			
94	20	Gradient Boosting classification metrics for periodontitis prediction	50
95			
96	21	Gut microbiome compositions in genus level	72
97			
98	22	Alpha-diversity indices in genus level	73
99			
100	23	Alpha-diversity indices with recurrence in genus level	74
101			
102	24	Alpha-diversity indices with OS in genus level	75
103			
104	25	Beta-diversity indices in genus level	76
105			
106	26	Beta-diversity indices with recurrence in genus level	77
107			
108	27	Beta-diversity indices with recurrence in genus level	78
109			
110	28	DAT with recurrence in species level	79
111			
112	29	DAT with OS in species level	80
113			
114	30	Random forest classification and regression	81
115			

List of Tables

105	1	Confusion matrix	6
106	2	Standard clinical information of PTB study participants	13
107	3	Clinical characteristics of the study participants	32
108	4	Feature combinations and their evaluations	33
109	5	List of DAT among the periodontally healthy and periodontitis stages	34
110	6	Feature the importance of taxa in the classification of different periodontal statuses.	35
111	7	Beta-diversity pairwise comparisons on the periodontitis statuses	36
112	8	Clinical characteristics of CRC study participants	66
113	9	DAT list for CRC recurrence	67
114	10	DAT list for CRC OS	68
115	11	Random forest classification and their evaluations	70
116	12	Random forest regression and their evaluations	71

List of Abbreviations

- 118 **ACC** Accuracy
- 119 **ACE** Abundance-based coverage estimator
- 120 **ASV** Amplicon sequence variant
- 121 **AUC** Area-under-curve
- 122 **BA** Balanced accuracy
- 123 **BMI** Body mass index
- 124 **C-section** Cesarean section
- 125 **DAT** Differentially abundant taxa
- 126 **F1** F1 score
- 127 **Faith PD** Faith's phylogenetic diversity
- 128 **FC** Fold change
- 129 **FN** False negative
- 130 **FP** False positive
- 131 **FTB** Full-term birth
- 132 **GA** Gestational age
- 133 **MAE** Mean absolute error
- 134 **MSI** Microsatellite instability
- 135 **MSI-H** MSI-High
- 136 **MSI-L** MSI-Low
- 137 **MSS** Microsatellite stable
- 138 **MWU test** Mann-Whitney U-test
- 139 **OS** Overall survival
- 140 **PRE** Precision
- 141 **PROM** Prelabor rupture of membrane
- 142 **PTB** Preterm birth

- ¹⁴³ **qPCR** quantitative-PCR
- ¹⁴⁴ **RMSE** Root mean squared error
- ¹⁴⁵ **ROC curve** Receiver-operating characteristics curve
- ¹⁴⁶ **rRNA** Ribosomal RNA
- ¹⁴⁷ **SD** Standard deviation
- ¹⁴⁸ **SEN** Sensitivity
- ¹⁴⁹ **SPE** Specificity
- ¹⁵⁰ **t-SNE** t-distributed stochastic neighbor embedding
- ¹⁵¹ **TN** True negative
- ¹⁵² **TP** True positive

153 **1 Introduction**

154 The microbiome refers to the complex community of microorganisms, including bacteria, viruses, fungi,
155 and other microbes, that inhabit various environment within living organisms (Ursell, Metcalf, Parfrey,
156 & Knight, 2012; Gilbert et al., 2018). In humans, the microbiome plays a crucial role in maintaining
157 health (Lloyd-Price, Abu-Ali, & Huttenhower, 2016), influencing processes such as digestion (Lim, Park,
158 Tong, & Yu, 2020), immune response (Thaiss, Zmora, Levy, & Elinav, 2016; Kogut, Lee, & Santin, 2020;
159 C. H. Kim, 2018), and even mental health (Mayer, Tillisch, Gupta, et al., 2015; X. Zhu et al., 2017;
160 X. Chen, D'Souza, & Hong, 2013). These microbial communities are not static nor constant, but rather
161 dynamic ecosystem that interacts with their host and respond to environmental changes. Recent studies
162 have revealed that imbalances in the microbiome, known as dysbiosis, can contribute to a wide range of
163 diseases, including obesity (John & Mullin, 2016; Tilg, Kaser, et al., 2011; Castaner et al., 2018), diabetes
164 (Barlow, Yu, & Mathur, 2015; Hartstra, Bouter, Bäckhed, & Nieuwdorp, 2015; Sharma & Tripathi, 2019),
165 infections (Whiteside, Razvi, Dave, Reid, & Burton, 2015; Alverdy, Hyoju, Weigerinck, & Gilbert, 2017),
166 inflammatory conditions (Francescone, Hou, & Grivennikov, 2014; Peirce & Alviña, 2019; Honda &
167 Littman, 2012), and cancers (Helmink, Khan, Hermann, Gopalakrishnan, & Wargo, 2019; Cullin, Antunes,
168 Straussman, Stein-Thoeringer, & Elinav, 2021; Sepich-Poore et al., 2021; Schwabe & Jobin, 2013). Thus,
169 understanding the composition of the human microbiomes is essential for developing new therapeutic
170 approaches that target these microbial populations to promote health and prevent diseases.

171 The microbiome participates a crucial role in overall health, influencing not only digestion and immune
172 function but also systemic and neurological processes through the brain-gut axis (Martin, Osadchiy,
173 Kalani, & Mayer, 2018; Aziz & Thompson, 1998; R. Li et al., 2024). The gut microbiota interact with
174 the host through metabolic byproducts, immune signaling, and the production of neurotransmitters, *e.g.*
175 serotonin and dopamine, which are essential for brain function and cognition. Disruptions in microbial
176 composition, known as dysbiosis, have been linked to various diseases, including inflammatory bowel
177 disease (Sultan et al., 2021; Baldelli, Scaldaferrri, Putignani, & Del Chierico, 2021), obesity (Kang et al.,
178 2022; Hamjane, Mechita, Nourouti, & Barakat, 2024; Pezzino et al., 2023), diabetes (Cai et al., 2024;
179 X. Li et al., 2021; Y. Li et al., 2023), and cardiovascular diseases (Manolis, Manolis, Melita, & Manolis,
180 2022; Tian et al., 2021). Furthermore, the brain-gut axis, a bidirectional communication system between
181 the gut microbiome composition and the central nervous system, has been implicated in mental disorders,
182 *e.g.* anxiety disorder, depressive disorder, and neurodegenerative diseases. Emerging evidence suggested
183 that alterations in the host microbiome can influence mood, cognitive function, and even behavior through
184 immune modulation, vagus nerve signaling, and microbial metabolites. These findings highlight the
185 microbiome as a critical factor in maintaining host health and suggest that targeted interventions, namely
186 probiotics, antibiotics, dietary modification, and microbiome-based therapies, may hold promise for
187 improving both physical and mental comfort. Hence, understanding the microbial effects could lead to
188 novel therapeutic strategies for a wide range of health conditions.

189 16S ribosomal RNA (rRNA) gene sequencing is one of the most extensively applied methods for
190 characterizing microbial communities by targeting the conserved 16S rRNA gene, which contains both

191 highly conserved and variable regions in bacteria (Tringe & Hugenholtz, 2008; Janda & Abbott, 2007).
192 The conserved regions enable universal primer binding, while the variable regions provide the specificity
193 needed to differentiate microbial taxa. Among these regions, the V3-V4 region is frequently selected for
194 sequencing due to its balance between phylogenetic resolution and sequencing efficiency (Johnson et al.,
195 2019; López-Aladid et al., 2023). Therefore, the V3-V4 region offers sufficient variability to classify a
196 wide range of bacteria taxa while maintaining compatibility with widely used sequencing platforms.

197 The Anna Karenina principle, originally derived from literature of Leo Tolstoy, has been applied
198 to microbiome research to describe the manner that microbial communities in patients with diseases
199 tend to be more variable and unstable compared to those in healthy individuals (Ma, 2020; W. Li &
200 Yang, 2025). This Anna Karenina principle suggests that while healthy microbiomes exhibit relatively
201 stable and uniform compositions, while disease-associated microbiomes become highly dysregulated due
202 to various environmental, genetic, and pathological influences. Dysbiosis-driven mechanisms, such as
203 inflammation, genotoxic metabolic production, and immune modulation, can contribute pathogenesis
204 and progression of diseases, including periodontitis. In the context of cancer, this Anna Karenina
205 principle suggests that gut microbiome dysbiosis does not follow a single uniform pattern in patients
206 with CRC but rather presents as diverse and individualized disruption in microbial composition. This
207 instability may play a role in field cancerization, where microbial alteration extend beyond the tumor
208 site to adjacent normal-appearing tissues (Curtius, Wright, & Graham, 2018; Rubio, Lang-Schwarz,
209 & Vieth, 2022), potentially priming the tumor microenvironment for malignancy. Therefore, the high
210 inter-individual variability in microbiome alteration across these disease supports the Anna Karenina
211 principle, highlighting the complexity of dysbiosis-driven diseases and the necessity for personalized
212 microbiome-based diagnostic and interventions. Investigating the shared and disease-specific microbial
213 disruptions across these conditions may offer novel insights into microbiome-driven pathogenesis and
214 therapeutic strategies.

215 On the other hand, PathSeq is a computational pipeline designed for the identification and analysis
216 of microbial sequences within short-read human sequencing data, such as next-generation sequencing
217 (Kostic et al., 2011; Walker et al., 2018). PathSeq's scalable and effective processing of massive amounts
218 of sequencing data allows large-scale microbial profiling possible. PathSeq workflow consists of two
219 main phases: a subtractive phase and an analytic phase. The subtractive phase is removing human-derived
220 reads by aligning them to a human reference genome; and, the analytic phase is mapping remaining reads
221 to microbial reference databases, not only bacterial reference genome, but also archaeal, fungal, and viral
222 reference genomes. This approach allows for the comprehensive detection of microbiome compositions,
223 without a requirement for targeted amplification. PathSeq presents a more comprehensive and objective
224 evaluation of microbiome compositions than conventional microbiome profiling techniques including 16S
225 rRNA gene sequencing, capturing an assortment of microbial species beyond bacteria. Therefore, PathSeq
226 is an effective instrument for metagenomic research, infectious disease study, and microbiome analysis in
227 environmental and clinical contexts because of its capacity to operate with complex sequencing datasets
228 (Ojesina et al., 2013; Park et al., 2024; Tejeda et al., 2021).

229 Diversity indices are essential techniques for evaluating the complexity and variety of microbial

communities, in ecological and microbiological research (Tucker et al., 2017; Hill, 1973). Alpha-diversity index attributes to the heterogeneity within a specific community, obtaining the number of different taxa and the distribution of taxa among the individuals, *i.e.*, richness and evenness. On the other hand, beta-diversity index measures the variations in microbiome compositions between the individuals, highlighting differences among the microbiome compositions of the study participants (B.-R. Kim et al., 2017). Altogether, by providing a thorough understanding of microbiome compositions, diversity indices, *e.g.* alpha-diversity and beta-diversity, allow us to investigate factors that affect community variability and structure.

Differentially abundant taxa (DAT) detection is a key analytical approach in microbiome study to identify microbial taxa that significantly differ in abundance between distinct study participant groups. This DAT detection method is particularly valuable for understanding how microbial communities vary across different conditions, such as disease states, environmental factors, and/or experimental treatments. Various statistical and computational techniques, *e.g.* LEfSe (Segata et al., 2011), DESeq2 (Love, Huber, & Anders, 2014), ANCOM (Lin & Peddada, 2020), and ANCOM-BC (Lin, Eggesbø, & Peddada, 2022; Lin & Peddada, 2024), are commonly used to assess differential abundance while accounting for compositional and sparsity-related challenges in microbiome composition data (Swift, Cresswell, Johnson, Stilianoudakis, & Wei, 2023; Cappellato, Baruzzo, & Di Camillo, 2022). Thus, identifying DAT can provide insights into microbial biomarkers associated with specific health conditions or disease statuses, enabling potential applications in diagnostics and therapeutics. However, due to the nature of microbiome composition data and the influence of sequencing depth, appropriate normalization and statistically adjustments are necessary to ensure reliable and stable detection of differentially abundant microbes (Xia, 2023; Pan, 2021). Integrating DAT detection analysis with functional profiling further enhances our understanding of the biological significance of microbial shifts or dysbiosis. As microbiome research advances, improving methodologies for DAT selection remains essential for uncovering meaningful microbial association and their potential roles in human diseases.

Classification is one of the supervised machine learning techniques used to categorized data into predefined classes based on features within the data (Kotsiantis, Zaharakis, & Pintelas, 2006; Sen, Hajra, & Ghosh, 2020). In other words, the method learns the relationship between input features and their corresponding output classes through the process of training a classification model using labeled data. Classification models are essential for advising choices in a wide range of applications, including medical diagnostics (Omondiagbe, Veeramani, & Sidhu, 2019). Thus, researchers could uncover sophisticated connections in input features and corresponding classes and produce reliable prediction by utilizing machine learning classification.

Random forest classification is one of the ensemble machine learning methods that constructs several decision trees during training and aggregates their results to provide classification predictions (Breiman, 2001; Geurts, Ernst, & Wehenkel, 2006). A portion of the features and classes—known as bootstrapping (Jiang & Simon, 2007; Champagne, McNairn, Daneshfar, & Shang, 2014; J.-H. Kim, 2009) and feature bagging (Bryll, Gutierrez-Osuna, & Quek, 2003; Alelyani, 2021; Yaman & Subasi, 2019)—are utilized to construct each tree in the forest. The majority vote from each tree determines the final classification,

which lowers the possibility of overfitting in comparison to a single decision tree. Furthermore, random forest classifier offers several advantages, including its robustness to outliers and its ability to calculate the feature importance.

Furthermore, k -fold cross-validation is a widely applied resampling technique that enhances the reliability and robustness of machine learning models by iteratively evaluating their performance across multiple data partitions (Wong & Yeh, 2019; Ghojogh & Crowley, 2019). Instead of relying on a single train-test split, k -fold cross-validation divides the dataset into equally sized k folds, where the machine learning model is trained on $k - 1$ folds and tested on the remaining fold in an iterative manner. This process is repeated k times, with each fold serving as the test set once, and the final performance is averaged across all iterations to provide a more generalizable estimate of model metrics. By reducing the risk of overfitting and minimizing variance in performance evaluation, k -fold cross-validation ensures that the machine learning model is not overly dependent on a specific train-test split. By applying k -fold cross-validation, researchers can ensure that their machine learning models are both robust and reliable, leading to more accurate and reproducible results (Fushiki, 2011).

Evaluating the performance of a machine learning classification model is essential to ensure its reliability and effectiveness in real-world solutions and applications (Novaković, Veljović, Ilić, Papić, & Tomović, 2017; Hossin & Sulaiman, 2015; Hand, 2012). A confusion matrix is a tabular representation of predictions of classification, showing the counts of true positives (TP), true negatives (TN), false positives (FP), and false negatives (FN) (Table 1). From this matrix, evaluations can be derived: accuracy (ACC; Equation 1), balanced accuracy (BA; Equation 2), F1 score (F1; Equation 3), sensitivity (SEN; Equation 4), specificity (SPE; Equation 5), and precision (PRE; Equation 6). These metrics are in $[0, 1]$ range and high metrics are good metrics. The confusion matrix also helps in identifying specific types of errors, such as a tendency to produce false positive or false negatives, offering valuable insights for improving the classification model. By combining the confusion matrix with other evaluation metrics, researchers can comprehensively assess the classification metrics and refine it for real-world solutions and applications.

The receiver-operating characteristics (ROC) curve is a graphical representation used to evaluate the performance of a classification model by plotting the sensitivity against (1-specificity) at multiple threshold setting (Gonçalves, Subtil, Oliveira, & de Zea Bermudez, 2014; Obuchowski & Bullen, 2018; Centor, 1991). The ROC curve illustrates the trade-off between detecting true positives while minimizing false positives, suggesting determining the optimal decision threshold for classification. A key metric derived from the ROC curve is the area-under-curve (AUC), which quantifies overall ability of the classification model to discriminate between positive and negative predictions. An AUC value of 0.5 indicates a model performing no better than random chance, while value closer to 1.0 suggests high predictive accuracy. Thus, by analyzing the AUC value of the ROC curve, researchers can compare different models and select the better classification model that offers the best balance between sensitivity and specificity for a given application.

Regression is a powerful predictive machine learning approach used to analyze complex relationships between variables and make continuous value predictions (Maulud & Abdulazeez, 2020; Yildiz, Bilbao, & Sproul, 2017). Beside classification, which assigns discrete labels, regression models estimate numerical

308 outcomes based on input features, making them particularly useful in biological research and clinical
309 applications for predicting disease risk, patient outcomes, and biomarker selection. By leveraging high-
310 throughput biological techniques and clinical information, regression model enables the discovery of
311 hidden patterns and the development of precision medicine strategies. As computational methods advance,
312 integrating regression models with metagenomic data can improve predictive accuracy and facilitate
313 data-driven therapeutic guide in healthcare.

314 Evaluating the performance of machine learning regression models requires assessing their prediction
315 errors using appropriate metrics. Mean absolute error (MAE; Equation 7) and root mean squared error
316 (RMSE; Equation 8) are commonly used measures for quantifying the accuracy of regression models. By
317 optimizing regression models based on MAE and RMSE, researchers can improve prediction accuracy
318 and enhance the reliability of machine learning regression models.

319 This dissertation present a comprehensive, multi-disease human microbiome analysis, bridging the
320 association between preterm birth (PTB) (Section 2), periodontitis (Section 3), and colorectal cancer
321 (CRC) (Section 4) through a unified metagenomic approach. While previous studies have examined the
322 role and characteristics of human microbiome in these diseases individually, this dissertation uniquely
323 integrates human microbiome-driven insights across these diseases to identify shared and disease-specific
324 microbial signatures. By applying high-throughput metagenomic sequencing, microbial diversity analysis,
325 and advanced bioinformatics techniques, this dissertation aims to uncover novel microbiome-based
326 biomarkers and mechanistic insights into how microbial communities influence these conditions. These
327 findings contribute to a broader understanding of microbiome-mediated disease interactions and pave the
328 way for personalized medicine strategies, including microbiome-targeted diagnostics and therapeutics.

Table 1: Confusion matrix

		Predicted	
		Positive	Negative
Actual	Positive	True positive (TP)	False negative (FN)
	Negative	False positive (FP)	True negative (TN)

329

$$ACC = \frac{TP + TN}{TP + FN + FP + TN} \quad (1)$$

330

$$BA = \frac{1}{2} \times \left(\frac{TP}{TP + FP} + \frac{TN}{TN + FN} \right) \quad (2)$$

331

$$F1 = \frac{2 \times TP}{2 \times TP + FP + FN} \quad (3)$$

332

$$SEN = \frac{TP}{TP + FP} \quad (4)$$

333

$$SPE = \frac{TN}{TN + FN} \quad (5)$$

334

$$PRE = \frac{TP}{TP + FP} \quad (6)$$

335

$$MAE = \sum_{i=1}^n |Prediction_i - Real_i| / n \quad (7)$$

$$RMSE = \sqrt{\sum_{i=1}^n (Prediction_i - Real_i)^2 / n} \quad (8)$$

336 **2 Predicting preterm birth using random forest classifier in salivary mi-**
337 **crobiome**

338 **This section includes the published contents:**

339 Hong, Y. M., **Lee, Jaewoong**, Cho, D. H., Jeon, J. H., Kang, J., Kim, M. G., ... & Kim, J. K. (2023).
340 Predicting preterm birth using machine learning techniques in oral microbiome. *Scientific Reports*, 13(1),
341 21105.

342 **2.1 Introduction**

343 Preterm birth (PTB), characterized by the delivery of neonates prior to 37 weeks of gestation, is one
344 of the major cause to neonatal mortality and morbidity (Blencowe et al., 2012). Multiple pregnancies
345 including twins, short cervical length, and infection on genitourinary tract are known risk factor for
346 PTB (Goldenberg, Culhane, Iams, & Romero, 2008). Nevertheless, the extent to which these aspects
347 affect birth outcomes is still up for debate. Henceforth, strategies to boost gestation and enhance delivery
348 outcomes can be more conveniently implemented when pregnant women at high risk of PTB are identified
349 early (Iams & Berghella, 2010).

350 Prediction models that can be utilized as a foundation for intervention methods still have an unac-
351 ceptable amount of classification evaluations, including accuracy, sensitivity, and specificity, despite a
352 great awareness of the risk factors that trigger PTB (Sotiriadis, Papatheodorou, Kavvadias, & Makrydi-
353 mas, 2010). Several attempts have been made to predict PTB through integrating data such as human
354 microbiome composition, inflammatory markers, and prior clinical data with predictive machine learn-
355 ing methods (Berghella, 2012). Because it is affordable and straightforward to use, fetal fibronectin is
356 commonly used in medical applications. However, with a sensitivity of only 56% that merely similar to
357 random prediction, it has a low classification evaluation (Honest et al., 2009). Due to the difficulty and
358 imprecision of the method in general, as well as the requirement for a qualified specialist cervical length
359 measuring is also restricted (Leitich & Kaider, 2003).

360 Preterm prelabor rupture of membranes (PROM) brought on by gestational inflammation and infection
361 contribute to about 70% of PTB cases (Romero, Dey, & Fisher, 2014). Nevertheless, as antibiotics and
362 anti-inflammatory therapeutic strategies were ineffective to decrease PTB occurrence rates, the pathology
363 of PTB has not been entirely elucidated by inflammatory and infectious pathways (Romero, Hassan, et al.,
364 2014). Recent researches on maternal microbiomes were beginning to examine unidentified connections
365 of PTB as a consequence of developmental processes in molecular biological technology (Fettweis et al.,
366 2019).

367 However, as anti-inflammatory and antibiotic therapies were insufficient to lower PTB occurrence
368 rates, infectious and inflammatory processes are insufficient to exhaustively clarify the pathogenesis and
369 pathophysiology of PTB. It has been hypothesized that the microbiota linked to PTB originate from either
370 a hematogenous pathway or the female genitourinary tract increasing through the vagina and/or cervix
371 (Han & Wang, 2013). Vaginal microbiome compositions have been found in women who eventually

372 acquire PTB, and recent studies have tried to predict PTB risk using cervico-vaginal fluid (Kindinger et
373 al., 2017). Even though previous investigation have confirmed the potential relationships between the
374 vaginal microbiome compositions and PTB, these studies are only able to clarify an upward trajectory.

375 Multiple unfavorable birth outcomes, including PROM and PTB, have been linked to periodontitis
376 as an independence risk factor, according to numerous epidemiological researches (Offenbacher et al.,
377 1996). It is expected that the oral microbiome will be able to explain additional hematogenous pathways
378 in light of these precedents; however, the oral microbiome composition of fetuses is limited understood.

379 Hence, in order to identify the salivary microbiome linked to PTB and to establish a machine learning
380 prediction model of PTB determined by oral microbiome compositions, this study examined the salivary
381 microbiome compositions of PTB study participants with a full-term birth (FTB) study participants.

382 **2.2 Materials and methods**

383 **2.2.1 Study design and study participants**

384 Between 2019 and 2021, singleton pregnant women who received treatment to Jeonbuk National University Hospital for childbirth were the participants of this study. This study was conducted according to the
385 Declaration of Helsinki (Goodyear, Krleza-Jeric, & Lemmens, 2007). The Institutional Review Board
386 authorized this study (IRB file No. 2019-01-024). Participants who were admitted for elective cesarean
387 sections (C-sections) or induction births, as well as those who had written informed consent obtained
388 with premature labor or PROM, were eligible.
389

390 **2.2.2 Clinical data collection and grouping**

391 Questionnaires and electronic medical records were implemented to gather information on both previous
392 and current pregnancy outcomes. The following clinical data were analyzed:

- 393 • maternal age at delivery
- 394 • diabetes mellitus
- 395 • hypertension
- 396 • overweight and obesity
- 397 • C-section
- 398 • history PROM or PTB
- 399 • gestational week on delivery
- 400 • birth weight
- 401 • sex

402 **2.2.3 Salivary microbiome sample collection**

403 Salivary microbiome samples were collected 24 hours before to delivery using mouthwash. The standard
404 methods of sterilizing were performed. Medical experts oversaw each stage of the sample collecting
405 procedure. Participants received instruction not to eat, drink, or brush their teeth for 30 minutes before
406 sampling salivary microbiome. Saliva samples were gathered by washing the mouth for 30 seconds with
407 12 mL of a mouthwash solution (E-zен Gargle, JN Pharm, Pyeongtaek, Gyeonggi, Korea). The samples
408 were tagged with the anonymous ID for each participant and kept in low temperature (4 °C) until they
409 underwent further processing. Genomic DNA was extracted using an ExgeneTM Clinic SV kit (GeneAll
410 Biotechnology, Seoul, Korea) following with the manufacturer instructions and store at -20 °C.

411 **2.2.4 16s rRNA gene sequencing**

412 Salivary microbiome samples were transported to the Department of Biomedical Engineering of the
413 Ulsan National Institute of Science and Technology . 16S rRNA sequencing was then carried out using a
414 commissioned Illumina MiSeq Reagent Kit v3 (Illumina, San Diego, CA, USA). Library methods were
415 utilized to amplify the V3-V4 areas. 300 base-pair paired-end reads were produced by sequencing the

416 pooled library using a v3 \times 600 cycle chemistry after the samples had been diluted to a final concentration
417 of 6 pM with a 20% PhiX control.

418 **2.2.5 Bioinformatics analysis**

419 The independent *t*-test was utilized to evaluate the differences of continuous values between from the
420 PTB participants than the FTB participants; χ^2 -square test was applied to decide statistical differences of
421 categorical values. Clinical measurement comparisons were conducted using SPSS (version 20.0) (Spss
422 et al., 2011). At $p < 0.05$, statistical significance was taken into consideration.

423 QIIME2 (version 2022.2) was implemented to import 16S rRNA gene sequences from salivary
424 microbiome samples of study participants for additional bioinformatics processing (Bolyen et al., 2019).
425 DADA2 was used to verify the qualities of raw sequences (Callahan et al., 2016). The remain sequences
426 were clustered into amplicon sequence variants (ASVs). Diversity indices, namely Faith PD for alpha
427 diversity index (Faith, 1992) and Hamming distance for beta diversity index (Hamming, 1950), were
428 calculated. MWU test (Mann & Whitney, 1947), and PERMANOVA multivariate test were evaluated for
429 measuring statistical significance (Anderson, 2014; Kelly et al., 2015).

430 Taxonomic assignment were implemented with HOMD (version 15.22) (T. Chen et al., 2010).
431 Afterward, DESeq2 was implemented to identify differentially abundant taxa (DAT) that could dis-
432 tinguish between salivary microbiome from PTB and FTB participants (Love et al., 2014). Taxa with
433 $|\log_2 \text{FoldChange}| > 1$ and $p < 0.05$ were considered as statistically significant.

434 The taxa for predicting PTB using salivary microbiome data were determined using a random forest
435 classifier (Breiman, 2001). Through stratified *k*-fold cross-validation (*k* = 5) that preserves the existence
436 rate of PTB and FTB participants, consistency and trustworthy classification were ensured (Wong & Yeh,
437 2019).

438 **2.2.6 Data and code availability**

439 All sequences from the 59 study participants have been published to the Sequence Read Archives
440 (project ID PRJNA985119): <https://dataview.ncbi.nlm.nih.gov/object/PRJNA985119>. Docker
441 image that employed throughout this study is available in the DockerHub: https://hub.docker.com/r/fumire/helixco_premature. Every code used in this study can be found on GitHub: https://github.com/CompbioLabUnist/Helixco_Premature.

444 **2.3 Results**

445 **2.3.1 Overview of clinical information**

446 In the beginning, 69 volunteer mothers were recruited for this study. However, due to insufficient clinical
447 information or twin pregnancies, 10 participants were excluded from the study participants. Demographic
448 and clinical information of the study participants are displayed in Table 2. Because PROM is one of the
449 leading factors of PTB, it was prevalent in the PTB group than the FTB group. Other maternal clinical
450 factors did not significantly differ between the FTB and PTB groups. There were no cases in both groups
451 that had a history of simultaneous periodontal disease or cigarette smoking.

452 **2.3.2 Comparison of salivary microbiomes composition**

453 The salivary microbiome composition was composed of 13953804 sequences from 59 study participants,
454 with 102305.95 ± 19095.60 and 64823.41 ± 15841.65 (mean \pm SD) reads/sample before and following
455 the quality-check stage, accordingly. There was not a significant distinction between the PTB and FTB
456 groups with regard to on alpha diversity nor beta diversity metrics (Figure 4).

457 DESeq2 was used to select 32 DAT that distinguish between the PTB and FTB groups out of the 465
458 species that were examined (Love et al., 2014): 26 FTB-enriched DAT and six PTB-enriched DAT. Seven
459 PROM-related DAT were removed from these 32 PTB-related DAT to lessen the confounding effect of
460 PROM (Figure 5). Therefore, there were a total of 25 PTB-related DAT: 22 FTB-enriched DAT and three
461 PTB-enriched DAT (Figure 1).

462 A significant negative correlation was found using Pearson correlation analysis between GW and
463 differences between PTB-enriched DAT and FTB-enriched DAT (Pearson correlation $r = -0.542$ and
464 $p = 7.8e-6$; Figure 5).

465 **2.3.3 Random forest classification to predict PTB risk**

466 To classify PTB according to DAT, random forest classifiers were constructed. The nine most significant
467 DAT were used to obtain the best BA (0.765 ± 0.071 ; Figure 3a). Moreover, random forest classification
468 model determined each DAT's importance (Figure 3b). We conducted a validation procedure on nine
469 twin pregnancies that were excluded in the initial study design in order to confirm the reliability and
470 dependability of our random forest-based PTB prediction model (Figure 6). Comparable to the PTB
471 prediction model on the 59 initial singleton study participants, the validation classification on PTB risk of
472 these twin participants have an accuracy of 87.5%.

Table 2: Standard clinical information of PTB study participants.

Continuous variable for independent *t*-test. Categorical variable for Pearson's χ^2 -square test. Continuous variable: mean \pm SD. Categorical variable: count (proportion)

	PTB (n=30)	FTB (n=29)	p-value
Maternal age (years)	31.8 \pm 5.2	33.7 \pm 4.5	0.687
C-section	20 (66.7%)	24 (82.7%)	0.233
Previous PTB history	4 (13.3%)	1 (3.4%)	0.353
PROM	12 (40.0%)	1 (3.4%)	0.001
Pre-pregnant overweight	8 (26.7%)	7 (24.1%)	1.000
Gestational weight gain (kg)	9.0 \pm 5.9	11.5 \pm 4.6	0.262
Diabetes	2 (6.7%)	2 (6.9%)	1.000
Hypertension	11 (36.7%)	4 (13.8%)	0.072
Gestational age (weeks)	32.5 \pm 3.4	38.3 \pm 1.1	\leq 0.001
Birth weight (g)	1973.4 \pm 686.6	3283.4 \pm 402.7	\leq 0.001
Male	14 (46.7%)	13 (44.8%)	1.000

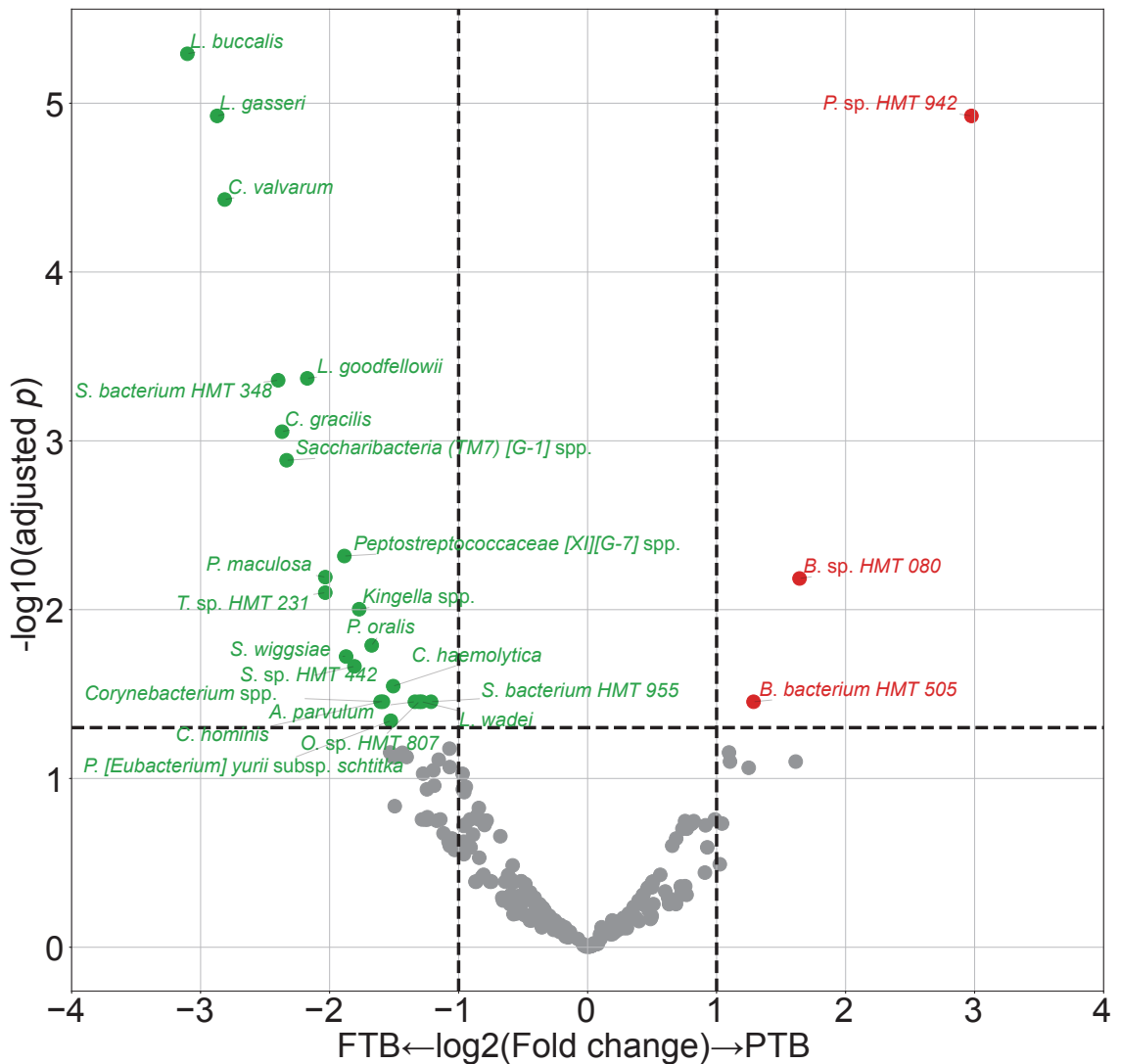


Figure 1: DAT volcano plot for PTB prediction.

Red dots represent PTB-enriched DAT, while green dots represent FTB-enriched DAT.

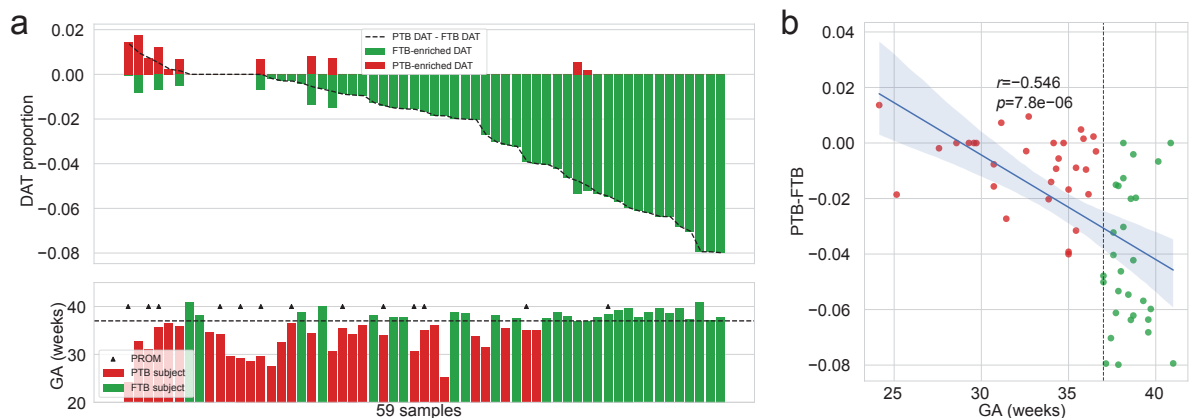


Figure 2: **Salivary microbiome compositions over DAT for PTB prediction.**

(a) Frequencies of DAT of study subjects. The study participants are arranged in respect of (PTB-enriched DAT – FTB-enriched DAT). The study participants' GA is displayed in accordance with the upper panel's order (PTB: red bar, FTB: green bar. PROM: arrow head.) **(b)** Correlation plot with GA and (PTB-enriched DAT – FTB-enriched DAT). Strong negative correlation is found with Pearson correlation.

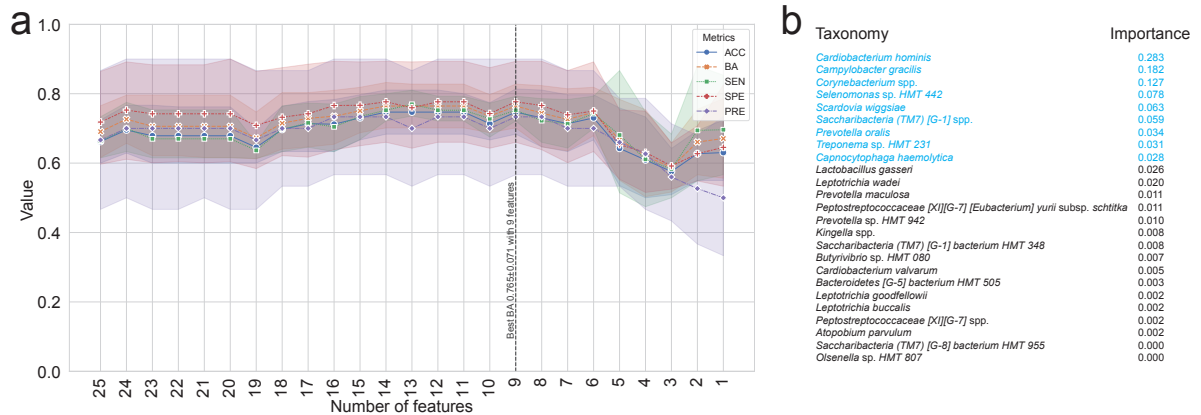


Figure 3: **Random forest-based PTB prediction model.**

(a) Machine learning evaluations upon number of features (DAT). Random Forest classifier has the best BA (0.765 ± 0.071 ; Mean \pm SD) with the nine most important DAT. **(b)** Importance of DAT.

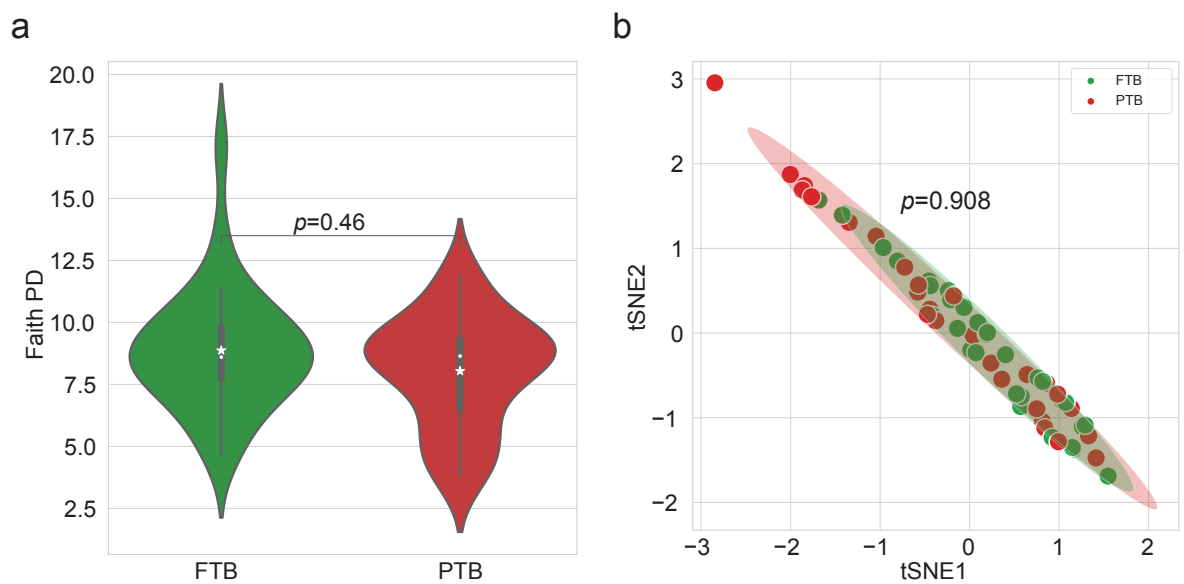


Figure 4: **Diversity indices.**

(a) Alpha diversity index (Faith PD). There is no statistically significant difference between the PTB and FTB group (MWU test $p = 0.46$). **(b)** t-SNE plot with beta diversity index (Hamming distance). There is no statistically significant difference between the PTB and FTB group (PERMANOVA test $p = 0.908$)

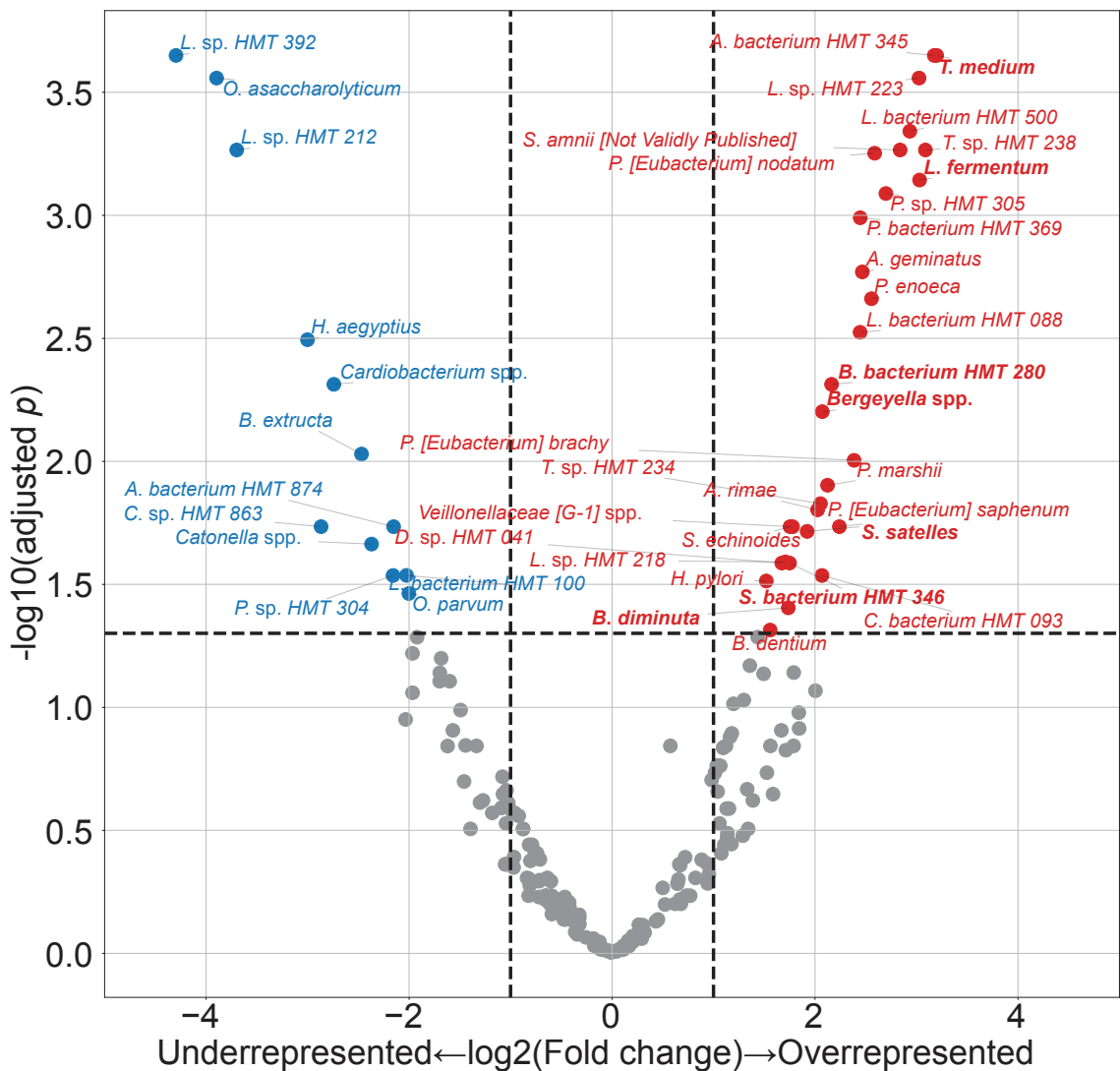


Figure 5: PROM-related DAT between FTB and PTB.

Only seven of these 42 PROM-related DAT overlapped with PTB-related DAT (bold text). Blue dots represented PROM-underrepresented DAT, while red dots represented PROM-overrepresented DAT.

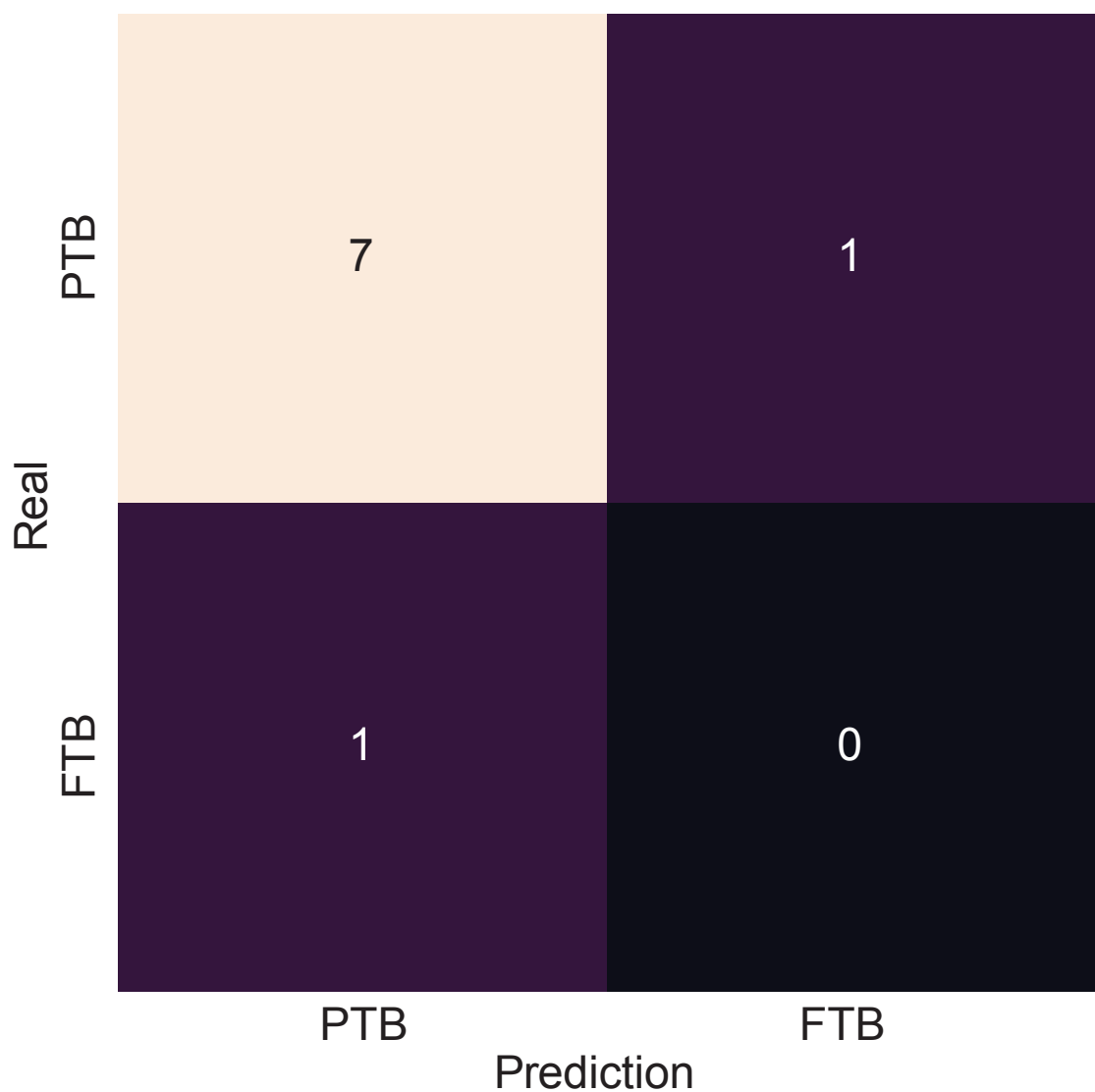


Figure 6: Validation of random forest-based PTB prediction model.

Nine twin pregnancies (eight PTB subjects and a FTB subject) that were excluded in the initial study subjects were subjected to a validation procedure. The random forest-based PTB prediction model shows 87.5% accuracy, comparable to the PTB classification evaluations on the singleton study subjects (0.714 ± 0.061 . Mean \pm SD)

473 **2.4 Discussion**

474 In this study, we employed salivary microbiome compositions to develop the random forest-based PTB
475 prediction models to estimate PTB risks. Previous reports have indicated bidirectional associations
476 between pregnancy outcomes and salivary microbiome compositions (Han & Wang, 2013). Nevertheless,
477 the salivary microbiome composition is not yet elucidated. Salivary microbial dysbiosis, including gingival
478 inflammation and periodontitis, have been connected to unfavorable pregnancy outcomes, such as PTB
479 (Ide & Papapanou, 2013). However, the techniques utilized in recent research that primarily focus on
480 recognized infections have led to inconsistent outcomes.

481 One of the most common salivary taxa that has been examined is *Fusobacterium nucleatum*, that is a
482 Gram-negative, anaerobic, and filamentous bacteria (Han, 2015; Brennan & Garrett, 2019; Bolstad, Jensen,
483 & Bakken, 1996). *Fusobacterium nucleatum* can be separated from not only the salivary microbiome
484 but also the vaginal microbiome (Vander Haar, So, Gyamfi-Bannerman, & Han, 2018; Witkin, 2019). In
485 both animal and human investigation, *Fusobacterium nucleatum* infection has been linked to risk of PTB
486 (Doyle et al., 2014). According to recent researches, the placenta women who give birth prematurely may
487 include additional salivary microbiome dysbiosis, such as *Bergeyella* spp. and *Porphyromonas gingivalis*
488 (León et al., 2007; Katz, Chegini, Shiverick, & Lamont, 2009). Although *Bergeyella* spp. were one of the
489 PROM-overrepresented DAT (Figure 5), it was excluded in the final 25 PTB-related DAT. Furthermore,
490 *Porphyromonas gingivalis* and *Campylobacter gracilis* were pathogens of periodontitis in sub-gingival
491 microbiome (Yang et al., 2022). *Lactobacillus gasseri* was also one of the FTB-enriched DAT (Figure
492 1), and it is well established that early PTB risk can be reduced by *Lactobacillus gasseri* in the vaginal
493 microbiome (Basavaprabhu, Sonu, & Prabha, 2020; Payne et al., 2021).

494 With DAT comprising 22 FTB-enriched DAT and three PTB-enriched DAT (Figure 1), we discovered
495 that the FTB study participants had the majority of the essential DAT that distinguished between the PTB
496 and FTB groups. Thus, we hypothesize that the pathogenesis and pathophysiology of PTB may have been
497 triggered by an absence of species with protective characteristics. The association between unfavorable
498 pregnancy outcomes and a dysfunctional microbiome has been explained through two distinct processes.
499 According to the first hypothesis, periodontal pathogens originating in the gingival biofilm might spread
500 from the infected salivary microbiome over the placenta microbiome, invade the intra-amniotic fluid
501 and fetal circulation, and then have a direct impact on the fetoplacental unit, leading to bacteremia
502 (Hajishengallis, 2015). Based on the second hypothesis, inflammatory mediators and endotoxins that
503 generated by the sub-gingival inflammation and derived from dental plaque of periodontitis may spread
504 throughout the body and reach the fetoplacental unit (Stout et al., 2013; Aagaard et al., 2014). Despite
505 belonging to the same species, some subgroups of the salivary microbiome may influence pregnancy
506 outcomes in both favorable and adverse manners. Following this line of argumentation, the salivary
507 microbiome composition or their dysbiosis are more significant than the existence of particular bacteria.

508 Notably, microbial alteration that take place throughout pregnancy may be expected results of a healthy
509 pregnancy. Those pregnancy-related vulnerabilities to dental problem like periodontitis can be explained
510 by three factors. Because of hormone-driven gingival hyper-reactivity to the salivary microbiome in the

511 oral biofilm including sub-gingival biofilm, these conditions are prevalent in pregnant women. For insight
512 at the relationship between the salivary microbiome compositions and PTB, further studies with pathway
513 analysis are warranted.

514 Our study confirmed that salivary microbiome composition could provide potential biomarkers for
515 predicting pregnancy complications including PTB risks using random forest-based classification models,
516 despite a limited number of study participants and a tiny validation sample size. Another limitation of our
517 study was 16S rRNA gene sequencing. In other words, unlike the shotgun sequencing, 16S rRNA gene
518 sequencing only focused on bacteria, not viruses nor fungi. We did not delve into other variables like
519 nutrition status and socioeconomic statuses of study participants that might affect the salivary microbiome
520 composition.

521 Notwithstanding these limitations, this prospective examination showed the promise of the random
522 forest-based PTB prediction models based on mouthwash-derived salivary microbiome composition.
523 Before applying the methods developed in this study in a clinical context, more multi-center and extensive
524 research is warranted to validate our findings.

525 **3 Random forest prediction model for periodontitis statuses based on the**
526 **salivary microbiomes**

527 **3.1 Introduction**

528 Saliva microbial dysbiosis brought on by the accumulation of plaque results in periodontitis, a chronic
529 inflammatory disease of the tissue that surrounds the tooth (Kinane, Stathopoulou, & Papapanou, 2017).
530 Loss of periodontal attachment is a consequence of periodontitis, which may lead to irreversible bone loss
531 and, eventually, permanent tooth loss if left untreated. A new classification criterion of periodontal diseases
532 was created in 2018, about 20 years after the 1999 statements of the previous one (Papapanou et al.,
533 2018). Even with this evolution, radiographic and clinical markers of periodontitis progression remain the
534 primary methods for diagnosing periodontitis (Papapanou et al., 2018). Such tools, nevertheless, frequently
535 demonstrate the prior damage from periodontitis rather than its present condition. Certain individuals have
536 a higher risk of periodontitis, a higher chance of developing severe generalized periodontitis, and a worse
537 response to common salivary bacteria control techniques utilized to prevent and treat periodontitis. As a
538 result, the 2017 framework for diagnosing periodontitis additionally allows for the potential development
539 of biomarkers to enhance diagnosis and treatment of periodontitis (Tonetti, Greenwell, & Kornman, 2018).
540 Instead of only depending on the progression of periodontitis, a new etiological indication based on the
541 current state must be introduced in order to enable appropriate intervention through early detection of
542 periodontitis. Thus, the current clinical diagnostic techniques that rely on periodontal probing can be
543 uncomfortable for patients with periodontitis (Canakci & Canakci, 2007).

544 Due to the development of salivaomics, in this manner, the examination of saliva has emerged as
545 a significant alternative to the conventional ways of identifying periodontitis (Altingöz et al., 2021;
546 Melguizo-Rodríguez, Costela-Ruiz, Manzano-Moreno, Ruiz, & Illescas-Montes, 2020). Given that saliva
547 sampling is non-invasive, painless, and accessible to non-specialists, it may be a valuable instrument for
548 diagnosing periodontitis (Zhang et al., 2016). Furthermore, much research has suggested that periodontitis
549 could be a trigger in the development and exacerbation of metabolic syndrome (Morita et al., 2010; Nesbitt
550 et al., 2010). Consequently, alteration in these levels of salivary microbiome markers may serve as high
551 effective diagnostic, prognostic, and therapeutic indicators for periodontitis and other systemic diseases
552 (Miller, Ding, Dawson III, & Ebersole, 2021; Čižmárová et al., 2022). The pathogenesis of periodontitis
553 typically comprises qualitative as well as quantitative alterations in the salivary microbial community,
554 despite that it is a complex disease impacted by a number of contributing factors including age, smoking
555 status, stress, and nourishment (Abusleme, Hoare, Hong, & Diaz, 2021; Lafaurie et al., 2022). Depending
556 on the severity of periodontitis, the salivary microbial community's diversity and characteristics vary
557 (Abusleme et al., 2021), indicating that a new etiological diagnostic standards might be microbial
558 community profiling based on clinical diagnostic criteria. As a consequence, salivary microbiome
559 compositions have been characterized in numerous research in connection with periodontitis. High-
560 throughput sequencing, including 16S rRNA gene sequencing, has recently used in multiple studies to
561 identify variations in the bacterial composition of sub-gingival plaque collections from periodontal healthy

562 individuals and patients with periodontitis (Altabtbaei et al., 2021; Iniesta et al., 2023; Nemoto et al., 2021).
563 This realization has rendered clear that alterations in the salivary microbial community—especially, shifts to
564 dysbiosis—are significant contributors to the pathogenesis and development of periodontitis (Lamont, Koo,
565 & Hajishengallis, 2018). Yet most of these research either focused only on the microbiome alterations in
566 sub-gingival plaque collection, comprised a limited number of periodontitis study participants, or did not
567 account for the impact of multiple severities of periodontitis.

568 For the objective of diagnosing periodontitis, previous research has developed machine learning-based
569 prediction models based on oral microbiome compositions, such as the sub-gingival microbial dysbiosis
570 index (T. Chen, Marsh, & Al-Hebshi, 2022; Chew, Tan, Chen, Al-Hebshi, & Goh, 2024), which have
571 demonstrated good diagnostic evaluation and could be applied to individual saliva collection. Despite
572 offering valuable details, these indicators are frequently restricted by their limited emphasis on classifying
573 the multiple severities of periodontitis. Furthermore, many of these machine learning models currently in
574 practice are trained solely upon the existence of periodontitis rather than on the multiple severities of
575 periodontitis.

576 Recently, we employed multiplex quantitative-PCR (qPCR) and machine learning-based classification
577 model to predict the severity of periodontitis based on the amount of nine pathogens of periodontitis from
578 saliva collections (E.-H. Kim et al., 2020). On the other hand, the fact that we focused merely at nine
579 pathogens for periodontitis and neglected the variety bacterial species associated to the various severities
580 of periodontitis constrained the breadth of our investigation. By developing a machine learning model
581 that could classify multiple severities of periodontitis based on the salivary microbiome composition,
582 this study aims to fill these knowledge gaps and produce more accurate and therapeutically useful
583 guidance to evaluate progression of periodontitis. Hence, in order to examine the salivary microbiome
584 composition of both healthy controls and patients with periodontitis in multiple stages, we applied
585 16S rRNA gene sequencing. Furthermore, employing the 2018 classification criteria, we sought to find
586 biomarkers (bacterial species) for the precise prediction of periodontitis severities (Papapanou et al.,
587 2018; Chapple et al., 2018).

588 **3.2 Materials and methods**

589 **3.2.1 Study participants enrollment**

590 Between 2018-08 and 2019-03, 250 study participants—100 healthy controls, 50 patients with stage I
591 periodontitis, 50 patients with stage II periodontitis, and 50 patients with stage III periodontitis—visited
592 visited the Department of Periodontics at Pusan National University Dental Hospital. The Institutional
593 Review Board of the Pusan National University Dental Hospital accepted this study protocol and design
594 (IRB No. PNUDH-2016-019). Every study participants provided their written informed authorization after
595 being fully informed about this study's objectives and methodologies. Exclusion criteria for the study
596 participants are followings:

- 597 1. People who, throughout the previous six months, underwent periodontal therapy, including root
598 planing and scaling.
- 599 2. People who struggle with systemic conditions that may affect periodontitis developments, such as
600 diabetes.
- 601 3. People who, throughout the previous three months, were prescribed anti-inflammatory medications
602 or antibiotics.
- 603 4. Women who were pregnant or breastfeeding.
- 604 5. People who have persistent mucosal lesions, *e.g.* pemphigus or pemphigoid, or acute infection, *e.g.*
605 herpetic gingivostomatitis.
- 606 6. Patient with grade C periodontitis or localized periodontitis (< 30% of teeth involved).

607 **3.2.2 Periodontal clinical parameter diagnosis**

608 A skilled periodontist conducted each clinical procedure. Six sites per tooth were used to quantify
609 gingival recession and probing depth: mesiobuccal, midbuccal, distobuccal, mesiolingual, midlingual,
610 and distolingual (Huang et al., 2007). A periodontal probe (Hu-Friedy, IL, USA) was placed parallel to
611 the major axis of the tooth at each tooth location in order to gather measurements. The cementoenamel
612 junction of the tooth was analyzed to determine the clinical attachment level, and the deepest point of
613 probing was taken to determine the periodontal pocket depth from the marginal gingival level of the
614 tooth. Plaque index was measured by probing four surfaces per tooth: mesial, distal, buccal, and palatal
615 or lingual. Plaque index was scored by the following criteria:

- 616 0. No plaque present.
- 617 1. A thin layer of plaque that adheres to the surrounding tissue of the tooth and free gingival margin.
618 Only through the use of a periodontal probe on the tooth surface can the plaque be existed.
- 619 2. Significant development of soft deposits that are visible within the gingival pocket, which is a
620 region between the tooth and gingival margin.

621 3. Considerable amount of soft matter on the tooth, the gingival margin, and the gingival pocket.

622 The arithmetic average of the plaque indices collected from every tooth was determined to calculate
623 plaque index of each study participant. By probing four surfaces per tooth, mesial, distal, buccal, and
624 palatal or lingual, to assess gingival bleeding, the gingival index was scored by the following criteria:

625 0. Normal gingiva: without inflammation nor discoloration.

626 1. Mild inflammation: minimal edema and slight color changes, but no bleeding on probing.

627 2. Moderate inflammation: edema, glazing, redness, and bleeding on probing.

628 3. Severe inflammation: significant edema, ulceration, redness, and spontaneous bleeding.

629 The arithmetic average of the gingival indices collected from every tooth was determined to calculate
630 gingival index of each study participant. The relevant data was not displayed, despite that furcation
631 involvement and bleeding on probing were thoroughly utilized into account during the diagnosis process.

632 Periodontitis was diagnosed in respect to the 2018 classification criteria for periodontitis (Papapanou
633 et al., 2018; Chapple et al., 2018). An experienced periodontist diagnosed the periodontitis severity
634 by considering complexity, depending on clinical examinations including radiographic images and
635 periodontal probing. Periodontitis is categorized into healthy, stage I, stage II, and stage III with the
636 following criteria:

637 • Healthy:

638 1. Bleeding sites < 10%

639 2. Probing depth: \leq 3 mm

640 • Stage I:

641 1. No tooth loss because of periodontitis.

642 2. Inter-dental clinical attachment level at the site of the greatest loss: 1-2 mm

643 3. Radiographic bone loss: < 15%

644 • Stage II:

645 1. No tooth loss because of periodontitis.

646 2. Inter-dental clinical attachment level at the site of the greatest loss: 3-4 mm

647 3. Radiographic bone loss: 15-33%

648 • Stage III:

649 1. Teeth loss because of periodontitis: \leq 3 teeth

650 2. Inter-dental clinical attachment level at the site of the greatest loss: \geq 5 mm

651 3. Radiographic bone loss: > 33%

652 **3.2.3 Saliva sampling and DNA extraction procedure**

653 All study participants received instructions to avoid eating, drinking, brushing, and using mouthwash for
654 at least an hour prior to the saliva sample collection process. These collections were conducted between
655 09:00 and 11:00. Mouth rinse was collected by rinsing the mouth for 30 seconds with 12 mL of a solution
656 (E-zen Gargle, JN Pharm, Korea). All saliva samples were tagged with anonymous ID and stored at -4 °C.

657 Bacteria DNA was extracted from saliva samples using an Exgene™Clinic SV DNA extraction kit
658 (GeneAll, Seoul, Korea), and quality and quantity of bacterial DNA was measured using a NanoDrop
659 spectrophotometer (Thermo Fisher Scientific, Wilmington, DE, USA). Hyper-variable regions (V3-V4)
660 of the 16S rRNA gene were amplified using the following primer:

- 661 • Forward: 5'-TCGTCGGCAGCGTCAGATGTGTATAAGAGACAGCCTACGGGNNGCWGCAG-3'
662 • Reverse: 5'-GTCTCGTGGGCTCGGAGATGTGTATAAGAGACAGGACTACHVGGGTATCTAATCC-3'

663 The standard protocols of the Illumina 16S Metagenomic Sequencing Library Preparation were
664 followed in the preparation of the libraries. The PCR conditions were as follows:

- 665 1. Heat activation for 30 seconds at 95 °C.
666 2. 25 cycles for 30 seconds at 95 °C.
667 3. 30 seconds at 55 °C.
668 4. 30 seconds at 72 °C.

669 NexteraXT Indexed Primer was applied to amplification 10 µL of the purified initial PCR products for
670 the final library creation. The second PCR used the same conditions as the first PCR conditions but with
671 10 cycles. 16S rRNA gene sequencing was performed via 2×300 bp paired-end sequencing at Macrogen
672 Inc. (Macrogen, Seoul, Korea) using Illumina MiSeq platform (Illumina, San Diego, CA, USA).

673 **3.2.4 Bioinformatics analysis**

674 We computed alpha-diversity and beta-diversity indices to quantify the divergence of phylogenetic
675 information. Following alpha-diversity indices were calculated using the scikit-bio Python package
676 (version 0.5.5) (Rideout et al., 2018), and these alpha-diversity indices were compared using the MWU
677 test:

- 678 • Abundance-based Coverage Estimator (ACE) (Chao & Lee, 1992)
679 • Chao1 (Chao, 1984)
680 • Fisher (Fisher, Corbet, & Williams, 1943)
681 • Margalef (Magurran, 2021)
682 • Observed ASVs (DeSantis et al., 2006)
683 • Berger-Parker *d* (Berger & Parker, 1970)
684 • Gini (Gini, 1912)

- Shannon (Weaver, 1963)
- Simpson (Simpson, 1949)

Aitchison index for a beta-diversity index was calculated using QIIME2 (version 2020.8) (Aitchison, Barceló-Vidal, Martín-Fernández, & Pawlowsky-Glahn, 2000; Bolyen et al., 2019). We employed the t-SNE algorithm to illustrate multi-dimensional data from the beta-diversity index computation (Van der Maaten & Hinton, 2008). The beta-diversity index was compared using the PERMANOVA test (Anderson, 2014; Kelly et al., 2015) and MWU test.

DAT between multiple periodontitis stages were identified by ANCOM (Lin & Peddada, 2020). The log-transformed absolute abundances of DAT were analyzed by hierarchical clustering in order to identify sub-groups with similar abundance patterns on periodontitis severities. Additionally, we examined the relative proportions among the 20 DAT in order to reduce the effect of salivary bacteria that differ insignificantly across the multiple severities of periodontitis.

Differentially abundant taxa (DAT) among multiple periodontitis severities were selected from the salivary microbiome compositions by ANCOM (Lin & Peddada, 2020). In contrast to conventional techniques that examine raw abundance counts, ANCOM applies log-ratio between taxa to account for the salivary microbiome composition data. The log-transformed abundances of DAT were subjected to hierarchical clustering to discover subgroups of DAT with similar patterns on periodontitis severities. Furthermore, we examined the relative proportion among the DAT in order to reduce the effects of other salivary bacteria that differ non-significantly across the multiple periodontitis severities.

As previously stated (E.-H. Kim et al., 2020), we used stratified k -fold cross-validation ($k = 10$) by severity of periodontitis to achieve consistent and trustworthy classification results (Wong & Yeh, 2019). Additionally, we utilized various features with confusion matrices and their derivations to evaluate the classification outcomes in order to identify which features optimize classification evaluations and decrease sequencing efforts. Using the DAT discovered by ANCOM, we iteratively removed the least significant taxa from the input features (taxa) of the random forest (Breiman, 2001) and gradient boosting (Friedman, 2002) classification models using the backward elimination method. Random forest classifier builds multiple decision trees independently using bootstrapped samples and aggregates their predictions, enhancing stability and reducing overfitting problems. In contrast, Gradient boosting constructs trees sequentially, where each new tree improves the errors of the previous ones using gradient descent, leading to higher classification evaluations.

We investigated external datasets from Spanish individuals (Iniesta et al., 2023) and Portuguese individuals (Relvas et al., 2021) to confirm that our random forest classification was consistent. To ascertain repeatability and dependability, the external datasets were processed using the same pipeline and parameters as those used for our study participants.

3.2.5 Data and code availability

All sequences from the 250 study participants have been published to the Sequence Read Archives (project ID PRJNA976179): <https://www.ncbi.nlm.nih.gov/Traces/study/?acc=PRJNA976179>. Docker

722 image that employed throughout this study is available in the DockerHub: <https://hub.docker.com/>
723 repository/docker/fumire/periodontitis_16s. Every code used in this study can be found on
724 GitHub: https://github.com/CompbioLabUnist/Periodontitis_16S.

725 **3.3 Results**

726 **3.3.1 Summary of clinical information and sequencing data**

727 Among clinical information of the study participants, clinical attachment level, probing depth, plaque
728 index, and gingival index, were significantly increased with periodontitis severity (Kruskal-Wallis test
729 $p < 0.001$), while sex were observed no significant difference (Table 2). Notably, clinical attachment level
730 and probing depth have significant differences among the periodontitis severities (MWU test $p < 0.01$;
731 Figure 15). Additionally, 71461.00 ± 11792.30 and 45909.78 ± 11404.65 reads per sample were obtained
732 before and after filtering low-quality reads and trimming extra-long tails, respectively (Figure 16). In 250
733 study subjects, we have found a total of 425 bacterial taxa (Figure 13).

734 **3.3.2 Diversity indices reveal differences among the periodontitis severities**

735 Rarefaction curves showed that the sequencing depth was sufficient (Figure 12). Alpha-diversity indices
736 indicated significant differences between the healthy and the periodontitis stages (MWU test $p < 0.01$;
737 Figure 7a-e); however, there were no significant differences between the periodontitis stages. This
738 emphasizes how essential it is to classify the salivary microbiome compositions and distinguish between
739 the stages of periodontitis using machine learning approaches.

740 The confidence ellipses of the tSNE-transformed beta-diversity index (Aitchison index) indicated
741 distinct distributions among the periodontitis severities (PERMANOVA $p \leq 0.001$; Figure 7f). Aitchison
742 index demonstrated significant differences every pairwise of the periodontitis severities (PERMANOVA
743 test $p \leq 0.001$; Table 7). Significant differences in the distances between periodontitis severities further
744 demonstrated the uniqueness of each severity of periodontitis (MWU test $p \leq 0.05$; Figure 7g-j).

745 **3.3.3 DAT among multiple periodontitis severities and their correlation**

746 Of the 425 total taxa that identified in the salivary microbiome composition (Figure 13), 20 DAT were
747 identified (Table 5). Three separate subgroups were formed from the participants-level abundances of the
748 DAT using a hierarchical clustering methodology (Figure 8a):

- 749 • Group 1
 - 750 1. *Treponema* spp.
 - 751 2. *Prevotella* sp. HMT 304
 - 752 3. *Prevotella* sp. HMT 526
 - 753 4. *Peptostreptococcaceae [XI][G-5]* saphenum
 - 754 5. *Treponema* sp. HMT 260
 - 755 6. *Mycoplasma faecium*
 - 756 7. *Peptostreptococcaceae [XI][G-9]* brachy
 - 757 8. *Lachnospiraceae [G-8]* bacterium HMT 500
 - 758 9. *Peptostreptococcaceae [XI][G-6]* nodatum
 - 759 10. *Fretibacterium* spp.

- 760 • Group 2
- 761 1. *Porphyromonas gingivalis*
- 762 2. *Campylobacter showae*
- 763 3. *Filifactor alocis*
- 764 4. *Treponema putidum*
- 765 5. *Tannerella forsythia*
- 766 6. *Prevotella intermedia*
- 767 7. *Porphyromonas* sp. HMT 285

- 768 • Group 3
- 769 1. *Actinomyces* spp.
- 770 2. *Corynebacterium durum*
- 771 3. *Actinomyces graevenitzii*

772 Ten DAT that were significant enriched in stage II and stage III, but deficient in healthy formed Group
773 1 (Figure 8). Furthermore, in comparison to the healthy, the seven DAT of Group 2 were significantly
774 enriched in each of the stages of periodontitis. On the other hand, three DAT in Group 3 were deficient in
775 stage II and stage III, but significantly enriched in healthy. The relative proportions of the DAT further
776 supported these findings (Figure 8b), suggesting that the DAT is primarily linked to periodontitis rather
777 than other salivary bacteria.

778 Correlation analysis from the DAT showed that DAT from Group 3 was negatively correlated with
779 Group 1 and Group 2 (Figure 9), and strong correlations were observed the nine pairs of DAT (Figure 14).

780 3.3.4 Classification of periodontitis severities by random forest models

781 To confirm that using selected DAT bacterial profiles could have enhanced sequencing expenses without
782 losing the classification evaluations, we built the random forest classification models based on DAT and
783 full microbiome compositions (Figure 18). DAT based classifier showed non-significant different or better
784 evaluations, by removing confounding taxa.

785 Based on the proportion of DAT, random forest classifier were trained to classify the periodontitis
786 severities (Table 6). We conducted multi-label classification for the multiple periodontitis severities,
787 namely healthy, stage I, stage II, and stage III. In this setting, we classified multiple periodontitis
788 severities with the highest BA of 0.779 ± 0.029 (Table 4). AUC ranged between 0.81 and 0.94 (Figure
789 10b).

790 Since timely detection in dentistry is demanding (Tonetti et al., 2018), we implemented a random
791 forest classification for both healthy and stage I. Remarkably, the random forest classifier had the highest
792 BA at 0.793 ± 0.123 (Table 4). In this setting, this model showed high AUC value for the classifying of
793 stage I from healthy (AUC=0.85; Figure 10d).

794 Based on the findings that the salivary microbiome composition in stage II is more comparable to
795 those in stage III than to other severities (Figure 7f and Figure 7j), we combined stage II and stage III to

796 perform a multi-label classification.

797 To examine alternative classification algorithms in comparison to random forest classification, we
798 selected gradient boost algorithm because it is another algorithm of the few classification algorithms
799 that can provide feature importances, which is essential for identifying key taxa contributing to the
800 classification of periodontitis severities. Thus, we assessed gradient boosting algorithms (Figure 20).
801 However, the classification evaluations obtained from gradient boosting have non-significant differences
802 compared to random forest classification.

803 Finally, to confirm the reliability and consistency of our random forest classifier, we validated our
804 classification model using openly accessible 16S rRNA gene sequencing from Spanish participants
805 (Iniesta et al., 2023) and Portuguese participants (Relvas et al., 2021) (Figure 11). Although some
806 evaluations, *e.g.* SPE, were low, the other were comparable.

Table 3: Clinical characteristics of the study participants.

Significant differences were assessed using the Kruskal-Wallis test. NA: Not applicable.

Index	Healthy	Stage I	Stage II	Stage III	p-value
Age (year)	33.83±13.04	43.30±14.28	50.26±11.94	51.08±11.13	6.18E-17
Gender (Male)	44 (44.0%)	22 (44.0%)	25 (50.0%)	25 (50.0%)	NA
Smoking (Never)	83 (83.0%)	36 (72.0%)	34 (68.0%)	29 (58.0%)	NA
Smoking (Ex)	12 (12.0%)	7 (14.0%)	9 (18.0%)	10 (20.0%)	NA
Smoking (Current)	2 (2.0%)	7 (14.0%)	7 (14.0%)	10 (20.0%)	NA
Number of teeth	28.03±2.23	27.36±1.80	26.72±2.89	25.74±4.34	8.07E-05
Attachment level (mm)	2.45±0.29	2.75±0.38	3.64±0.83	4.54±1.14	1.82E-35
Probing depth (mm)	2.42±0.29	2.61±0.40	3.27±0.76	3.95±0.88	6.43E-28
Plaque index	17.66±16.21	35.46±23.75	54.40±23.79	58.30±25.25	3.23E-22
Gingival index	0.09±0.16	0.44±0.46	0.85±0.52	1.06±0.52	2.59E-32

Table 4: Feature combinations and their evaluations

Classification performance with the most important taxon, the two most important taxa, and taxa with the best-balanced accuracy. *P.gingivalis* and *Act.* are *Porphyromonas gingivalis* and *Actinomyces* spp., respectively.

Classification	Features	ACC	AUC	BA	F1	PRE	SEN	SPE
Healthy vs. Stage I vs. Stage II vs. Stage III	<i>P.gingivalis</i>	0.758±0.051	0.716±0.177	0.677±0.068	0.839±0.034	0.839±0.034	0.516±0.102	
	<i>P.gingivalis+Act.</i>	0.792±0.043	0.822±0.105	0.723±0.057	0.861±0.029	0.861±0.029	0.584±0.086	
Top 5 taxa		0.834±0.022	0.870±0.079	0.779±0.029	0.889±0.015	0.889±0.015	0.668±0.033	
Healthy vs. Stage I	<i>Act.</i>	0.687±0.116	0.725±0.145	0.647±0.159	0.762±0.092	0.760±0.128	0.781±0.116	0.513±0.224
	<i>Act.+P.gingivalis</i>	0.733±0.119	0.831±0.081	0.713±0.122	0.797±0.097	0.798±0.126	0.798±0.082	0.627±0.191
Top 9 taxa		0.800±0.103	0.852±0.103	0.793±0.123	0.849±0.080	0.850±0.112	0.857±0.090	0.730±0.193
Healthy vs. Stage I vs. Stages II/III	<i>P.gingivalis</i>	0.776±0.042	0.736±0.196	0.748±0.047	0.832±0.031	0.832±0.031	0.664±0.062	
	<i>P.gingivalis+Act.</i>	0.843±0.035	0.876±0.109	0.823±0.039	0.882±0.026	0.882±0.026	0.764±0.052	
Top 6 taxa		0.885±0.036	0.914±0.027	0.871±0.038	0.914±0.025	0.914±0.025	0.828±0.051	
Healthy vs. Stages I/II/III	<i>P.gingivalis</i>	0.792±0.114	0.856±0.105	0.819±0.088	0.776±0.089	0.840±0.092	0.756±0.175	0.883±0.054
	<i>P.gingivalis+Act.</i>	0.828±0.121	0.926±0.074	0.847±0.116	0.797±0.123	0.800±0.126	0.830±0.191	0.864±0.074
Top 4 taxa		0.860±0.078	0.953±0.049	0.885±0.066	0.832±0.079	0.840±0.128	0.864±0.157	0.905±0.070

Table 5: List of DAT among healthy status and periodontitis stages

No.	Taxonomy	ANCOM W score
1	<i>Porphyromonas gingivalis</i>	424
2	<i>Actinomyces</i> spp.	424
3	<i>Filifactor alocis</i>	421
4	<i>Prevotella intermedia</i>	419
5	<i>Treponema putidum</i>	418
6	<i>Tannerella forsythia</i>	415
7	<i>Porphyromonas</i> sp. HMT 285	412
8	<i>Peptostreptococcaceae [XI][G-6] nodatum</i>	412
9	<i>Fretibacterium</i> spp.	411
10	<i>Mycoplasma faecium</i>	411
11	<i>Prevotella</i> sp. HMT 304	411
12	<i>Lachnospiraceae [G-8] bacterium</i> HMT 500	409
13	<i>Treponema</i> spp.	408
14	<i>Prevotella</i> sp. HMT 526	401
15	<i>Peptostreptococcaceae [XI][G-9] brachy</i>	400
16	<i>Peptostreptococcaceae [XI][G-5] saphenum</i>	398
17	<i>Campylobacter showae</i>	395
18	<i>Treponema</i> sp. HMT 260	393
19	<i>Corynebacterium durum</i>	393
20	<i>Actinomyces graevenitzii</i>	387

Table 6: Feature the importance of taxa in the classification of different periodontal statuses
 Taxa are ranked in descending order of importance; from most important to least important.

Condition	Healthy vs. Stage I vs. Stage II vs. Stage III			Healthy vs. Stage I			Healthy vs. Stage I vs. Stage II/III			Healthy vs. Stage I/II/III		
	Rank	Taxa	Importance	Taxa	Importance	Taxa	Importance	Taxa	Importance	Taxa	Importance	
1	<i>Porphyromonas gingivalis</i>	0.297	<i>Actinomyces spp.</i>	0.195	<i>Porphyromonas gingivalis</i>	0.360	<i>Porphyromonas gingivalis</i>	0.426	<i>Porphyromonas gingivalis</i>	0.461		
2	<i>Actinomyces spp.</i>	0.195	<i>Actinomyces graevenitzii</i>	0.054	<i>Actinomyces spp.</i>	0.125	<i>Actinomyces spp.</i>	0.244	<i>Actinomyces spp.</i>	0.257		
3	<i>Prevotella intermedia</i>	0.054	<i>Actinomyces graevenitzii</i>	0.052	<i>Porphyromonas sp. HMT 285</i>	0.055	<i>Actinomyces graevenitzii</i>	0.049	<i>Actinomyces graevenitzii</i>	0.059		
4	<i>Actinomyces graevenitzii</i>	0.052	<i>Lachnospiraceae (G-8) bacterium HMT 500</i>	0.050	<i>Porphyromonas sp. HMT 285</i>	0.062	<i>Corynebacterium durum</i>	0.046	<i>Corynebacterium durum</i>	0.035		
5	<i>Filifactor alocis</i>	0.050	<i>Campylobacter showae</i>	0.042	<i>Campylobacter showae</i>	0.052	<i>Filifactor alocis</i>	0.036	<i>Filifactor alocis</i>	0.032		
6	<i>Campylobacter showae</i>	0.042	<i>Porphyromonas sp. HMT 285</i>	0.040	<i>Corynebacterium durum</i>	0.052	<i>Prevotella intermedia</i>	0.033	<i>Campylobacter showae</i>	0.023		
7	<i>Porphyromonas sp. HMT 285</i>	0.040	<i>Treponema spp.</i>	0.032	<i>Treponema spp.</i>	0.038	<i>Tannerella forsythia</i>	0.025	<i>Porphyromonas sp. HMT 285</i>	0.022		
8	<i>Corynebacterium durum</i>	0.032	<i>Tannerella forsythia</i>	0.026	<i>Tannerella forsythia</i>	0.037	<i>Prevotella intermedia</i>	0.023	<i>Prevotella intermedia</i>	0.022		
9	<i>Treponema spp.</i>	0.032	<i>Prevotella intermedia</i>	0.025	<i>Prevotella intermedia</i>	0.029	<i>Treponema spp.</i>	0.021	<i>Treponema spp.</i>	0.022		
10	<i>Tannerella forsythia</i>	0.026	<i>Prevotella intermedia</i>	0.025	<i>Peptostreptococcaceae (XII)(G-9) brachy</i>	0.026	<i>Peptostreptococcaceae (XII)(G-9) brachy</i>	0.018	<i>Peptostreptococcaceae (XII)(G-9) brachy</i>	0.015		
11	<i>Treponema putidum</i>	0.025	<i>Freibacterium spp.</i>	0.023	<i>Peptostreptococcaceae (XII)(G-9) brachy</i>	0.018	<i>Lachnospiraceae (G-8) bacterium HMT 500</i>	0.014	<i>Lachnospiraceae (G-8) bacterium HMT 500</i>	0.010		
12	<i>Freibacterium spp.</i>	0.023	<i>Peptostreptococcaceae (XII)(G-9) brachy</i>	0.021	<i>Peptostreptococcaceae (XII)(G-9) brachy</i>	0.018	<i>Peptostreptococcaceae (XII)(G-6) nodatum</i>	0.011	<i>Tannerella forsythia</i>	0.009		
13	<i>Peptostreptococcaceae (XII)(G-9) brachy</i>	0.021	<i>Treponema putidum</i>	0.019	<i>Treponema putidum</i>	0.014	<i>Treponema putidum</i>	0.010	<i>Freibacterium spp.</i>	0.009		
14	<i>Treponema sp. HMT 260</i>	0.019	<i>Prevotella sp. HMT 526</i>	0.018	<i>Prevotella sp. HMT 526</i>	0.011	<i>Prevotella sp. HMT 526</i>	0.009	<i>Prevotella sp. HMT 526</i>	0.006		
15	<i>Prevotella sp. HMT 526</i>	0.018	<i>Peptostreptococcaceae (XII)(G-6) nodatum</i>	0.018	<i>Peptostreptococcaceae (XII)(G-6) nodatum</i>	0.008	<i>Freibacterium spp.</i>	0.008	<i>Peptostreptococcaceae (XII)(G-6) nodatum</i>	0.004		
16	<i>Peptostreptococcaceae (XII)(G-6) nodatum</i>	0.018	<i>Prevotella sp. HMT 304</i>	0.017	<i>Peptostreptococcaceae (XII)(G-6) nodatum</i>	0.008	<i>Treponema sp. HMT 260</i>	0.008	<i>Treponema sp. HMT 260</i>	0.004		
17	<i>Prevotella sp. HMT 304</i>	0.017	<i>Mycoplasma faecium</i>	0.014	<i>Mycoplasma faecium</i>	0.004	<i>Prevotella sp. HMT 304</i>	0.005	<i>Mycoplasma faecium</i>	0.003		
18	<i>Mycoplasma faecium</i>	0.014	<i>Prevotella sp. HMT 304</i>	0.014	<i>Peptostreptococcaceae (XII)(G-5) saphenum</i>	0.003	<i>Peptostreptococcaceae (XII)(G-5) saphenum</i>	0.005	<i>Peptostreptococcaceae (XII)(G-5) saphenum</i>	0.002		
19	<i>Peptostreptococcaceae (XII)(G-5) saphenum</i>	0.014	<i>Lachnospiraceae (G-8) bacterium HMT 500</i>	0.013	<i>Peptostreptococcaceae (XII)(G-5) saphenum</i>	0.003	<i>Prevotella sp. HMT 304</i>	0.004	<i>Prevotella sp. HMT 304</i>	0.001		
20	<i>Lachnospiraceae (G-8) bacterium HMT 500</i>	0.013										

Table 7: Beta-diversity pairwise comparisons on the periodontitis statuses

Statistically significant (p-value) was determined by the PERMANOVA test.

Group 1	Group 2	p-value
Healthy	Stage I	0.001
Healthy	Stage II	0.001
Healthy	Stage III	0.001
Stage I	Stage II	0.001
Stage I	Stage III	0.001
Stage II	Stage III	0.737

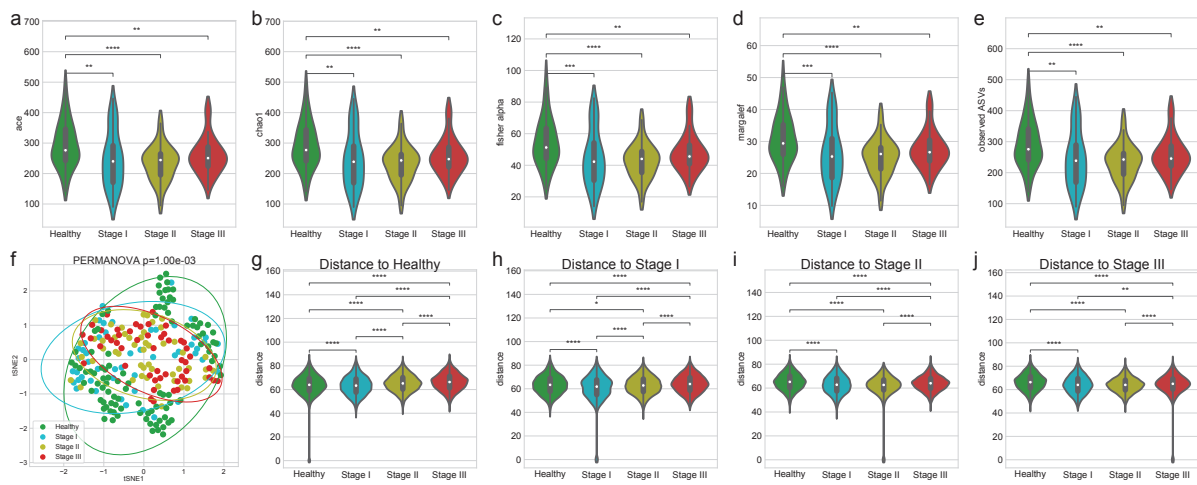


Figure 7: Diversity indices for periodontitis.

Alpha-diversity indices (**a-e**) indicate that healthy controls have increased heterogeneity than periodontitis stages as measured by: **(a)** ACE **(b)** Chao1 **(c)** Fisher alpha **(d)** Margalef, and **(e)** observed ASVs. **(f)** The beta-diversity index (weighted UniFrac) was visualized using a tSNE-transformed plot. The confidence ellipses are shown to display the distribution of each periodontitis stage. The distance to each stage demonstrated that each periodontitis stage was distinguished from the other periodontitis stages: **(g)** distance to Healthy **(h)** distance to Stage I **(i)** distance to Stage II, and **(j)** distance to Stage III. Statistical significance determined by the MWU test and the PERMANOVA test: $p < 0.05$ (*), $p < 0.01$ (**), $p < 0.001$ (***) ≤ 0.0001 (****).

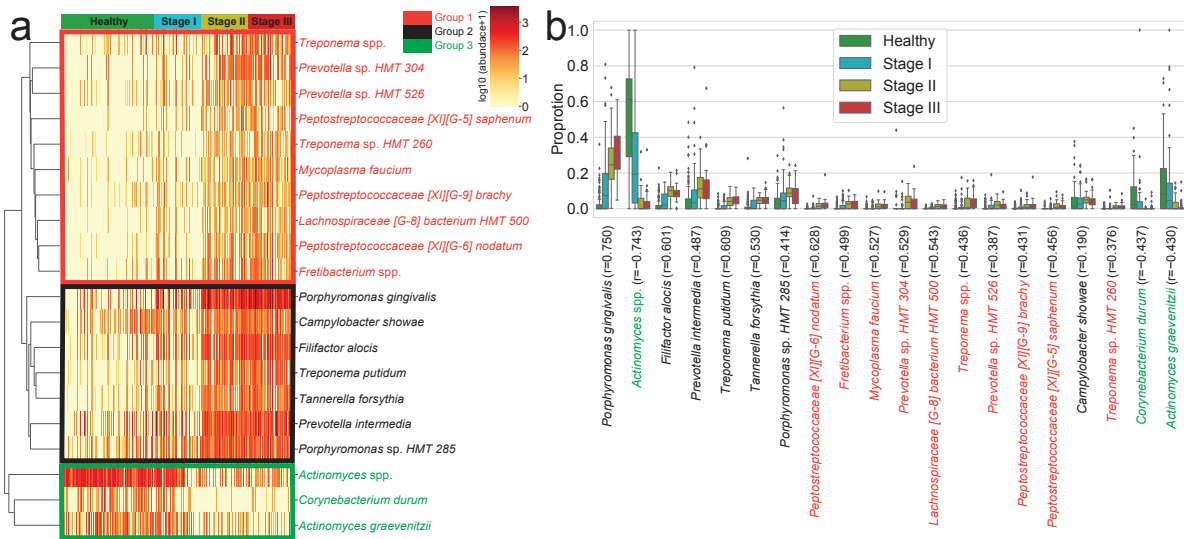


Figure 8: DAT for periodontitis.

DAT that were identified by ANCOM. **(a)** Heatmap of clustered DAT with similar distribution among subjects. Group 1, Group 2, and Group 3 are marked in red, black, and green, respectively. **(b)** Box plots showing the proportions of DAT. Taxa were sorted by their importance according to ANCOM.

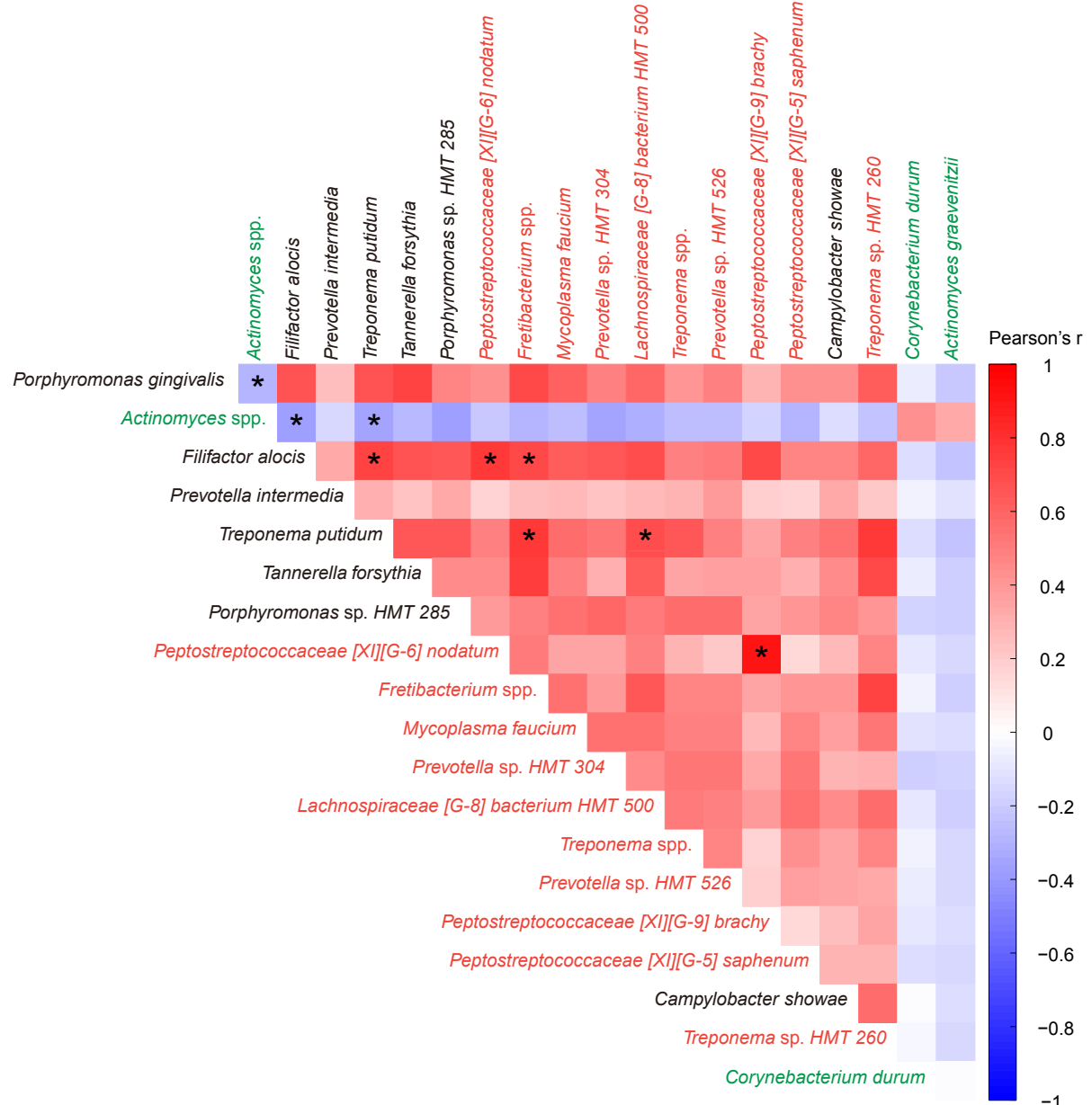


Figure 9: Correlation heatmap between periodontitis DAT.

Pearson's correlations between DAT in healthy status and periodontitis stages. Statistical significance was determined by strong correlation, i.e., $| \text{coefficient} | \geq 0.5$ (*).

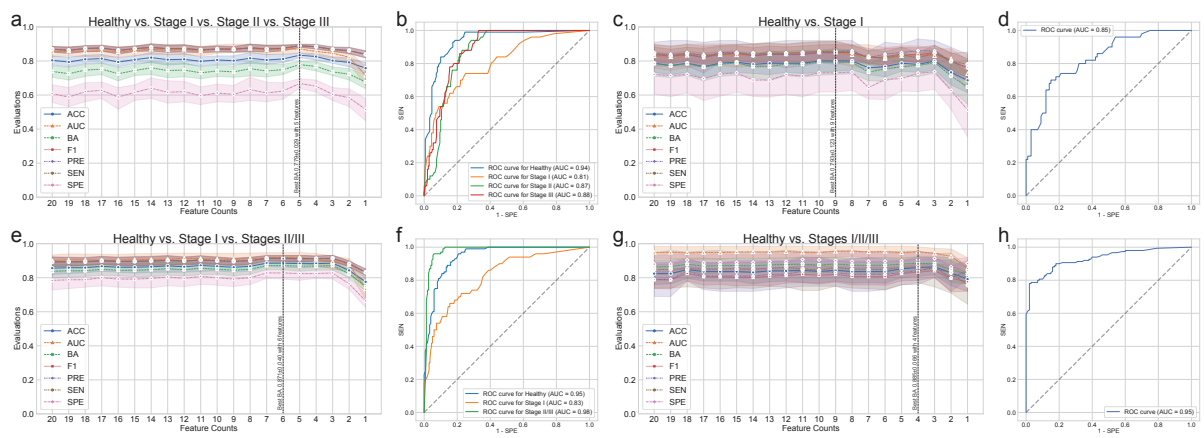


Figure 10: Random forest classification metrics for periodontitis prediction.

The classification metrics in the random forest classifications were as follows: ACC, AUC, BA, F1, PRE, SEN, and SPE. **(a)** Classification performance for healthy vs. stage I vs. stage II vs. stage III. **(b)** ROC curve for the highest BA of (a). **(c)** Classification performance for healthy vs. stage I. **(d)** ROC curve on the highest BA of (c). **(e)** Classification performance for healthy vs. stage I vs. stages II/III. **(f)** ROC curve for the highest BA of (e). **(g)** Classification performance for healthy vs. stages I/II/III. **(h)** ROC curve for the highest BA of (h).

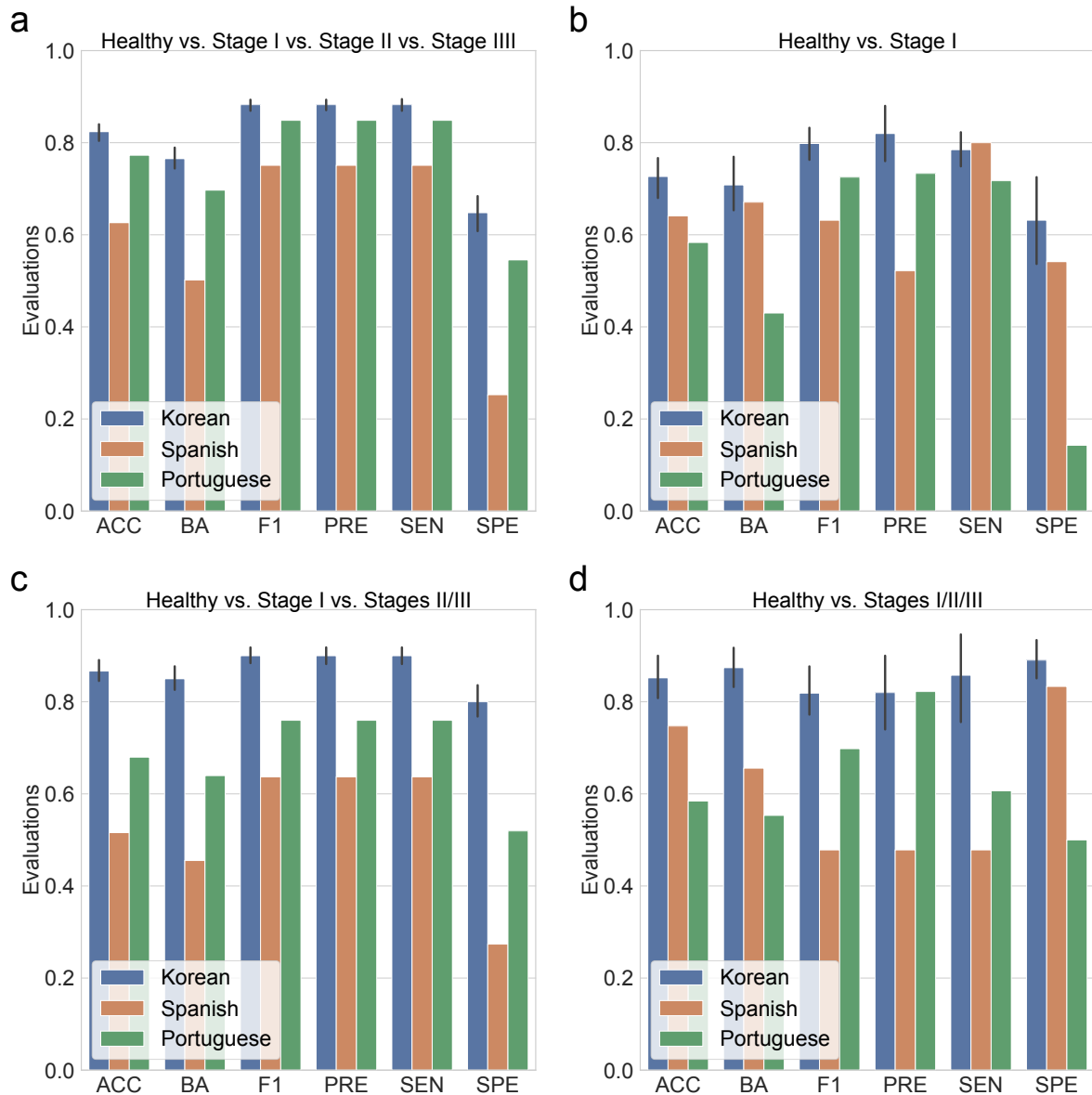


Figure 11: **Random forest classification metrics from external datasets.**

The classification metrics in the random forest classifications were as follows: ACC, AUC, BA, F1, PRE, SEN, and SPE. **(a)** Classification performance for healthy vs. stage I vs. stage II vs. stage III. **(b)** Classification performance for healthy vs. stage I. **(c)** Classification performance for healthy vs. stage I vs. stages II/III. **(d)** Classification performance for healthy vs. stages I/II/III.

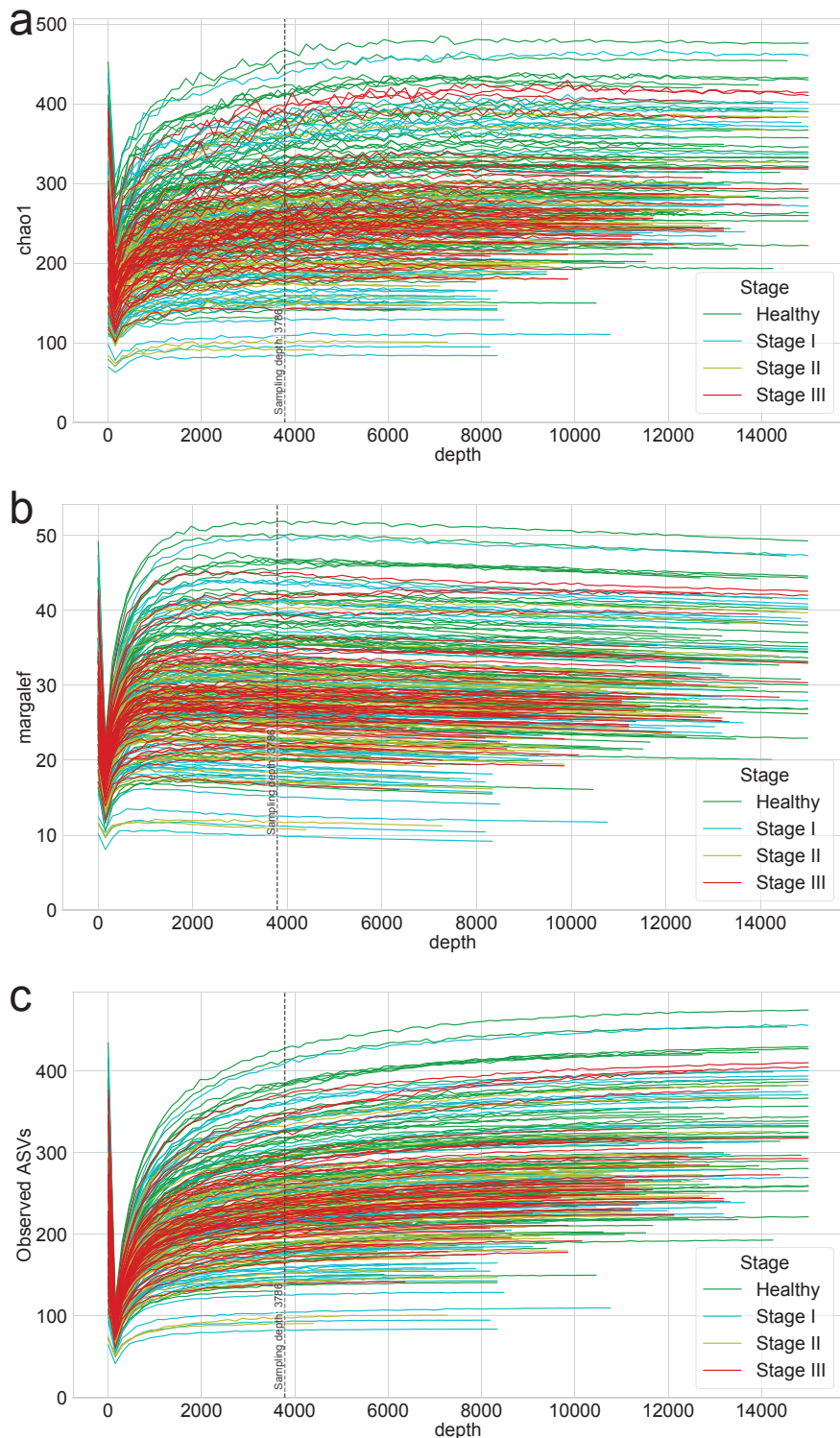


Figure 12: Rarefaction curves for alpha-diversity indices.

Rarefaction of (a) chao1 (b) margalef, and (c) observed ASVs were generated to measure species richness and determine the sampling depth of each sample.

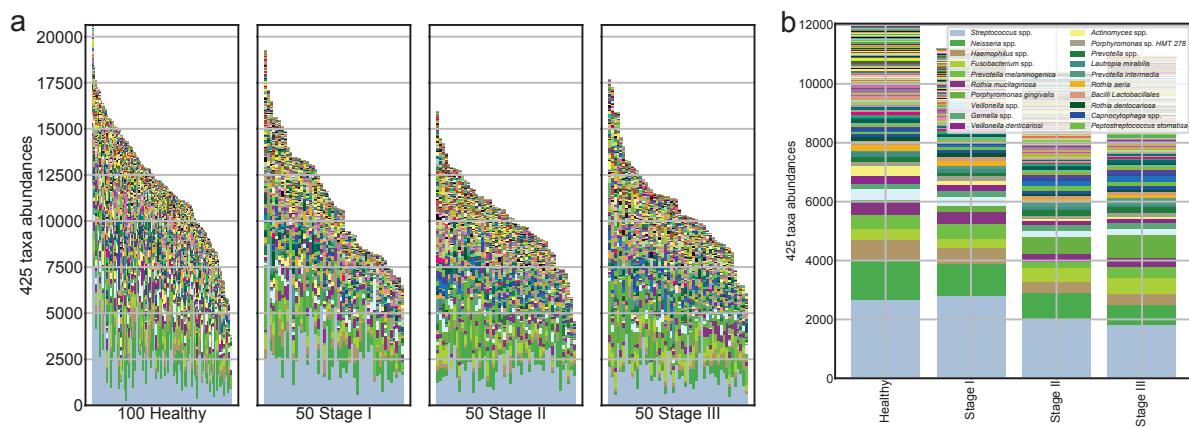


Figure 13: Salivary microbiome compositions in the different periodontal statuses.

Stacked bar plot of the absolute abundance of bacterial species for all samples (a) and the mean absolute abundance of bacterial species in the healthy, stage I, stage II, and stage III groups (b).

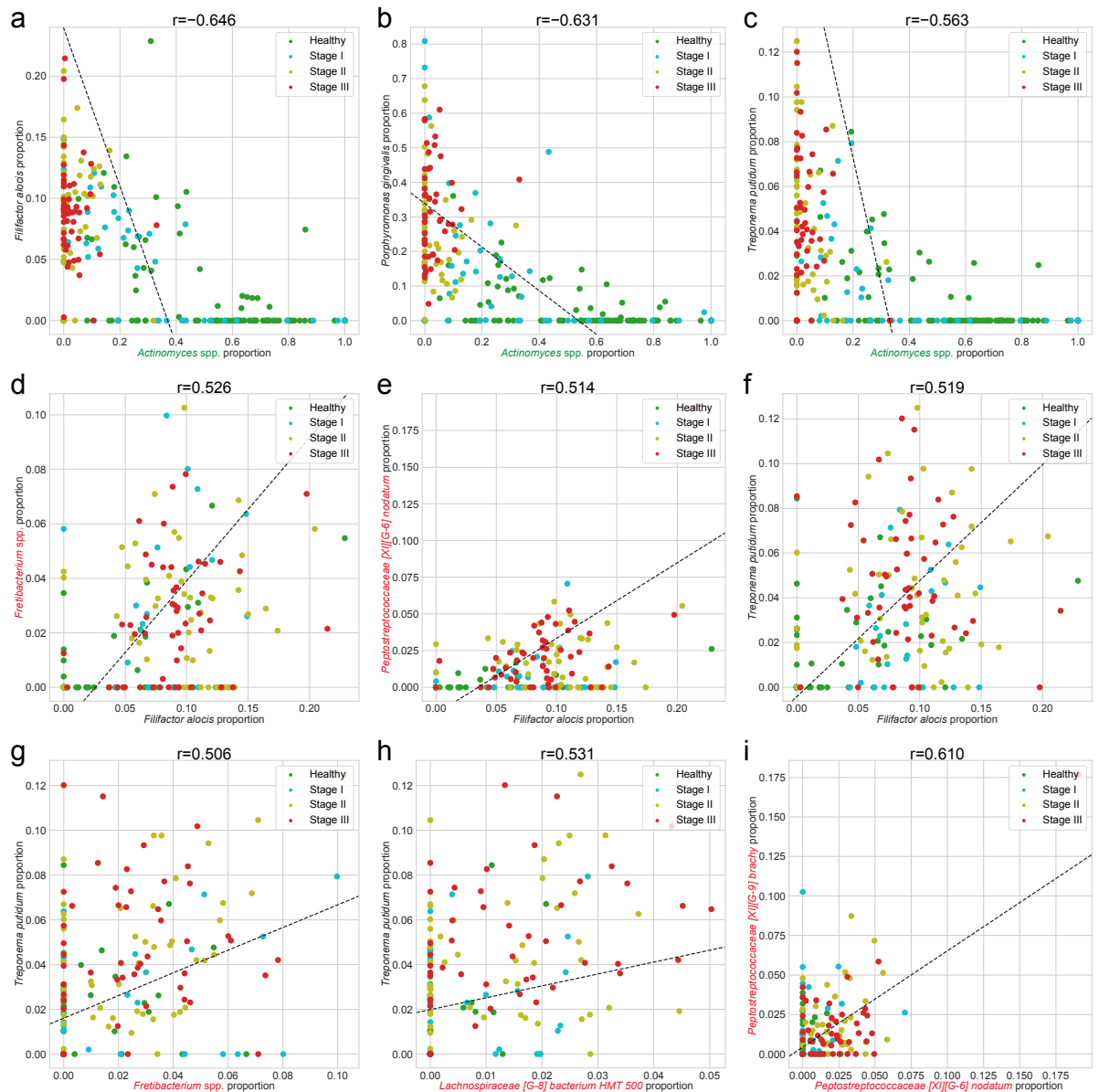


Figure 14: Correlation plots for periodontitis DAT.

We selected the combinations of DAT with absolute Spearman correlation coefficients greater than 0.5. The color represents periodontal healthy periodontal statuses (green: healthy, cyan: stage I, yellow: stage II, and red: stage III).

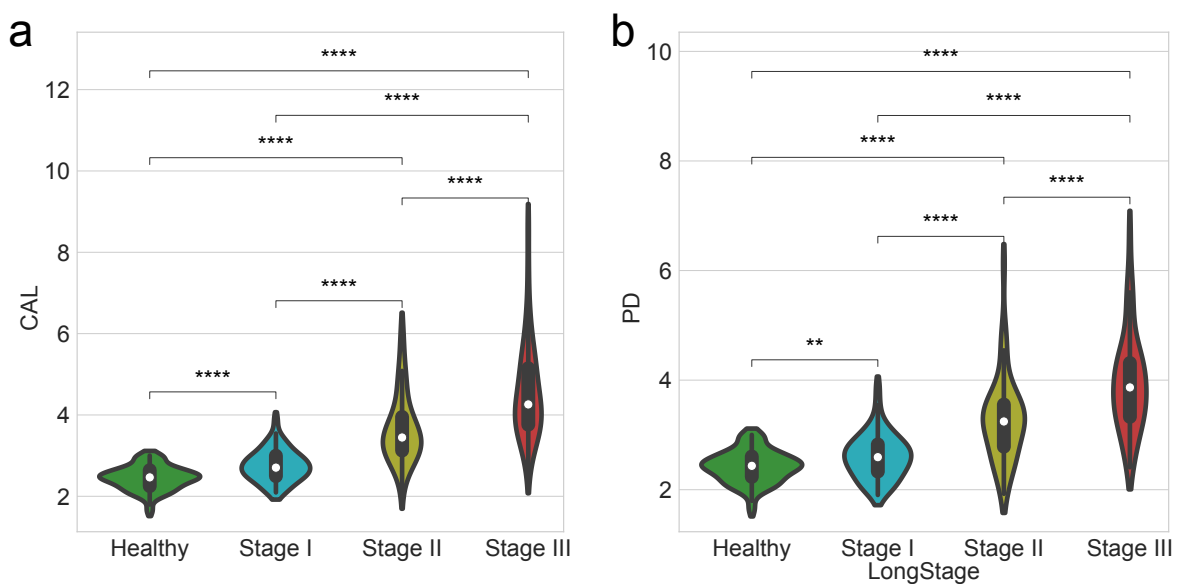


Figure 15: Clinical measurements by the periodontitis statuses.

Comparisons of clinical measurement among healthy controls and patients with various periodontitis stages. **(a)** Clinical attachment level (CAL) **(b)** Probing depth (PD). Statistical significance determined by the MWU test: $p < 0.01$ (**) and $p < 0.0001$ (****).

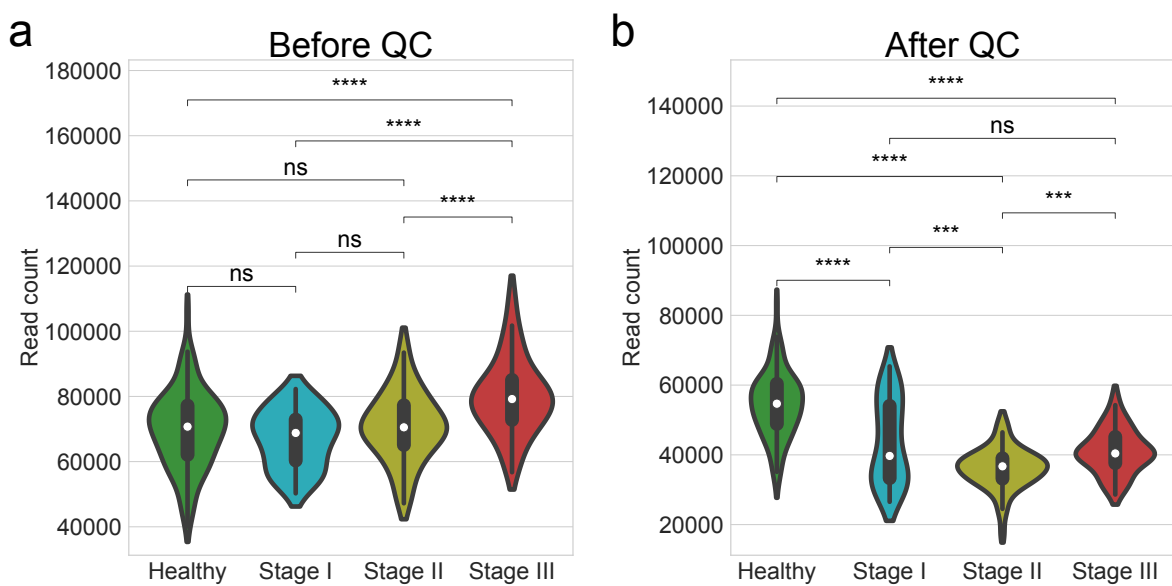


Figure 16: Number of read counts by the periodontitis statuses.

Comparisons of the number of read counts among healthy controls and patients with various periodontitis stages. **(a)** Before quality check **(b)** After quality check. Statistical significance determined by the MWU test: $p \geq 0.05$ (ns), $p < 0.05$ (*), $p < 0.01$ (**), $p < 0.001$ (***), and $p < 0.0001$ (****).

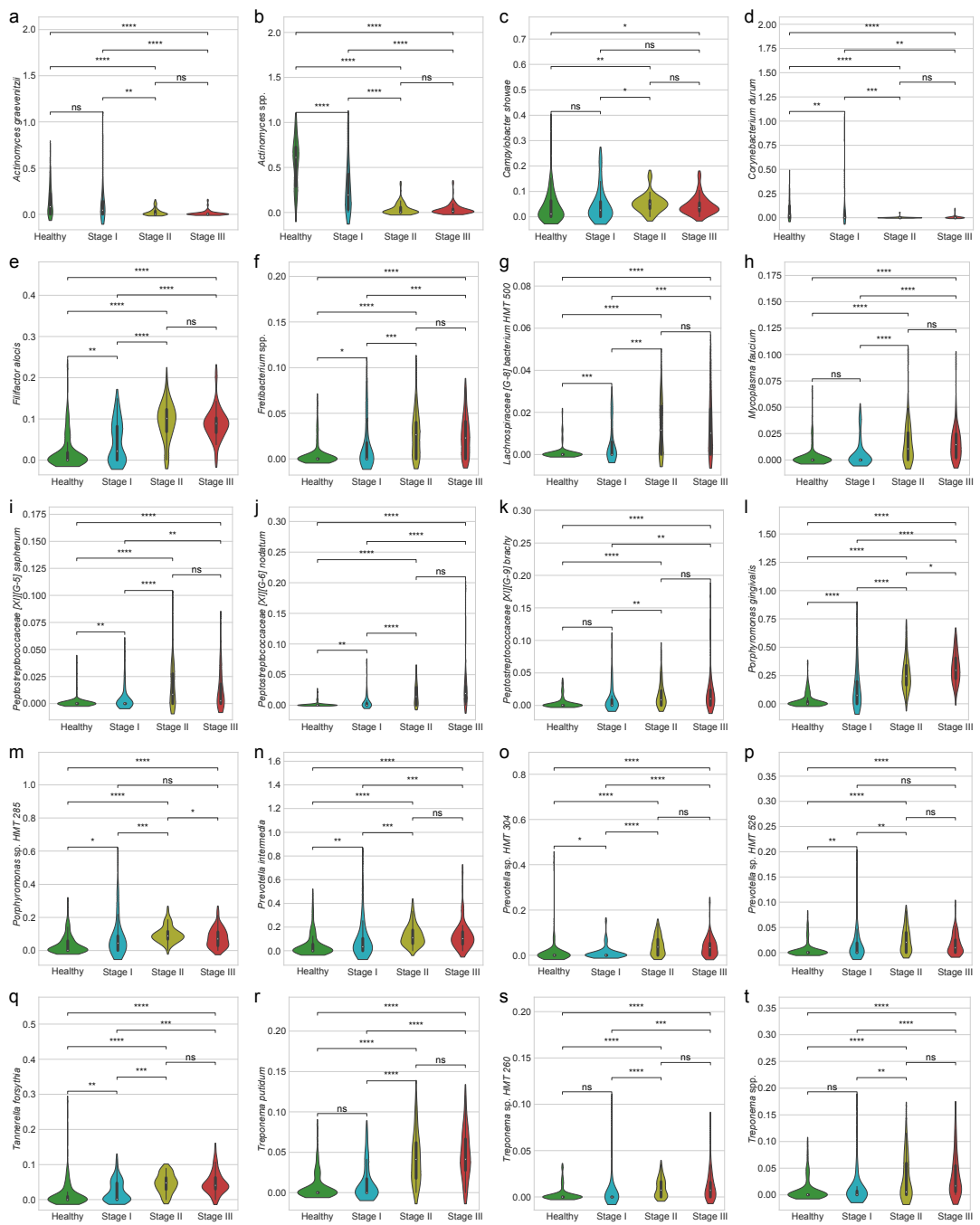


Figure 17: Proportions of periodontitis DAT.

(a) *Actinomyces graevenitzii* **(b)** *Actinomyces* spp. **(c)** *Campylobacter showae* **(d)** *Corynebacterium durum* **(e)** *Filifactor alocis* **(f)** *Fretibacterium* spp. **(g)** *Lachnospiraceae [G-8] bacterium HMT 500* **(h)** *Mycoplasma faecium* **(i)** *Peptostreptococcaceae [XI][G-5] saphenum* **(j)** *Peptostreptococcaceae [XI][G-6] nodatum* **(k)** *Peptostreptococcaceae [XI][G-9] brachy* **(l)** *Porphyromonas gingivalis* **(m)** *Porphyromonas* sp. HMT 285 **(n)** *Prevotella intermedia* **(o)** *Prevotella* sp. HMT 304 **(p)** *Prevotella* sp. HMT 526 **(q)** *Tannerella forsythia* **(r)** *Treponema putidum* **(s)** *Treponema* sp. HMT 260 **(t)** *Treponema* spp. Statistical significance determined by the MWU test: $p \geq 0.05$ (ns), $p < 0.05$ (*), $p < 0.01$ (**), $p < 0.001$ (***) , and $p < 0.0001$ (****).

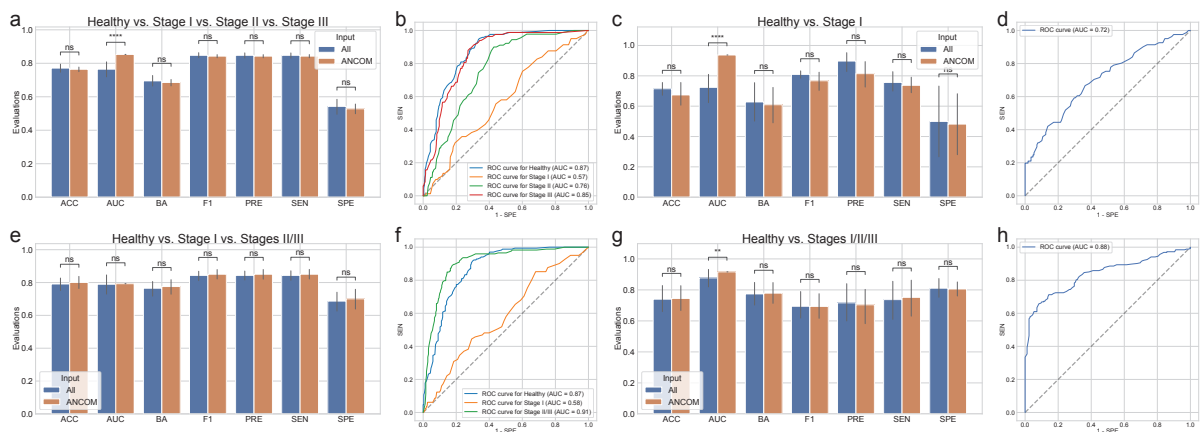


Figure 18: Random forest classification metrics with the full microbiome compositions and ANCOM-selected DAT compositions.

The classification metrics in the random forest classifications were as follows: ACC, AUC, BA, F1, PRE, SEN, and SPE. **(a)** Classification performance for healthy vs. stage I vs. stage II vs. stage III. **(b)** ROC curve for the highest BA of (a). **(c)** Classification performance for healthy vs. stage I. **(d)** ROC curve on the highest BA of (c). **(e)** Classification performance for healthy vs. stage I vs. stages II/III. **(f)** ROC curve for the highest BA of (e). **(g)** Classification performance for healthy vs. stages I/II/III. **(h)** ROC curve for the highest BA of (g). Statistical significance determined by the MWU test: $p \geq 0.05$ (ns), $p < 0.01$ (**), and $p < 0.0001$ (***).

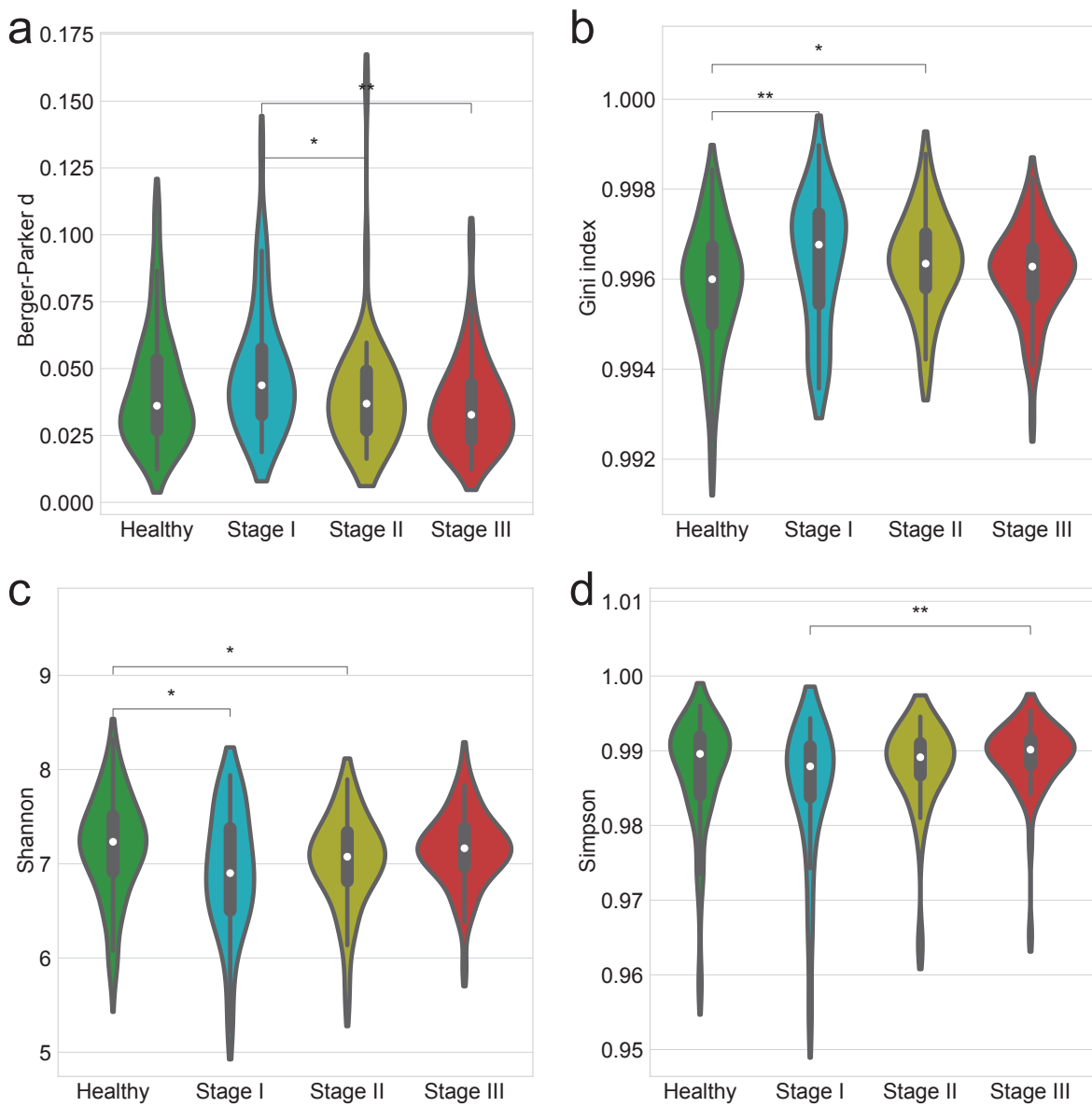


Figure 19: **Alpha-diversity indices account for evenness.**

Alpha-diversity indices (**a-d**) indicate that the heterogeneity between the periodontitis stages as measured by: **(a)** Berger-Parker *d* **(b)** Gini **(c)** Shannon **(d)** Simpson. Statistical significance determined by the MWU test: $p < 0.05$ (*) and $p < 0.01$ (**)

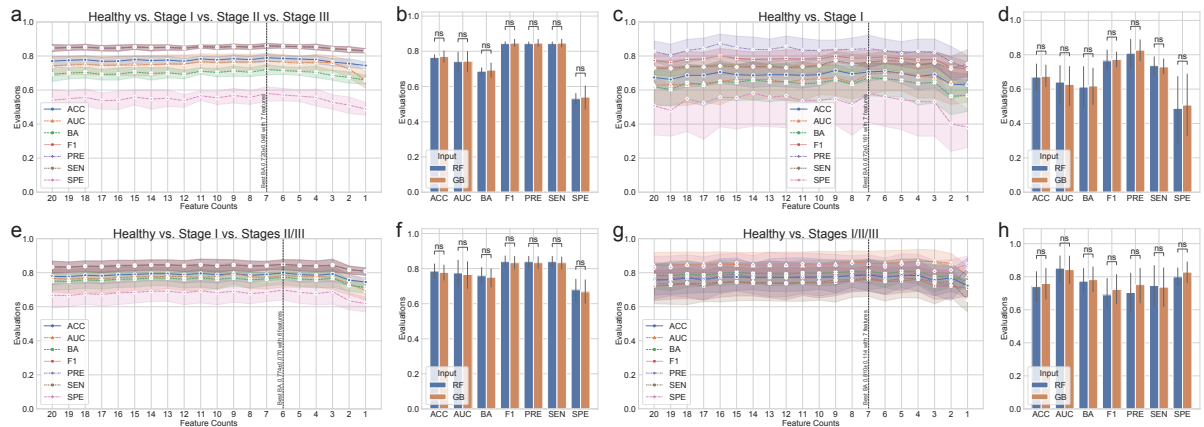


Figure 20: Gradient Boosting classification metrics for periodontitis prediction.

The classification metrics in the random forest classifications were as follows: ACC, AUC, BA, F1, PRE, SEN, and SPE. The feature counts mean that the classification model trained on the most important n features as the Table 5. **(a)** Comparison of Random forest (RF) and Gradient boosting (GB) for healthy vs. stage I vs. stage II vs. stage III. **(b)** Comparison of RF and GB for the highest BA of (a). **(c)** Classification performance for healthy vs. stage I. **(d)** Comparison of RF and GB for healthy vs. stage I vs. stages II/III. **(e)** Comparison of RF and GB for the highest BA of (d). **(f)** Comparison of RF and GB for Healthy vs. Stage I vs. Stages II/III. **(g)** Classification performance for healthy vs. stages I/II/III. **(h)** Comparison of RF and GB for Healthy vs. Stages I/II/III. MWU test: $p \geq 0.05$ (ns)

807 **3.4 Discussion**

808 In order to investigate at potential alterations in the salivary microbiome compositions based on periodontal
809 statuses, including healthy, stage I, stage II, and stage III, we employed 16S rRNA gene sequencing to
810 perform a cross-sectional periodontitis analysis. In this study, the 2018 periodontitis classification served
811 as the basis for the classification of periodontitis severities (Papapanou et al., 2018). There were notable
812 variations in the salivary microbiome composition among the multiple severities of periodontitis (Figure
813 13). Furthermore, our random forest classification model based on the proportions of DAT in the salivary
814 microbiome compositions across study participants to predict multiple periodontitis statuses with high
815 AUC of 0.870 ± 0.079 (Table 4).

816 Previous research identified the red complex as the primary pathogens of periodontitis (Listgarten,
817 1986): *Porphyromonas gingivalis*, *Tannerella forsythia*, and *Treponema denticola*. Other studies, however,
818 have shown that periodontal pathogens communicate with other bacteria in the salivary microbiome
819 networks to generate dental plaque prior to the pathogenesis and development of periodontitis (Lamont &
820 Jenkinson, 2000; Rosan & Lamont, 2000; Yoshimura, Murakami, Nishikawa, Hasegawa, & Kawaminami,
821 2009).

822 Using subgingival plaque collections, recent researches have suggested a connection between the
823 periodontitis severity and the salivary microbiome compositions (Altabtbaei et al., 2021; Iniesta et al.,
824 2023; Nemoto et al., 2021). Therefore, we have examined the salivary microbiome compositions of
825 patients with multiple severities of periodontitis and periodontally healthy controls, extending on earlier
826 studies.

827 According to our findings, the salivary microbiome compositions have 425 taxa (Figure 13). We
828 computed the alpha-diversity indices to determine the variability within each salivary microbiome
829 composition, including ace (Chao & Lee, 1992), chao1 (Chao, 1984), fisher alpha (Fisher et al., 1943),
830 margalef (Magurran, 2021), observed ASVs (DeSantis et al., 2006), Berger-Parker *d* (Berger & Parker,
831 1970), Gini (Gini, 1912), Shannon (Weaver, 1963), and Simpson (Simpson, 1949) (Figure 7 and Figure
832 19). Alpha-diversity indices suggested that the microbial richness of periodontally healthy controls was
833 higher than that of patients with periodontitis (Figure 7a-e and Figure 19). These results are in line with
834 findings with that patients with advanced periodontitis, namely stage II and stage III, have less diversified
835 communities than periodontally healthy controls (Jorth et al., 2014). Recognizing that the periodontitis
836 severity increases the amount of *Porphyromonas gingivalis*, the salivary microbiome compositions from
837 periodontally healthy controls conserved microbial networks dominated by *Streptococcus* spp. (Figure
838 13). *Porphyromonas gingivalis* is one of the known periodontal pathogen that could cause dysbiosys
839 in the salivary microbiomes, suggesting in the pathophysiology of periodontitis. Despite this finding,
840 earlier research found that subgingival microbiome of patients with periodontitis had a greater alpha-
841 diversity index (observed ASVs) than that of healthy controls (Iniesta et al., 2023), might due to the
842 different sampling sites between saliva and subgingival plaque. On the other hand, another research
843 has addressed significant discrepancies in alpha-diversity indices from subgingival plaque, saliva, and
844 tongue biofilms from healthy controls and periodontitis patients, resulting the highest alpha-diversity

845 index in saliva collections (Belstrøm et al., 2021). Moreover, early-stage periodontitis, namely stage I,
846 did not determine statistically significant differences in alpha-diversity indices compared to advanced
847 periodontitis, including stage II and stage III (Figure 7a-e). Accordingly, saliva collection of stage I
848 periodontitis may exhibit heterogeneity, indicating a midpoint condition between a healthy state and
849 advanced periodontitis (stage II and stage III). Likewise, gingivitis is often associated with low abundances
850 of the majority of periodontal pathogens, including *Porphyromonas gingivalis*, *Tannerella forsythia*, and
851 *Treponema denticola* (Abusleme et al., 2021). Compared to healthy controls, patients with stage I
852 periodontitis have higher detection rates of *Porphyromonas gingivalis* and *Tannerella forsythia* (Tanner et
853 al., 2006, 2007).

854 Therefore, we calculated beta-diversity indices to analyze the differences between the study partici-
855 pants. The distances for the multiple stages of periodontitis, including stage I, stage II, and stage III, as
856 well as healthy controls (Figure 4g-j and Table 7), suggesting notable differences among the multiple
857 periodontitis severities. In other words, the composition of the salivary microbiome compositions varies
858 depending on the periodontitis stages, so that supporting the findings from a previous study (Iniesta et al.,
859 2023). Taken together that it is nearly impossible to fully restore the attachment level after it has been lost
860 due to the progression and development of periodontitis, the ability to rapidly screen for periodontitis in
861 its early phases using saliva collections would be highly beneficial for effective disease management and
862 treatment.

863 Of the total of 425 taxa in the salivary microbiome composition that have been identified (Figure 13),
864 ANCOM was applied to select 20 taxa as the DAT that indicated notable abundance variation among
865 the periodontitis severities (Figure 8 and Table 5). Three sub-groups were formed from the DAT using
866 hierarchical clustering (Figure 8a). Surprisingly, two of the red complex pathogens (Rôças, Siqueira Jr,
867 Santos, Coelho, & de Janeiro, 2001), *Porphyromonas gingivalis* and *Tannerella forsythia*, were classified
868 in Group 2 and were more prevalent in stage II and stage III periodontitis compared to healthy controls.
869 *Campylobacter showae* was additionally placed in Group 2 of the orange complex pathogens (Gambin et
870 al., 2021). Furthermore, some of the DAT in Group 2 have reported their crucial roles in pathogenesis
871 and development of periodontitis: *Filifactor alocis* (Aruni et al., 2015), *Treponema putidum* (Wyss et
872 al., 2004), *Tannerella forsythia* (Stafford, Roy, Honma, & Sharma, 2012; W. Zhu & Lee, 2016), and
873 *Prevotella intermedia* (Karched, Bhardwaj, Qudeimat, Al-Khabbaz, & Ellepolo, 2022). Taken together,
874 this indicates that DAT in Group 2 is essential to periodontitis. The portion of some Group 1 DAT,
875 including *Peptostreptococcaceae[XI][G-5] saphenum*, *Peptostreptococcaceae[XI][G-6] nodatum*, and
876 *Peptostreptococcaceae[XI][G-9] brachy*, in healthy controls and patients with periodontitis significantly
877 differed, according to earlier research (Lafaurie et al., 2022). These outcomes support our research,
878 implying that Group 1 DAT are also essential to the etiology and progression of periodontitis. However,
879 in contrast to patients with periodontitis, Group 3 DAT, namely *Corynebacterium durum* and *Actinomyces*
880 *graevenitzii*, were enriched in healthy controls, which is consistent with earlier research (Redanz et al.,
881 2021; Nibali et al., 2020).

882 In our correlation analysis (Figure 9), we have discovered strongly negative correlations (coefficient \leq
883 -0.5) between DAT of Group 3 and these of Group 1 and Group 2; we have also identified nine DAT

pairs with strong correlations (coefficient $\leq -0.5 \vee$ coefficient ≥ 0.5) (Figure 14). Interestingly, there were strongly negative correlations (coefficient ≤ -0.5) between Group 2 DAT and *Actinomyces* spp., taxa which belong to Group 3: *Filifactor alocis* (Figure 14a), *Porphyromonas gingivalis* (Figure 14b), and *Treponema putidum* (Figure 14c). Taken together that pathogens, including *Filifactor alocis* (Aja, Mangar, Fletcher, & Mishra, 2021; Hiranmayi, Sirisha, Rao, & Sudhakar, 2017), *Porphyromonas gingivalis* (Rôças et al., 2001), and *Treponema putidum* (Wyss et al., 2004), become dominant taxa in patients with stage III periodontitis. On the other hand, commensal salivary bacteria, such as *Actinomyces* spp., gradually declined. Additionally, several DAT from Group 1 and Group 2 exhibited strong positive correlations (coefficient ≥ 0.5) (Figure 14d-i). It has been established that all of these DAT from Group 1 and Group 2 are periodontal pathogens: *Filifactor alocis* (Aja et al., 2021; Hiranmayi et al., 2017), *Fretibacterium* spp. (Teles, Wang, Hajishengallis, Hasturk, & Marchesan, 2021), *Lachnospiraceae[G-8] bacterium HMT 500* (Lafaurie et al., 2022), *Peptostreptococcaceae[XI][G-6] nodatum* (Lafaurie et al., 2022; Haffajee, Teles, & Socransky, 2006), *Peptostreptococcaceae[XI][G-9] brachy* (Lafaurie et al., 2022), and *Treponema putidum* (Wyss et al., 2004). Thus, these fundamental roles of identified periodontal pathogens in the pathophysiology and progression of periodontitis are further supported by these strong positive correlations (coefficient ≥ 0.5), suggesting that advanced periodontitis, i.e., stage III, might arise from the additional DAT from Group 1 and Group 2.

Moreover, to predict periodontitis statuses from salivary microbiome composition, we have constructed machine-learning classification models based on random forest for four classification settings:

1. healthy vs. stage I vs. stage II vs. stage III
2. healthy vs. stage I
3. healthy vs. stage I vs. stages II/III
4. healthy vs. stages I/II/III

Porphyromonas gingivalis and *Actinomyces* spp. were the two most important taxa (feature) in all classification settings (Table 6). This finding aligns with a recent study that identifies *Actinomyces* spp. as the most prevalent bacteria in both the healthy gingivitis controls, while *Porphyromonas gingivalis* is recognized as the most predominant taxon within the periodontitis subjects, based on analyses of subgingival plaque samples (Nemoto et al., 2021). We have previously developed machine learning models for the classification of periodontitis, with the objective of predicting the severities of chronic periodontitis by analyzing the copy numbers of nine known salivary bacteria species. We classified healthy controls and patients with periodontitis utilizing bacterial combinations in conjunction with a random forest model (E.-H. Kim et al., 2020):

- AUC: 94%
- BA: 84%
- SEN: 95%
- SPE: 72%

Another study established a machine-learning model for the classification of periodontitis, employing 266 species derived from the buccal microbiome (Na et al., 2020):

- AUC: 92%

- 923 • BA: 84%
- 924 • SEN: 94%
- 925 • SPE: 74%

926 By separating patients with periodontitis from healthy controls using only four DAT, *e.g.* *Actinomyces*
927 *graevenitzii*, *Actinomyces* spp., *Corynebacterium durum*, and *Porphyromonas gingivalis*, our machine
928 learning model performed better than previously published models (Figure 10, Table 4, and Table 6):

- 929 • AUC: $95.3\% \pm 4.9\%$
- 930 • BA: $88.5\% \pm 6.6\%$
- 931 • SEN: $86.4\% \pm 15.7\%$
- 932 • SPE: $90.5\% \pm 7.0\%$

933 This result showed that by detecting Group 3 bacteria that were substantially abundant in health
934 controls than patients with periodontitis, our study increased BA by at least 5% and SPE by at least 17%.

935 Furthermore, we have validated our machine-learning prediction model using openly accessible 16S
936 rRNA gene sequencing data from Portuguese (Iniesta et al., 2023) and Spanish participants (Relvas et
937 al., 2021) in order to ensure the consistency of our random forest classification model (Figure 11). Our
938 classification models employed in this study were primarily developed and assessed on Korean study par-
939 ticipants, which may limit their generalizability to other ethnic groups with different salivary microbiome
940 compositions (Premaraj et al., 2020; Renson et al., 2019). Therefore, the evaluations of this periodonti-
941 tis classification models can be affected by ethnic-specific variances and differences, highlighting the
942 necessity for additional validation and adjustment across a spectrum of ethnic backgrounds.

943 Regarding the clinical characteristics and potential confounders influencing the analysis of salivary
944 microbiome compositions connected with periodontitis severity, this study had a number of limitations
945 that were pointed out. We did not offer clinical information, such as the percentage of teeth, the percentage
946 of bleeding on probing, nor dental furcation involvement, even though we did gather information on
947 attachment level, probing depth, plaque index, and gingival index (Renvert & Persson, 2002); this might
948 have it challenging to present thorough and in-depth data about periodontal health. Moreover, the broad age
949 range may make it tougher to evaluate the relationship between age and periodontitis statuses, providing
950 the necessity for future studies to consider into account more comprehensive clinical characteristics
951 associated with periodontitis. Additionally, potential confounders—*e.g.* body mass index (Bombin, Yan,
952 Bombin, Mosley, & Ferguson, 2022) and e-cigarette use (Suzuki, Nakano, Yoneda, Hirofumi, & Hanioka,
953 2022)—which might have affected dental health and salivary microbiome composition were disregarding
954 consideration in addition to smoking status and systemic diseases. Thus, future research incorporating
955 these components would offer a more thorough knowledge of how lifestyle factors interact and affect the
956 salivary microbiome composition and periodontal health. Throughout, resolving these limitations will
957 advance our understanding in pathogenesis and development of periodontitis, offering significant novel
958 insights on the causal connection between systemic diseases and the salivary microbiome compositions.

959 **4 Metagenomic signature analysis of Korean colorectal cancer**

960 **4.1 Introduction**

961 Colorectal cancer (CRC) is one of the most prevalent and life-threatening malignancies worldwide
962 (Kuipers et al., 2015; Center, Jemal, Smith, & Ward, 2009; N. Li et al., 2021), with its incidence
963 influenced by a combination of genetic (Zhuang et al., 2021; Peltomaki, 2003), environmental (O'Sullivan
964 et al., 2022; Raut et al., 2021), and lifestyle factors (X. Chen et al., 2021; Bai et al., 2022; Zhou et
965 al., 2022; X. Chen, Li, Guo, Hoffmeister, & Brenner, 2022). Established risk factors include a often
966 diet in red and processed meats (Kennedy, Alexander, Taillie, & Jaacks, 2024; Abu-Ghazaleh, Chua,
967 & Gopalan, 2021), obesity (Mandic, Safizadeh, Niedermaier, Hoffmeister, & Brenner, 2023; Bardou
968 et al., 2022), cigarette smoking (X. Chen et al., 2021; Bai et al., 2022), alcohol consumption (Zhou et
969 al., 2022; X. Chen et al., 2022), and a sedentary lifestyle (An & Park, 2022), all of which contribute to
970 chronic inflammation, mutagenesis, and metabolic regulation. Additionally, underlying conditions, e.g.
971 Lynch syndrome (Vasen, Mecklin, Khan, & Lynch, 1991; Hampel et al., 2008) and familial adenomatous
972 polyposis (Inra et al., 2015; Burt et al., 2004), significantly increase risk of CRC due to persistent mucosal
973 inflammation and somatic mutations that promote tumorigenesis.

974 The gut microbiome plays a fundamental role in maintaining host health by helping digestion
975 (Joscelyn & Kasper, 2014; Cerqueira, Photenhauer, Pollet, Brown, & Koropatkin, 2020), regulating
976 metabolism (Dabke, Hendrick, Devkota, et al., 2019; Utzschneider, Kratz, Damman, & Hullarg, 2016;
977 Magnúsdóttir & Thiele, 2018), adjusting immune function (Kau, Ahern, Griffin, Goodman, & Gordon,
978 2011; Shi, Li, Duan, & Niu, 2017; Broom & Kogut, 2018), and even coordinating neurological processes
979 by the brain-gut axis (Martin et al., 2018; Aziz & Thompson, 1998; R. Li et al., 2024). Comprising
980 these gut microbiota, including, archaea, bacteria, fungi, and viruses, the gut microbiome contributes
981 to the synthesis of essential vitamins, and production of fatty acids, which influence intestinal integrity
982 and immune responses. Thus, well-balanced gut microbiome composition modulates systemic immune
983 function by interacting with gut-associated lymphoid tissue, shaping immune tolerance and response
984 to infections. Hence, emerging evidence suggests that dysbiosis in the gut microbiome composition are
985 associated not only a narrow range of diseases, e.g. diarrhea and enteritis (Paganini & Zimmermann,
986 2017; Gao, Yin, Xu, Li, & Yin, 2019) but also a wide range of diseases, e.g. obesity, diabetes, and cancers
987 (Barlow et al., 2015; Hartstra et al., 2015; Helmink et al., 2019; Cullin et al., 2021).

988 Recent studies have highlighted the crucial role of the gut microbiome in tumorigenesis and progres-
989 sion of CRC (Song, Chan, & Sun, 2020; Rebersek, 2021), with dysbiosis emerging as a potential risk
990 factor. Dysbiosis in gut microbiome compositions can promote tumorigenesis of many cancers, including
991 CRC, through several signaling cascades, including inflammation, mutagenesis, and altered metabolism
992 in host. Certain bacteria species, such as *Fusobacterium* genus (Hashemi Goradel et al., 2019; Bullman et
993 al., 2017; Flanagan et al., 2014), *Bacteroides* genus (Ulger Toprak et al., 2006; Boleij et al., 2015), and
994 *Escherichia coli* (Swidsinski et al., 1998; Bonnet et al., 2014), have been associated with development
995 and progression of CRC by producing pro-inflammatory signals, generating toxins including mutagens,

996 and disrupting the intestinal barriers including mucous surface. In contrast, beneficial bacteria, such as
997 *Lactobacillus* genus (Ghorbani et al., 2022; Ghanavati et al., 2020) and *Bifidobacterium* genus (Le Leu,
998 Hu, Brown, Woodman, & Young, 2010; Fahmy et al., 2019), are regarded to apply protective roles by
999 maintaining homeostasis of gut microbiome compositions and regulating immune responses including
1000 inflammation.

1001 Furthermore, identifying metagenome biomarkers in Korean CRC patients is essential, as the gut
1002 microbiome compositions significantly vary by ethnicity due to genetic, dietary, and environmental
1003 factor (Fortenberry, 2013; Merrill & Mangano, 2023; Parizadeh & Arrieta, 2023). Additionally, ethnicity-
1004 specific microbiome composition signatures may affect the reliability of previously established biomarkers
1005 derived from predominantly Western CRC cohorts (Network et al., 2012), necessitating population-
1006 specific investigations. By identifying metagenomic biomarkers tailored to Korean CRC patients, we
1007 can improve early detection rate of early-stage CRC, develop more accurate risk of CRC, and explore
1008 microbiome-targeted therapies that consider host-microbiome interactions within the Korean population.

1009 Accordingly, this study aims to identify microbiome-based biomarkers specific to CRC within
1010 the Korean population, addressing the critical demand for ethnicity-specific microbiome research. By
1011 leveraging metagenomic sequencing and advanced computational biology analysis, this study seeks to
1012 uncover novel microbial signatures associated with Korean CRC patients. As part of the larger "Multi-
1013 genomic analysis for biomarker development in colon cancer" project (NTIS No. 1711055951), this study
1014 investigates microbial signatures within next-generation sequencing data to enhance precision medicine
1015 approaches for CRC and to develop robust microbiome-based biomarkers for early detection, prognosis,
1016 and therapeutic stratification, complementing genomic and epigenomic markers. Hence, this research
1017 represents a crucial step toward personalized cancer diagnostic and therapeutic strategies tailored to the
1018 Korean population.

1019 **4.2 Materials and methods**

1020 **4.2.1 Study participants enrollment**

1021 To achieve metagenomic observations of CRC, a total of 211 Korean CRC patients were enrolled (Table
1022 8). The tissue samples were collected from both the tumor lesion and its corresponding adjacent normal
1023 lesion to enable comparative metagenomic analyses. Tumor tissue samples were obtained from confirmed
1024 CRC lesions, ensuring adequate representation of CRC-associated microbial alterations. Adjacent normal
1025 tissues were collected from non-cancerous regions away from the tumor margin to serve as a control
1026 for baseline molecular and microbial composition. Moreover, clinical information was collected for all
1027 study participants included in this study to investigate potential associations between gut microbiome
1028 compositions and clinical outcomes. Key clinical characteristics recorded included overall survival (OS)
1029 and recurrence. These clinical parameters were integrated with metagenomic data to explore potential
1030 microbiome-based biomarkers for CRC prognosis and progression. Ethical approval was obtained for
1031 clinical data collection, and all patient information was anonymized to ensure confidentiality in accordance
1032 with institutional guidelines.

1033 **4.2.2 DNA extraction procedure**

1034 Tissue samples were immediately processed under sterile conditions to prevent contamination and
1035 preserved in low temperature (-80°C) storage for downstream DNA extraction and whole-genome
1036 sequencing. Furthermore, produced sequencing data were provided by the "Multi-genomic analysis
1037 for biomarker development in colon cancer" project (NTIS No. 1711055951) in mapped BAM format,
1038 aligned to the hg38 human reference genome. The preprocessing pipeline utilized by the main project
1039 included high-throughput whole-genome sequencing using standardized alignment algorithm, BWA
1040 (H. Li & Durbin, 2009). In addition to the mapped human sequences, our whole-genome sequencing
1041 data retained unmapped sequences, which contain potential microbial reads that were not aligned to the
1042 human reference genome.

1043 **4.2.3 Bioinformatics analysis**

1044 To identify microbial signatures associated with CRC, we employed PathSeq (version 4.1.8.1) (Kostic
1045 et al., 2011; Walker et al., 2018), a computational pipeline designed for metagenomic analysis of high-
1046 throughput sequencing data including the whole-genome sequences. After processing these sequencing
1047 data through the PathSeq pipeline, a comprehensive bioinformatics analyses were conducted to characterize
1048 microbial signatures associated with CRC.

1049 Prevalent taxa identification was performed by determining microbial taxa present in the majority of
1050 the study participants, filtering out low-abundance and rare taxa to ensure robust downstream analyses.

1051 To assess microbial community structure, diversity indices were calculated, including alpha-diversity
1052 to evaluate single-sample diversity and beta-diversity to compare microbial composition between the
1053 tumor tissues and their corresponding adjacent normal tissues. Following alpha-diversity indices were

1054 calculated using the scikit-bio Python package (version 0.6.3) (Rideout et al., 2018), and these alpha-
1055 diversity indices were compared using the MWU test:

- 1056 1. Berger-Parker d (Berger & Parker, 1970)
- 1057 2. Chao1 (Chao, 1984)
- 1058 3. Dominance
- 1059 4. Doubles
- 1060 5. Fisher (Fisher et al., 1943)
- 1061 6. Good's coverage (Good, 1953)
- 1062 7. Margalef (Magurran, 2021)
- 1063 8. McIntosh e (Heip, 1974)
- 1064 9. Observed ASVs (DeSantis et al., 2006)
- 1065 10. Simpson d
- 1066 11. Singles
- 1067 12. Strong (Strong, 2002)

1068 Furthermore, these beta-diversity indices were measured and compared using the PERMANOVA
1069 test (Anderson, 2014; Kelly et al., 2015). To demonstrate multi-dimensional data from the beta-diversity
1070 indices, we utilized the t-SNE algorithm (Van der Maaten & Hinton, 2008).

- 1071 1. Bray-Curtis (Sorensen, 1948)
- 1072 2. Canberra
- 1073 3. Cosine (Ochiai, 1957)
- 1074 4. Hamming (Hamming, 1950)
- 1075 5. Jaccard (Jaccard, 1908)
- 1076 6. Sokal-Sneath (Sokal & Sneath, 1963)

1077 Differentially abundant taxa (DAT) were identified using statistical method, ANCOM (Lin & Peddada,
1078 2020), adjusting for sequencing depth and potential confounders to highlight taxa significantly associated
1079 with categorical clinical information in CRC, such as recurrence. Furthermore, to point attention to
1080 taxa that are substantially linked to continuous clinical measurement in CRC, including OS, DAT were
1081 found using the Spearman correlation and slope from linear regression (Equation 9). Note that both the
1082 Spearman correlation and the slope from linear regression were utilized to provide a more comprehensive
1083 assessment of the relationship between DAT proportions and OS. While the correlation coefficient
1084 measures the strength and direction of a linear relationship between these variables, it does not convey
1085 information about the magnitude of change in independent variable relative to dependent variable. The
1086 slope of the linear regression model, on the other hand, quantifies this change by indicating how much
1087 the dependent variable is expected to increase or decrease per unit change in the independent variable. By
1088 incorporating both the correlation coefficient and the slope from the linear regression, we ensured that
1089 the analysis captured not only whether two variables were associated but also the extent to which one
1090 variable influenced the other. This dual approach enhances the interpretability of results, particularly in
1091 biological and clinical studies where both statistical association and biological effect size are crucial for
1092 meaningful suggestions.

$$\text{slope} = \frac{\Delta \text{OS}}{\Delta \text{DAT proportion}} \quad (9)$$

1093 To assess the predictive potential of microbial signatures in CRC prognosis, we employed a random
1094 forest machine learning model using DAT proportions as input features. Random forest classification was
1095 utilized to predict CRC recurrence, where the classification model was trained to distinguish between
1096 CRC patients with or without recurrence based on the gut microbiome compositions. Additionally,
1097 random forest regression was applied to predict OS by estimating survival time as a continuous clinical
1098 outcome based on microbiome features. This approach allowed for the identification of microbial taxa
1099 that contribute significantly to CRC prognosis, offering insights into potential gut microbiome-based
1100 biomarkers for cancer progression. By integrating these random forest machine learning models, we
1101 aimed to improve CRC risk stratification and precision medicine strategies.

1102 This multi-layered bioinformatics approach enabled a comprehensive investigation of gut microbiome
1103 alteration in CRC, facilitating the identification of potential microbial biomarkers for diagnosis and
1104 prognosis of CRC.

1105 **4.2.4 Data and code availability**

1106 All sequences from the 211 study participants have been published to the Korea Bioinformation Center
1107 (data ID KGD10008857): <https://kbds.re.kr/KGD10008857>. Docker image that employed through-
1108 out this study is available in the DockerHub: <https://hub.docker.com/repository/docker/fumire/unist-crc-copm/general>. Every code used in this study can be found on GitHub: <https://github.com/CompbioLabUnist/CoPM-ColonCancer>.

1111 **4.3 Results**

1112 **4.3.1 Summary of clinical characteristics**

1113 Microsatellite instability (MSI) is one of the key molecular features and risk factors in CRC, resulting
1114 from defects in the DNA mismatch repair system (Boland & Goel, 2010). MSI leads to the accumulation
1115 of mutations in short repetitive DNA sequences (microsatellites), contributing to genomic instability and
1116 tumor development (Søreide, Janssen, Söiland, Körner, & Baak, 2006; Vilar & Gruber, 2010). Therefore,
1117 we compared clinical measurements with MSI status, including microsatellite stable (MSS), MSI-low
1118 (MSI-L), and MSI-high (MSI-H). There were no significant differences in the clinical measurements, *e.g.*
1119 recurrence, sex, OS, and age in diagnosis, in the total of 211 study participants (Table 8).

1120 **4.3.2 Gut microbiome compositions**

1121 In the total of 211 CRC study participants, these ten kingdoms were found in the gut microbiome
1122 composition:

- 1123 1. Archaea kingdom: 31 genera
- 1124 2. Bacteria kingdom: 1508 genera
- 1125 3. Bamfordvirae kingdom: 1 genus
- 1126 4. Eukaryota kingdom: 77 genera
- 1127 5. Fungi kingdom: 137 genera
- 1128 6. Loebvirae kingdom: 2 genera
- 1129 7. Orthornavirae kingdom: 1 genus
- 1130 8. Parnavirae kingdom: 3 genera
- 1131 9. Shotokuvirae kingdom: 6 genera
- 1132 10. Viruses kingdom: 76 genera

1133 Among these kingdoms, the proportions of four major kingdoms, which have at least 50 genera, in
1134 the gut microbiome composition were displayed (Figure 21): Bacteria kingdom, Eukaryota kingdom,
1135 Fungi kingdom, and Viruses kingdom. In the Bacteria kingdom (Figure 21a), *Bacteroides* genus is the
1136 most prevalent genus in the tumor tissue samples, followed by *Fusobacterium* and *Cutibacterium* genera.
1137 *Toxoplasma* and *Malassezia* genera were the dominant genus, which have over 90% of proportions, in
1138 the Eukaryota kingdom (Figure 21b) and the Fungi kingdom (Figure 21c), respectively. On the other
1139 hand, *Roseolovirus* genus is the most popular genus of the Viruses kingdom in the normal tissue samples
1140 (Figure 21d); contrarily, *Lymphocryptovirus* and *Cytomegalovirus* genera had been dominant genera in
1141 the tumor tissue samples. Taken together, these results suggest that the Anna Karenina principle (Ma,
1142 2020; W. Li & Yang, 2025), *i.e.* in human microbiome-associated diseases, every disease-associated
1143 microbiome, including dysbiosis, is unique and patient-specific, whereas all healthy microbiomes are
1144 similar, also applies to CRC.

1145 **4.3.3 Diversity indices**

1146 In alpha-diversity analysis, which measures within-sample microbial community, revealed a significant
1147 increase in tumor tissue samples compared to adjacent normal tissue samples (Figure 22). Alpha-diversity
1148 indices, including Chao1, Fisher α , and observed features, were consistently higher in CRC tumor tissues
1149 (MWU test $p < 0.05$), indicating a more heterogeneous microbial community, *e.g.* the Anna Karenina
1150 principle, potentially influenced by tumor-associated dysbiosis.

1151 To assess the microbial impact on CRC recurrence, alpha-diversity indices compared between normal
1152 and tumor tissue samples in accordance with recurrence information (Figure 23). In the recurrence
1153 patients, most alpha-diversity indices (11 out of 12), except McIntosh index, exhibited increasing in
1154 tumor tissue samples than normal tissue samples (MWU test $p < 0.05$; Figure 23); In the non-recurrence
1155 patients, on the other hand, some alpha-diversity indices (8 out of 12) amplified in tumor tissue samples
1156 than normal tissue samples (MWU test $p < 0.05$; Figure 23). What is interesting about the alpha-diversity
1157 analysis in this figure is that a few indices, namely Fisher α (Figure 28e) and Margalef (Figure 23g),
1158 presented augmentation in normal tissue sample of the recurrence patients than that of the non-recurrence
1159 patients (MWU test $p < 0.05$). Overall, these alpha-diversity results demonstrate that tumor tissue samples
1160 have more diverse microbiome composition than normal tissue samples. Furthermore, although only
1161 two indices significantly increased, the recurrence patients have diversified microbiome compositions
1162 than the non-recurrence patients in normal sample tissue, not in tumor sample tissues, indicating field
1163 cancerization by the gut microbiome leads to unfavorable prognosis such as recurrence (Curtius et al.,
1164 2018; Rubio et al., 2022).

1165 To determine the microbial impact on OS of CRC patients, the Spearman correlation compared
1166 between alpha-diversity indices and OS duration (Figure 24). No significant Spearman correlation was
1167 found between every alpha-diversity indices and OS (Spearman correlation $p \geq 0.1$; Figure 24). However,
1168 a few alpha-diversity indices, *e.g.* Chao1 (Figure 24b), Good's coverage (Figure 24f), and observed
1169 features (Figure 24i), showed negative correlations with OS (Spearman correlation $p < 0.05$). Together
1170 these correlation results provide important insights into heterogeneous microbiome leads to shorter OS,
1171 suggesting the Anna Karenina principle and the field cancerization.

1172 In beta-diversity analysis, which calculates inter-sample microbial community, explain significant
1173 disparity between tumor tissue samples and normal tissue samples (Figure 25). Every six beta-diversity
1174 indices presented discrepancy between normal tissue samples and tumor tissue samples (PERMANOVA
1175 test $p < 0.001$), implying that tumor tissue samples have distinct microbiome compositions from normal
1176 tissue samples.

1177 Beta-diversity indices were evaluated between normal and tumor tissue samples along with recurrence
1178 history in order to evaluate the microbial influence on CRC recurrence (Figure 26). All six beta-diversity
1179 indices examined significant difference in microbial community structure between the recurrence patients
1180 and the non-recurrence patients (PERMANOVA test $p < 0.001$; Figure 26), indicating that tumor-
1181 associated gut microbiome composition varies resulting on recurrence status. tSNE-transformed plots
1182 further illustrated clear clustering patterns (Figure 26), suggesting again that the recurrence patients

1183 harbor dissimilar microbial communities compared to the non-recurrence patients. These observed
1184 differences in beta-diversity represent that microbial shifts, including dysbiosis, may be associated with
1185 CRC progression and recurrence risk, possibly due to specific taxa contributing to a tumor-promoting
1186 microenvironment.

1187 Moreover, beta-diversity analysis suggested a potential associated with OS duration in CRC patients.
1188 In all six beta-diversity indices, tSNE-transformed plots showed clear clustering patterns along OS
1189 duration (Figure 27), implying that possible microbiome composition shifts related to survival outcomes
1190 in CRC. However, since OS is a continuous variable, statistical significance testing could not be directly
1191 performed for these clustering patterns. Despite this limitation, the observed microbial community
1192 variations suggest that alterations in the gut microbiome composition may be associated to CRC prognosis
1193 and survival duration.

1194 Together, diversity indices analyses revealed significant microbial community alterations between
1195 normal and tumor tissue samples, as well as between the recurrence and non-recurrence CRC patients.
1196 Alpha-diversity indices significantly increased in tumor tissue samples than normal tissue samples (MWU
1197 test $p < 0.05$; Figure 22). This increase was more pronounced in the recurrence patients (11 of 12
1198 indices) compared to non-recurrence patients (8 of 12 indices) (Figure 23), indicating a potential link
1199 between microbial diversity and CRC recurrence. Additionally, negative correlation between OS and
1200 alpha-diversity indices were observed in normal samples (Spearman correlation $p < 0.05$; Figure 24),
1201 suggesting that lower microbial diversity may be associated with longer survival in CRC. On the other
1202 hand, beta-diversity indices analysis, showed significant separation between tumor and tumor tissue
1203 samples across all six beta-diversity indices (PERMANOVA test $p < 0.001$; Figure 25). Furthermore,
1204 the recurrence and non-recurrence patients displayed significantly discrete microbial compositions
1205 (PERMONOVA test $p < 0.001$; Figure 26), implying that microbial community shifts may reflect CRC
1206 progression and recurrence risk. These findings highlight the importance of microbiome diversity and
1207 gut microbiome composition in CRC prognosis and warrant further investigation into their potential as
1208 predictive biomarkers.

1209 4.3.4 DAT selection

1210 The selection of differentially abundant taxa (DAT) aimed to identify microbial taxa that exhibit significant
1211 differences in relative abundance between clinical information, such as recurrence history or OS in CRC
1212 patients. Identifying and selection these microbial discrepancies is crucial for understanding the role of
1213 the gut microbiome composition in CRC progression, prognosis, and potential therapeutic interventions.

1214 We identified 19 DAT associated with recurrence history across the total samples by ANCOM (Figure
1215 28a), including 18 non-recurrence-enriched DAT and a recurrence-related DAT. When stratified by sample
1216 type, one DAT was enriched in normal samples of the non-recurrence patients (Figure 28b), whereas six
1217 DAT exhibited significant differential abundance in tumor samples (Figure 28c). These findings suggest
1218 that microbial composition variations in the tumor microenvironment are more pronounced in relation to
1219 recurrence status (Table 9), potentially indicating a microbial signature linked to CRC progression. These

1220 identified DAT may contribute to tumor-associated dysbiosis, influencing the likelihood of CRC recurrence
1221 through mechanisms such as inflammation, metabolic modulation, or immune system interaction.

1222 The non-recurrence-enriched DAT have decreased proportions both in normal and tumor samples of
1223 the recurrence patients than those in the non-recurrence patients (MWU test $p < 0.001$; Figure 28d-h).
1224 What is interesting about these non-recurrence-enriched DAT is that they belong to the *Micrococcus* genus.
1225 Among them, *Micrococcus aloeverae* was consistently identified in all three settings—total (Figure 28a),
1226 normal (Figure 28b), and tumor samples (Figure 28c)—indicating its stable presence regardless of tissue
1227 type. Variation in relative proportions of *Micrococcus aloeverae* (Figure 28d) suggests potential ecological
1228 adaptability within tumor microenvironment of CRC. The remaining *Micrococcus*-related DAT showed
1229 less variation between the recurrence and non-recurrence patients, reinforcing their limited associations
1230 with CRC recurrence. Moreover, only one taxon, *Pseudomonas* sp. *NBRC 111133*, was identified as
1231 recurrence-enriched DAT (Figure 28a). This suggests a potential association between *Pseudomonas* sp.
1232 *NBRC 111133* and CRC recurrence, indicating that its presence may contribute to a tumor-supportive
1233 microbial environment. *Pseudomonas* sp. *NBRC 111133* had higher relative proportions both in normal
1234 and tumor tissue samples of the recurrence patients than those of the non-recurrence patients (Figure
1235 28i). Likewise, *Pseudomonas* sp. *NBRC 111133* were prevalent in tumor tissue samples than normal
1236 tissue samples of the non-recurrence patients (MWU test $p < 0.01$; Figure 28i); however, no significant
1237 difference between normal and tumor tissue samples of the recurrence patients.

1238 These findings imply that while certain species belong to *Micrococcus* genus may be prevalent in CRC
1239 tissues, their roles in cancer progression and recurrence risk remain uncertain. Species of *Pseudomonas*
1240 genus are known for their metabolic involvement in biofilm formation, antibiotic resistance, and immune
1241 modulation, which could play a role in CRC progression.

1242 Furthermore, correlation analysis between DAT abundance and OS duration identified a total of 16
1243 over-represented DAT in the total samples (Figure 29a). When analyzed separately, 11 DAT, which consist
1244 of four under-represented and seven over-represented DAT showed significant correlations with OS in
1245 normal samples (Figure 29b), while four under-represented and 45 over-represented DAT were identified
1246 in tumor samples (Figure 29c), indicating that microbial composition shifts in tumor tissues may have a
1247 stronger association with survival outcomes. The higher number of survival-associated DAT in tumor
1248 tissue suggests that the tumor microbiome plays a more dynamic role in progression and prognosis
1249 of CRC. These findings highlight the potential of gut microbial composition as a prognostic indicator
1250 in CRC, warranting further investigation into the functional roles of these DAT in influencing clinical
1251 outcomes.

1252 Among a total of 57 OS-correlated DAT (Table 10) with Spearman correlation and the slope (Equation
1253 9). *Agaricus bisporus* (Figure 29d) and *Corynebacterium* sp. *KPLI824* (Figure 29h) are identified as
1254 over-represented DAT both in normal samples and tumor samples (Spearman correlation $p < 0.05$),
1255 whereas *Corynebacterium lowii* (Figure 29g) and *Paracoccus sphaerophysae* (Figure 29i) are selected
1256 as under-represented DAT both in normal samples and tumor samples (Spearman correlation $p < 0.05$).
1257 On the other hand, *Clostridiales bacterium* (Figure 29e) is classified as under-represented DAT only in
1258 normal samples (Spearman correlation $p < 0.01$), while *Corynebacterium kroppenstedtii* (Figure 29f) is

1259 described as over-represented DAT only in tumor samples (Spearman correlation $p < 0.001$).

1260 These findings highlight the potential influence of microbial dysbiosis on cancer progression and
1261 prognosis. The presence of these OS-correlated DAT in tumor and/or adjacent normal tissues suggests
1262 that microbial alterations may contribute to field cancerization, a phenomenon where histopathologically
1263 benign tissues surrounding the tumor undergo molecular, inflammatory, and microbial shifts, creating
1264 a microenvironment conducive to tumor development and progression. Therefore, these discoveries
1265 reinforce the importance of investigating the gut microbiome as a prognostic biomarker and suggest that
1266 targeting microbial dysbiosis could offer new therapeutic strategies for improving clinical outcomes of
1267 CRC.

1268 4.3.5 Random forest prediction

1269 We employed the random forest-based machine learning prediction to assess the predictive power of DAT
1270 from gut microbiome composition for CRC prognosis. To achieve this aim, we utilized random forest
1271 classification to predict recurrence status, training the model to differentiate between recurrence and
1272 non-recurrence patients based on microbial abundance patterns. Additionally, we applied random forest
1273 regression to predict OS, aiming to identify microbial taxa associated with survival duration. By leveraging
1274 random forest models, this study aimed to establish a microbiome-based predictive machine learning
1275 models for CRC recurrence risk assessment and survival prognosis, contributing to the development of
1276 prediction medicine strategies based on gut microbial signatures.

1277 To evaluate the predictive power of gut microbiome composition in CRC recurrence, we implemented
1278 a random forest classification model using two different input sets (Figure 30a-f): the entire gut mi-
1279 crobiome composition and DAT. Comparing these models allowed us to assess whether focusing on
1280 DAT-selected microbial features enhances classification performance. While the DAT-based classification
1281 models showed slightly improved classification metrics (MWU test $p \geq 0.05$), including ACC, AUC, and
1282 BA, over the entire microbiome-based model in the total sample (Figure 30a and Figure 29d), normal sam-
1283 ples (Figure 30b and Figure 30e), and tumor samples (Figure 30c and Figure 30f), overall classification
1284 metrics remained around 60%, suggesting moderated predictive capability. This relatively low metrics
1285 highlight the complexity of CRC recurrence, indicating that while dysbiosis may contribute to CRC
1286 progression, it is likely interwinded with host genetic factors such as germline and somatic mutations.
1287 Thus, the interplay between microbial shifts and tumor genomic alterations warrants further investigation,
1288 as integrating microbiome and genomic sequencing data may improve therapeutic strategies.

1289 To assess the predictive capability of the gut microbiome composition in OS of CRC patients, we
1290 implemented a random forest regression model, comparing two different input sets (Figure 30g-i): the
1291 entire gut microbiome composition and DAT. This comparison also aimed to determine whether focusing
1292 on key microbial features (DAT) enhances predictive accuracy. While DAT-based model showed a slight
1293 improvement over the entire microbiome-based model in normal samples (Figure 30h) and tumor samples
1294 (Figure 30i), the regression error remained high (about 700 days), indicating substantial variability in
1295 survival outcomes that cannot be fully explained by gut microbiome composition alone. This result

1296 suggest that while gut microbial dysbiosis may influence CRC progression, survival duration (OS) is
1297 likely also driven by host genetic factors, highlighting the requirement for multi-omics integration, where
1298 combining microbiome and genomic sequencing data may provide a more accurate and comprehensive
1299 predictive model for CRC patients survival.

Table 8: Clinical characteristics of CRC study participants.

Statistical significance were assessed using the χ -squared test for categorical values and the Kruskal-Wallis test for continuous values. OS: overall survival.

	Overall	MSS	MSI-L	MSI-H	p-value
n	211	181	7	18	
Recurrence, n (%)	False	132 (62.6%)	112 (61.9%)	4 (57.1%)	0.657
	True	79 (37.4%)	69 (38.1%)	3 (42.9%)	
Sex, n (%)	Male	137 (64.9%)	119 (65.7%)	6 (85.7%)	0.357
	Female	74 (35.1%)	62 (34.3%)	1 (14.3%)	
OS, mean±SD	1248.5±770.3	1268.1±769.5	1416.6±496.3	1097.7±903.2	0.580
Age, mean±SD	61.2±13.1	61.7±12.4	60.1±15.6	60.2±19.4	0.867

Table 9: DAT list for CRC recurrence.

Significance threshold is $|\log_2 \text{FC}| > 1.0| \wedge W > 9600$. Non-significant values remain blank. DAT are sorted in alphabetical order. FC: fold change

Taxonomy name	Entire-log ₂ FC	Entire-W	Normal-log ₂ FC	Normal-W	Tumor-log ₂ FC	Tumor-W
<i>Cutibacterium acnes</i>	-1.878	10570				
<i>Cutibacterium avidum</i>	-1.383	10266				
<i>Cutibacterium granulosum</i>	-1.476	10271				
<i>Micrococcus aloeverae</i>	-2.280	10740	-1.821	10462	-2.481	10591
<i>Micrococcus luteus</i>	-2.216	10744				
<i>Micrococcus</i> sp. <i>CH3</i>	-2.323	10740			-2.493	10527
<i>Micrococcus</i> sp. <i>CH7</i>	-2.321	10740			-2.493	10542
<i>Micrococcus</i> sp. <i>HMSC31B01</i>	-2.282	10739			-2.458	10519
<i>Micrococcus</i> sp. <i>MS-ASIII-49</i>	-2.284	10740			-2.470	10527
<i>Pseudomonas</i> sp. <i>NBRC 111133</i>	1.139	9732				
<i>Pseudonocardia</i> sp. <i>P2</i>	-2.200	10736			-2.394	10253
<i>Staphylococcus</i> sp. <i>HMSC034A07</i>	-1.341	10050				
<i>Staphylococcus</i> sp. <i>HMSC063F03</i>	-1.322	10001				
<i>Staphylococcus</i> sp. <i>HMSC064E11</i>	-1.064	10163				
<i>Staphylococcus</i> sp. <i>HMSC067B04</i>	-1.343	9952				
<i>Staphylococcus</i> sp. <i>HMSC068G12</i>	-1.344	10173				
<i>Staphylococcus</i> sp. <i>HMSC072H01</i>	-1.298	10197				
<i>Staphylococcus</i> sp. <i>HMSC077C03</i>	-1.331	10115				
<i>Treponema endosymbiont of Eucomonympha</i> sp.	-1.629	10472				

Table 10: DAT list for CRC OS.

Significance threshold is $\log_{10}|\text{slope}| > 2.0 \wedge |r| > 0.2$. Non-significant values remain blank. DAT are sorted in alphabetical order.

Taxonomy name	Entire-slope	Entire-r	Normal-slope	Normal-r	Tumor-slope	Tumor-r
<i>Acinetobacter venetianus</i>					3.087	0.203
<i>Actinotalea ferrariae</i>					2.574	0.200
<i>Agaricus bisporus</i>	2.329	0.287	2.925	0.276	2.258	0.306
<i>Bifidobacterium boum</i>					2.096	-0.216
<i>Brevundimonas</i> sp. <i>DS20</i>			2.180	0.279		
<i>Clostridiales bacterium</i>			2.631	-0.203		
<i>Corynebacterium kroppenstedtii</i>	2.117	0.220			2.117	0.302
<i>Corynebacterium lipophiloflavum</i>			2.137	0.227		
<i>Corynebacterium lowii</i>			2.006	-0.216		
<i>Corynebacterium</i> sp. <i>KPL1818</i>	2.101	0.209	2.487	0.220	2.044	0.215
<i>Corynebacterium</i> sp. <i>KPL1824</i>	2.057	0.207	2.511	0.212	2.003	0.226
<i>Corynebacterium</i> sp. <i>KPL1986</i>					2.205	0.202
<i>Corynebacterium</i> sp. <i>KPL1996</i>					2.205	0.202
<i>Corynebacterium</i> sp. <i>KPL1998</i>					2.205	0.202
<i>Corynebacterium</i> sp. <i>KPL2004</i>					2.205	0.202
<i>Kocuria flava</i>			2.729	0.214		
<i>Kytococcus sedentarius</i>					2.267	0.206
<i>Lachnospiraceae bacterium AD3010</i>			2.609	-0.203		
<i>Lachnospiraceae bacterium NK4A136</i>					2.538	-0.220
<i>Methylorum extorquens</i>					2.068	0.295
<i>Microbacterium barkeri</i>			2.071	0.389		
<i>Paracoccus sphaerophysae</i>					2.012	-0.209
<i>Pontibacillus litoralis</i>					2.580	-0.209
<i>Porphyromonas macacae</i>			2.476	-0.200		
<i>Pseudomonas balearica</i>					2.117	0.203
<i>Pseudomonas monteilii</i>					2.183	0.228
<i>Rodentibacter myodis</i>					2.444	0.245
<i>Roseovarius tolerans</i>					2.295	0.221
<i>Staphylococcus epidermidis</i>					2.243	0.214
<i>Staphylococcus</i> sp. <i>HMSC034A07</i>					2.183	0.209
<i>Staphylococcus</i> sp. <i>HMSC034D07</i>	2.278	0.206			2.252	0.253
<i>Staphylococcus</i> sp. <i>HMSC034G11</i>	2.362	0.208			2.357	0.261
<i>Staphylococcus</i> sp. <i>HMSC036A09</i>					2.308	0.239
<i>Staphylococcus</i> sp. <i>HMSC055A10</i>					2.168	0.222
<i>Staphylococcus</i> sp. <i>HMSC055B03</i>	2.134	0.202			2.134	0.266
<i>Staphylococcus</i> sp. <i>HMSC058E12</i>					2.106	0.216
<i>Staphylococcus</i> sp. <i>HMSC061C10</i>					2.882	0.207
<i>Staphylococcus</i> sp. <i>HMSC062B11</i>	2.391	0.203			2.377	0.253
<i>Staphylococcus</i> sp. <i>HMSC062D04</i>	2.278	0.202			2.274	0.259
<i>Staphylococcus</i> sp. <i>HMSC063F03</i>	2.376	0.201			2.367	0.251
<i>Staphylococcus</i> sp. <i>HMSC063F05</i>	2.387	0.210			2.381	0.266
<i>Staphylococcus</i> sp. <i>HMSC064E11</i>					2.276	0.218
<i>Staphylococcus</i> sp. <i>HMSC065D11</i>					2.329	0.245

Table 10 continued from previous page

Taxonomy name	Entire-slope	Entire-r	Normal-slope	Normal-r	Tumor-slope	Tumor-r
<i>Staphylococcus</i> sp. <i>HMSC066G04</i>					2.181	0.218
<i>Staphylococcus</i> sp. <i>HMSC067B04</i>	2.332	0.205			2.329	0.260
<i>Staphylococcus</i> sp. <i>HMSC068G12</i>					2.294	0.226
<i>Staphylococcus</i> sp. <i>HMSC070A07</i>	2.360	0.216			2.362	0.287
<i>Staphylococcus</i> sp. <i>HMSC073C02</i>	2.352	0.205			2.334	0.246
<i>Staphylococcus</i> sp. <i>HMSC073E10</i>					2.366	0.255
<i>Staphylococcus</i> sp. <i>HMSC074D07</i>	2.330	0.218			2.308	0.270
<i>Staphylococcus</i> sp. <i>HMSC076H12</i>					2.200	0.219
<i>Staphylococcus</i> sp. <i>HMSC077C03</i>					2.258	0.207
<i>Staphylococcus</i> sp. <i>HMSC077D09</i>					2.245	0.230
<i>Staphylococcus</i> sp. <i>HMSC077G12</i>	2.335	0.200			2.345	0.276
<i>Staphylococcus</i> sp. <i>HMSC077H01</i>					2.214	0.241
<i>Streptomyces cinnamoneus</i>					2.787	0.208
<i>Thauera terpenica</i>					2.975	0.226

Table 11: Random forest classification and their evaluations.

	Dataset	ACC	AUC	BA	F1	PRE	SEN	SPE
Entire	Total	0.544±0.139	0.667±0.141	0.561±0.141	0.544±0.139	0.559±0.152	0.562±0.192	0.559±0.152
	Normal	0.464±0.214	0.571±0.182	0.484±0.210	0.464±0.214	0.515±0.200	0.454±0.255	0.515±0.200
	Tumor	0.481±0.176	0.615±0.087	0.497±0.181	0.481±0.176	0.464±0.189	0.530±0.212	0.464±0.189
DAT	Total	0.582±0.112	0.656±0.109	0.592±0.120	0.582±0.112	0.558±0.114	0.626±0.167	0.558±0.114
	Normal	0.530±0.117	0.567±0.102	0.553±0.123	0.530±0.117	0.501±0.117	0.604±0.194	0.501±0.117
	Tumor	0.478±0.122	0.570±0.164	0.504±0.143	0.478±0.122	0.527±0.240	0.480±0.119	0.527±0.240

Table 12: **Random forest regression and their evaluations.**

Dataset		MAE	RMSE
Entire	Total	704.909 ± 249.010	894.943 ± 246.192
	Normal	803.487 ± 145.365	979.334 ± 158.813
	Tumor	811.505 ± 204.788	1005.182 ± 197.351
DAT	Total	823.700 ± 141.448	994.698 ± 157.983
	Normal	663.414 ± 147.203	825.461 ± 151.120
	Tumor	729.302 ± 179.940	884.863 ± 181.154

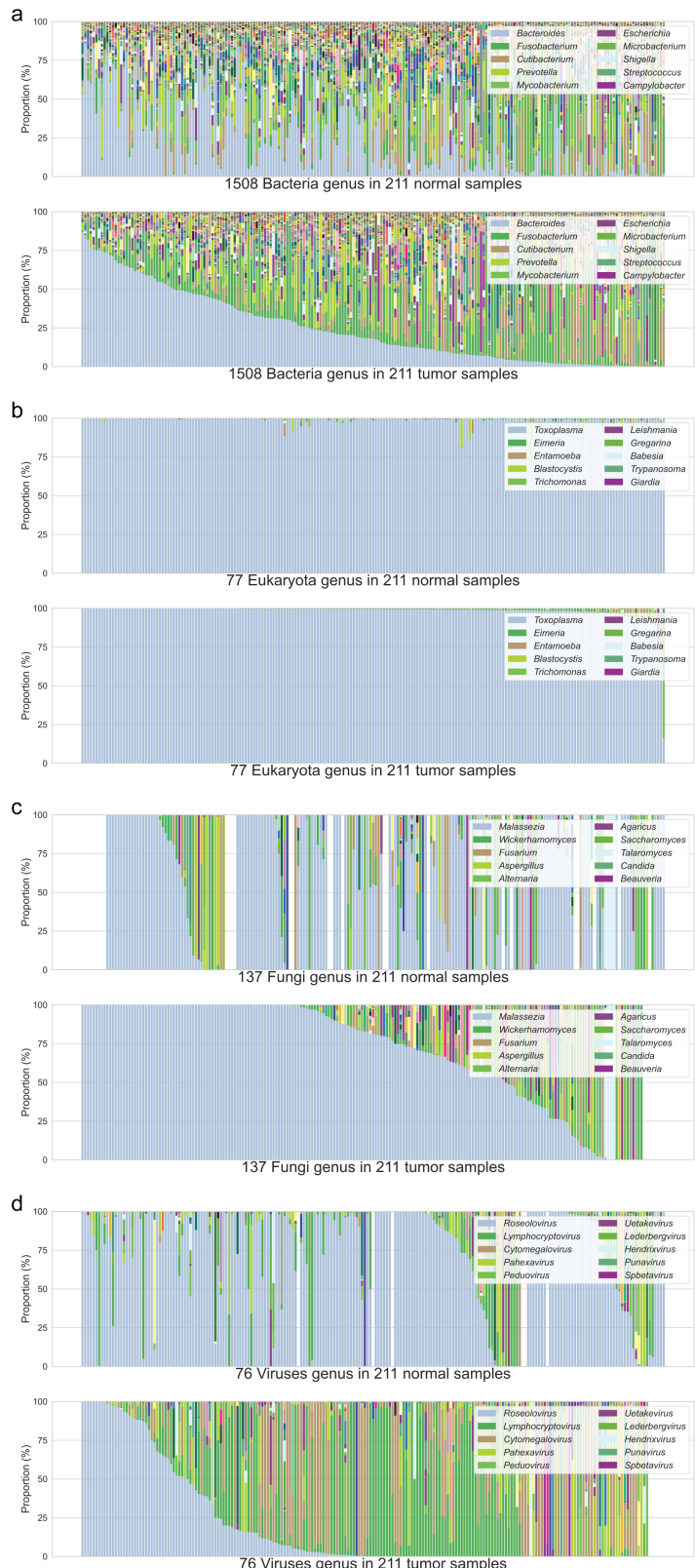


Figure 21: Gut microbiome compositions in genus level.

Taxa were sorted from the most prevalent taxon to the least prevalent taxon. CRC patients were sorted by the most prevalent taxon in descending order. **(a)** Bacteria kingdom **(b)** Eukaryota kingdom **(c)** Fungi kingdom **(d)** Viruses kingdom

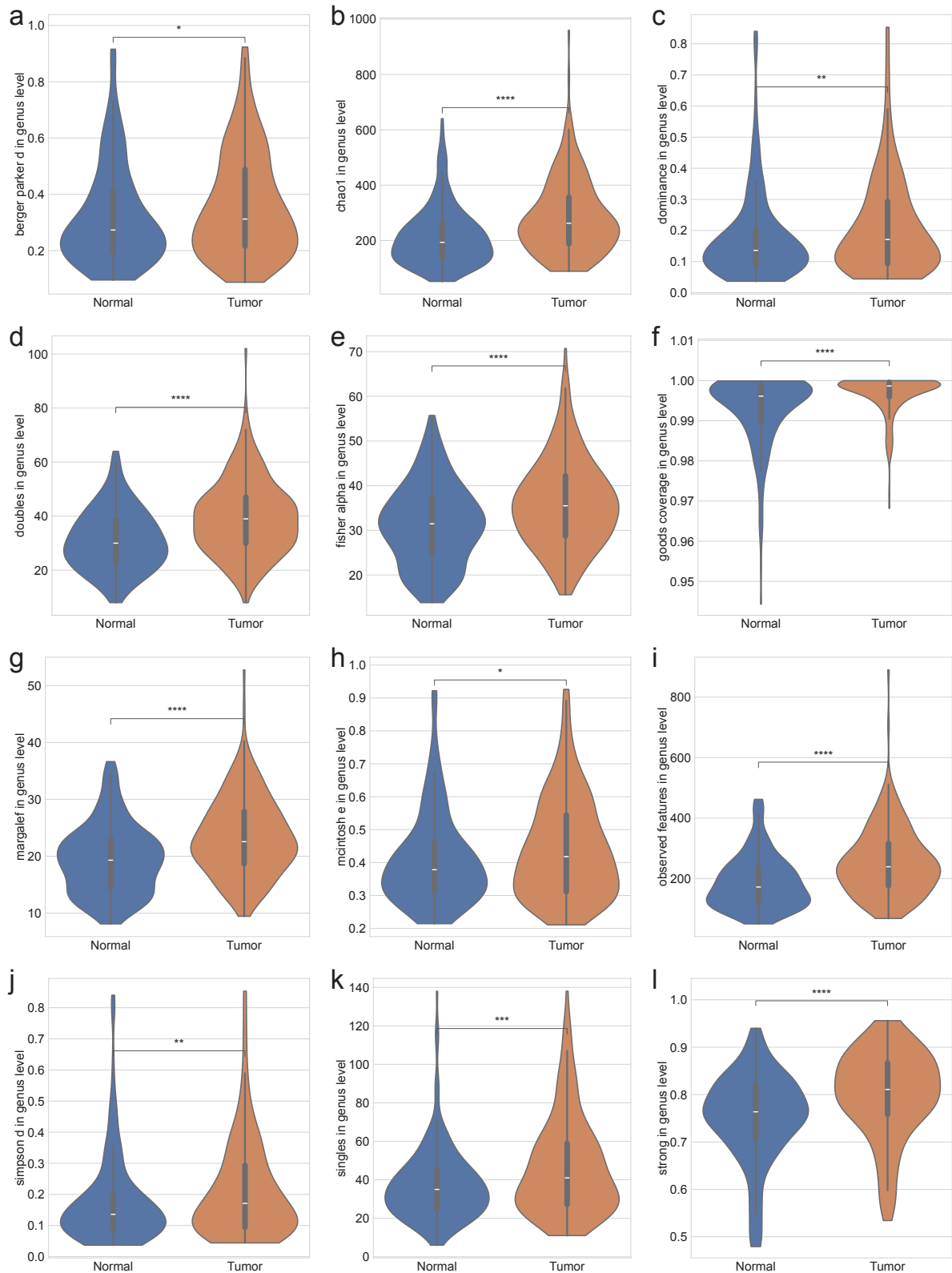


Figure 22: Alpha-diversity indices in genus level.

(a) Berger-Parker d (b) Chao1 (c) Dominance (d) Doubles (e) Fisher α (f) Good's coverage (g) Margalef (h) McIntosh (i) Observed features (j) Simpson d (k) Singles (l) Strong. MWU test: $p < 0.05$ (*), $p < 0.01$ (**), $p < 0.001$ (***), and $p < 0.0001$ (****)

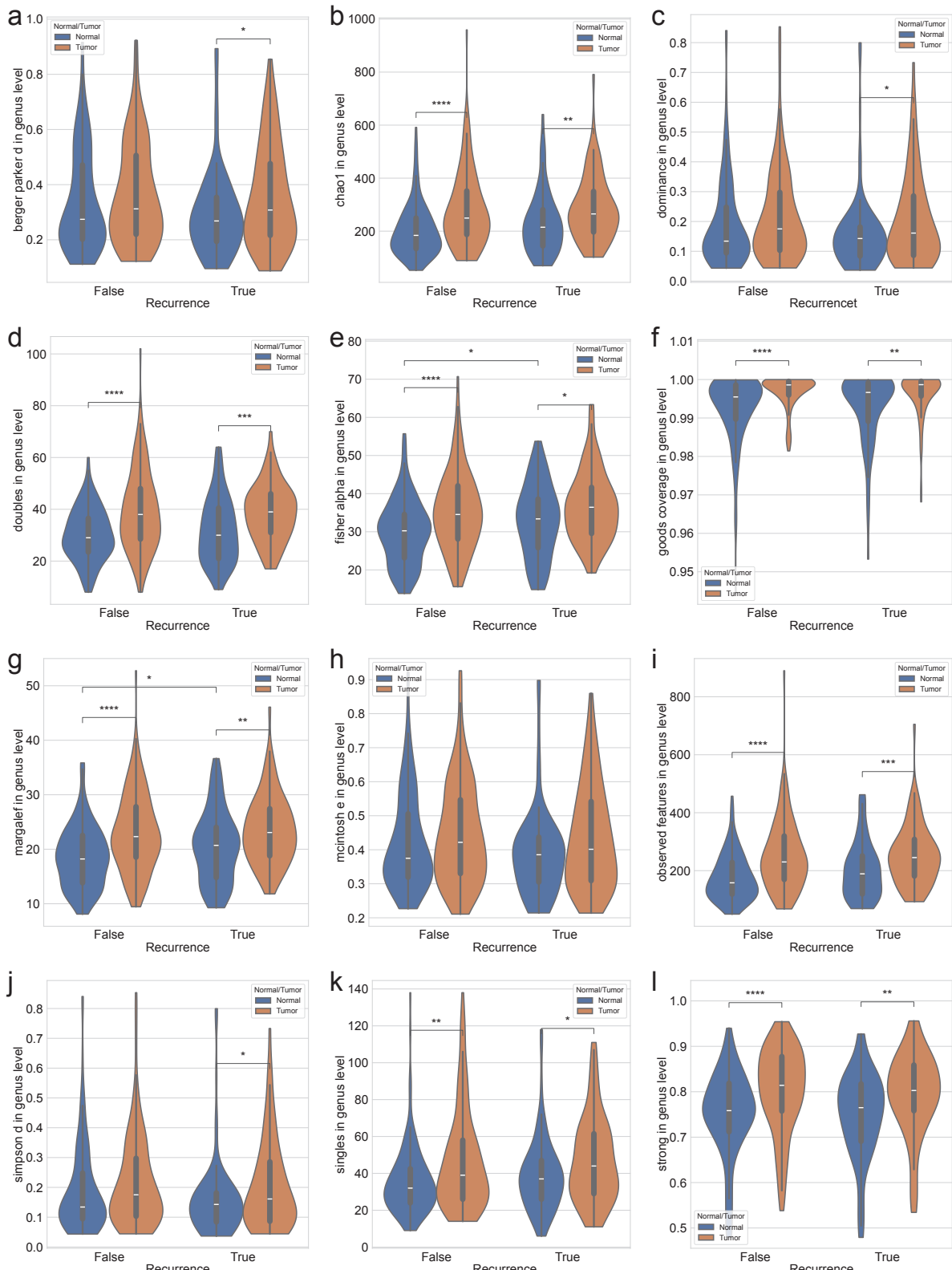


Figure 23: Alpha-diversity indices with recurrence in genus level.

(a) Berger-Parker d (b) Chao1 (c) Dominance (d) Doubles (e) Fisher α (f) Good's coverage (g) Margalef (h) McIntosh (i) Observed features (j) Simpson d (k) Singles (l) Strong. MWU test: $p < 0.05$ (*), $p < 0.01$ (**), $p < 0.001$ (***), and $p < 0.0001$ (****)

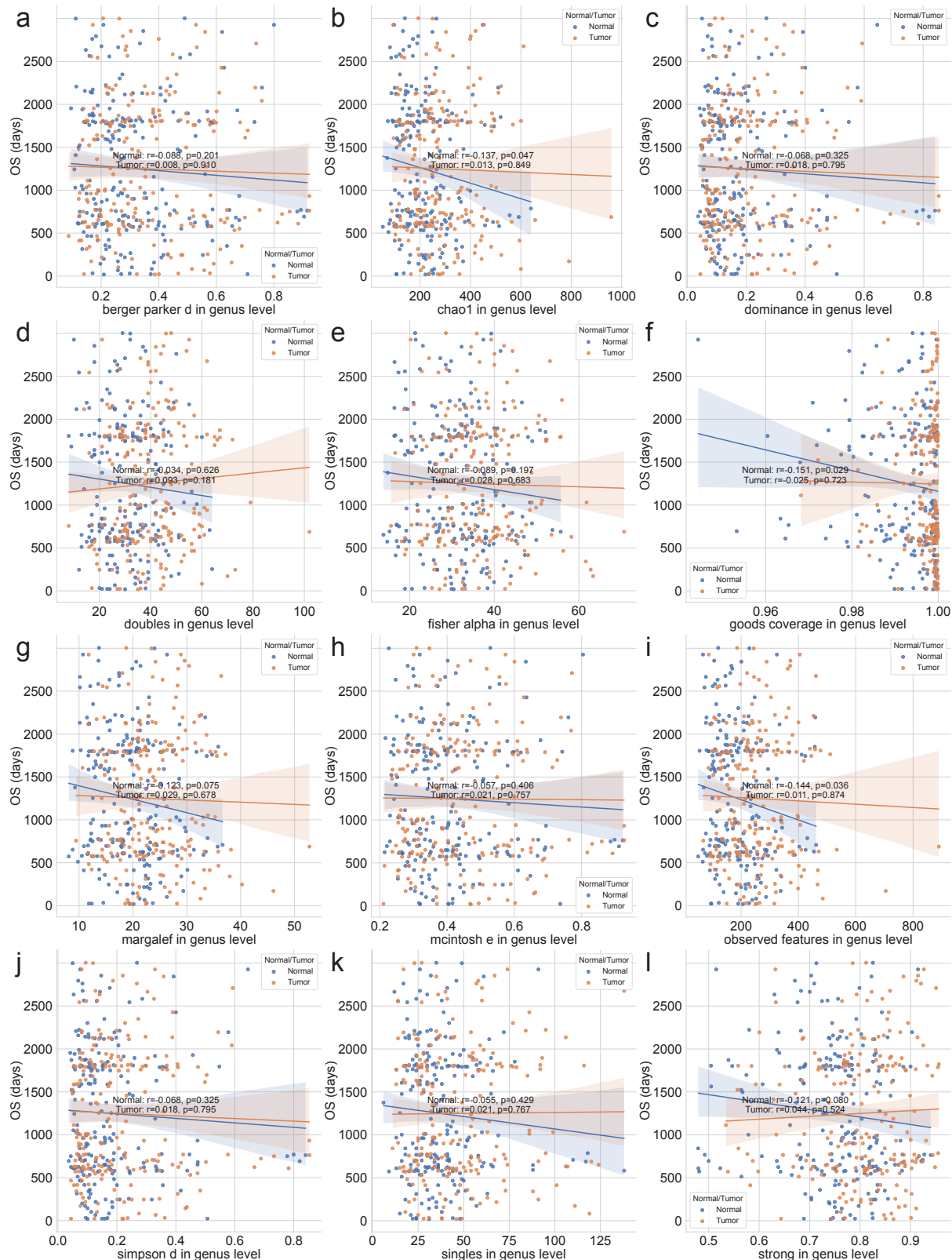


Figure 24: Alpha-diversity indices with OS in genus level.

(a) Berger-Parker d (b) Chao1 (c) Dominance (d) Doubles (e) Fisher α (f) Good's coverage (g) Margalef (h) McIntosh (i) Observed features (j) Simpson d (k) Singles (l) Strong. Statistical significance was calculated by the Spearman correlation.

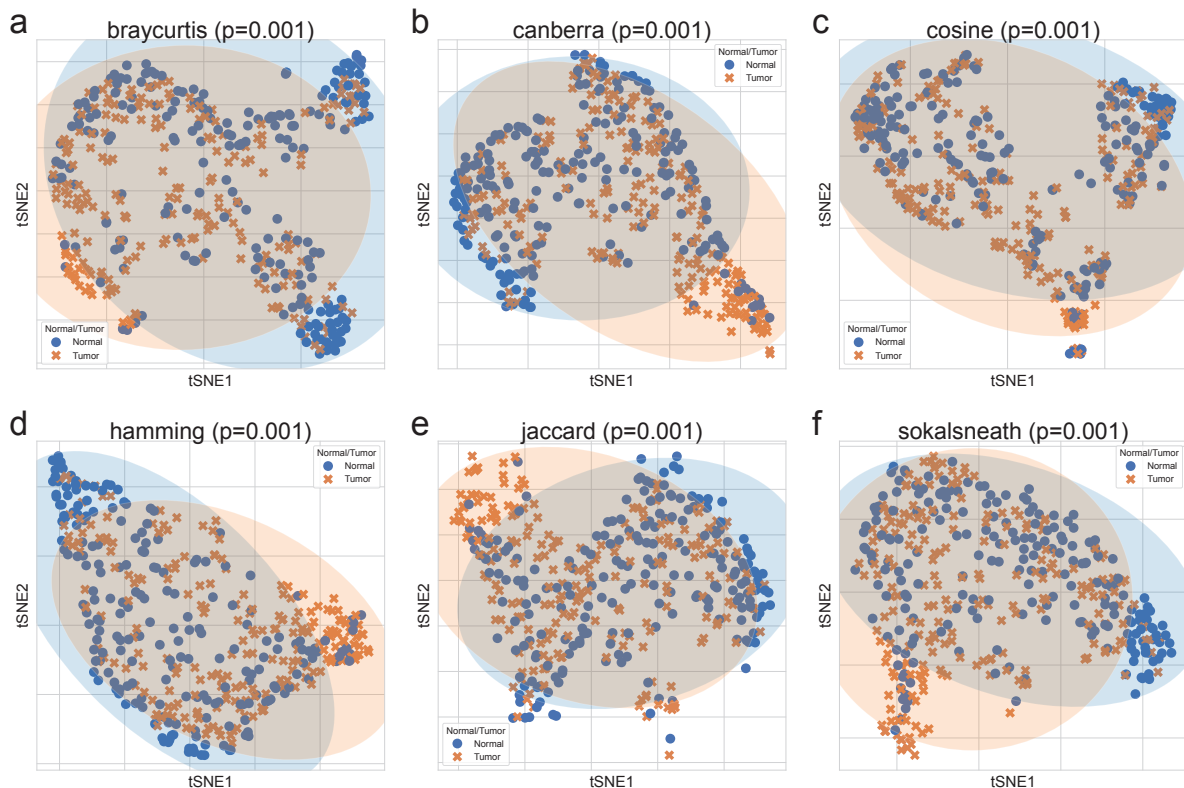


Figure 25: Beta-diversity indices in genus level.

Beta-diversity indices were visualized using a tSNE-transformed plot. The confidence ellipses are shown to display the distribution of each sub-group (Normal or Tumor). **(a)** Bray-Curtis **(b)** Canberra **(c)** Cosine **(d)** Hamming **(e)** Jaccard **(f)** Sokal-Sneath. Statistical significance were determined by PERMANOVA test.

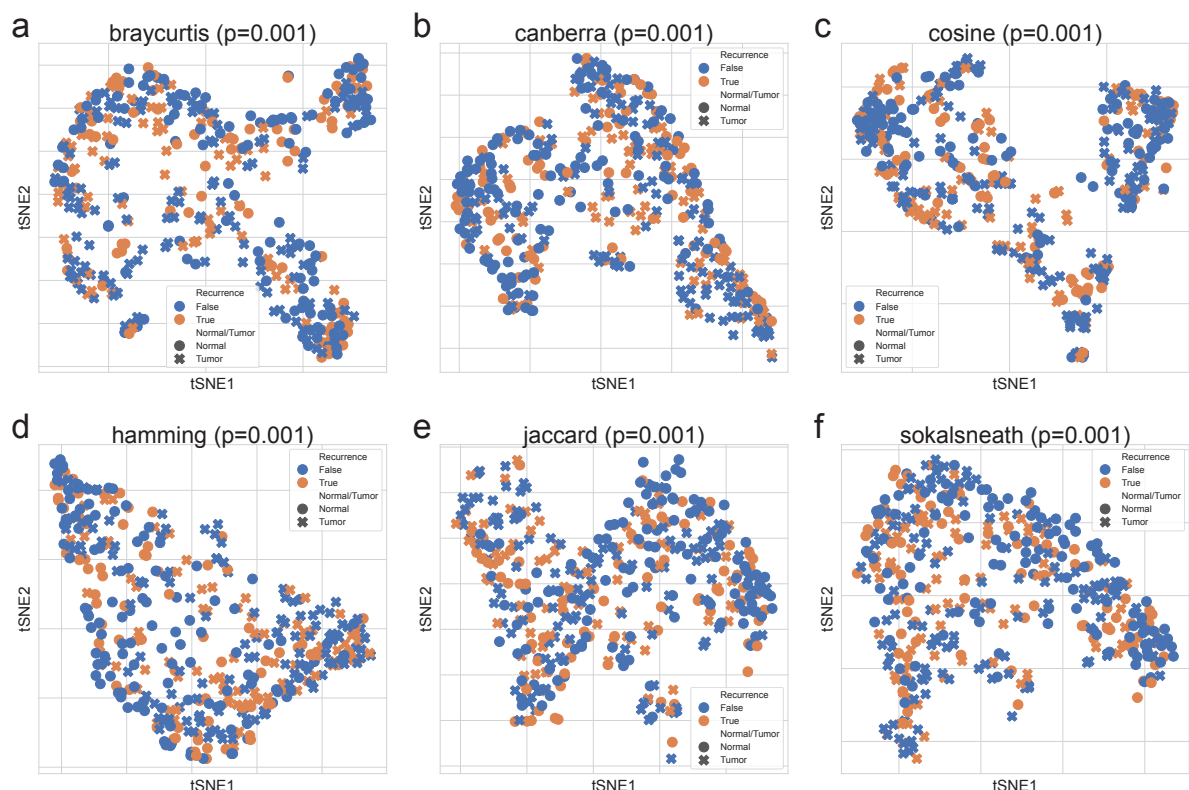


Figure 26: Beta-diversity indices with recurrence in genus level.

Beta-diversity indices were visualized using a tSNE-transformed plot. **(a)** Bray-Curtis **(b)** Canberra **(c)** Cosine **(d)** Hamming **(e)** Jaccard **(f)** Sokal-Sneath. Statistical significance were determined by PERMANOVA test.

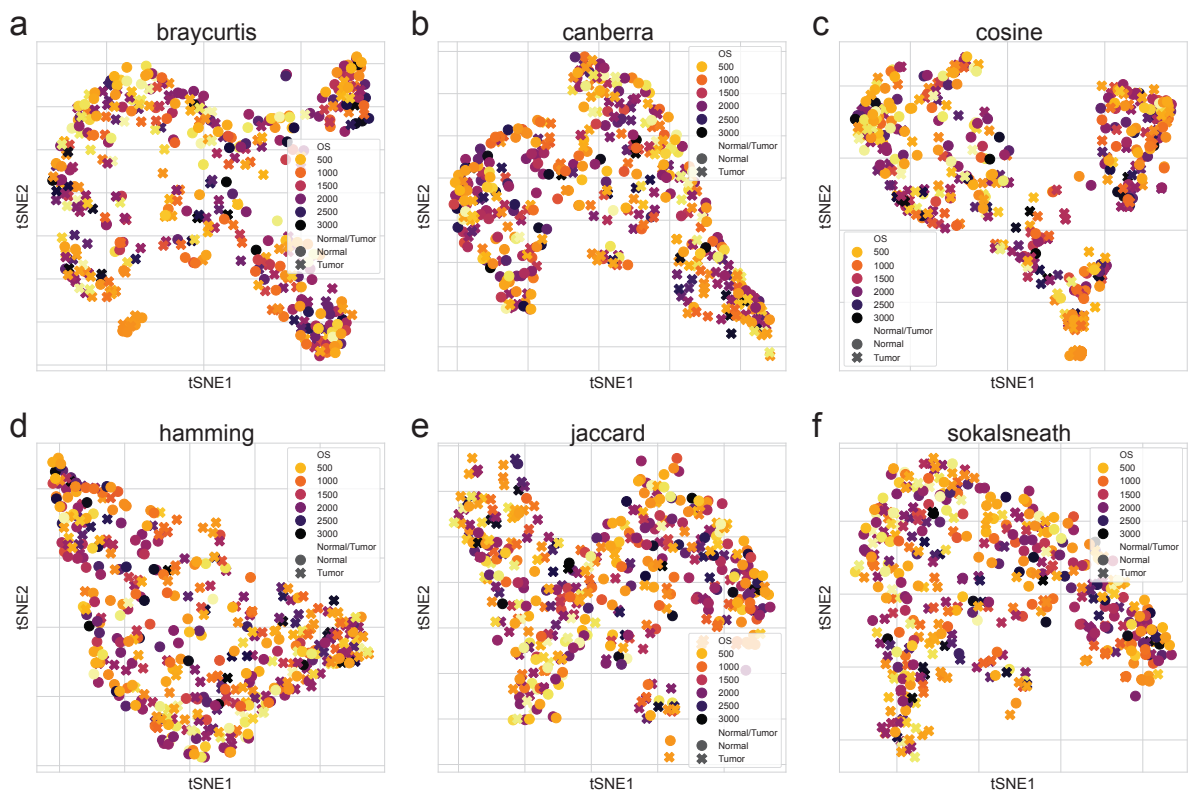


Figure 27: Beta-diversity indices with OS in genus level.

Beta-diversity indices were visualized using a tSNE-transformed plot. (a) Bray-Curtis (b) Canberra (c) Cosine (d) Hamming (e) Jaccard (f) Sokal-Sneath.

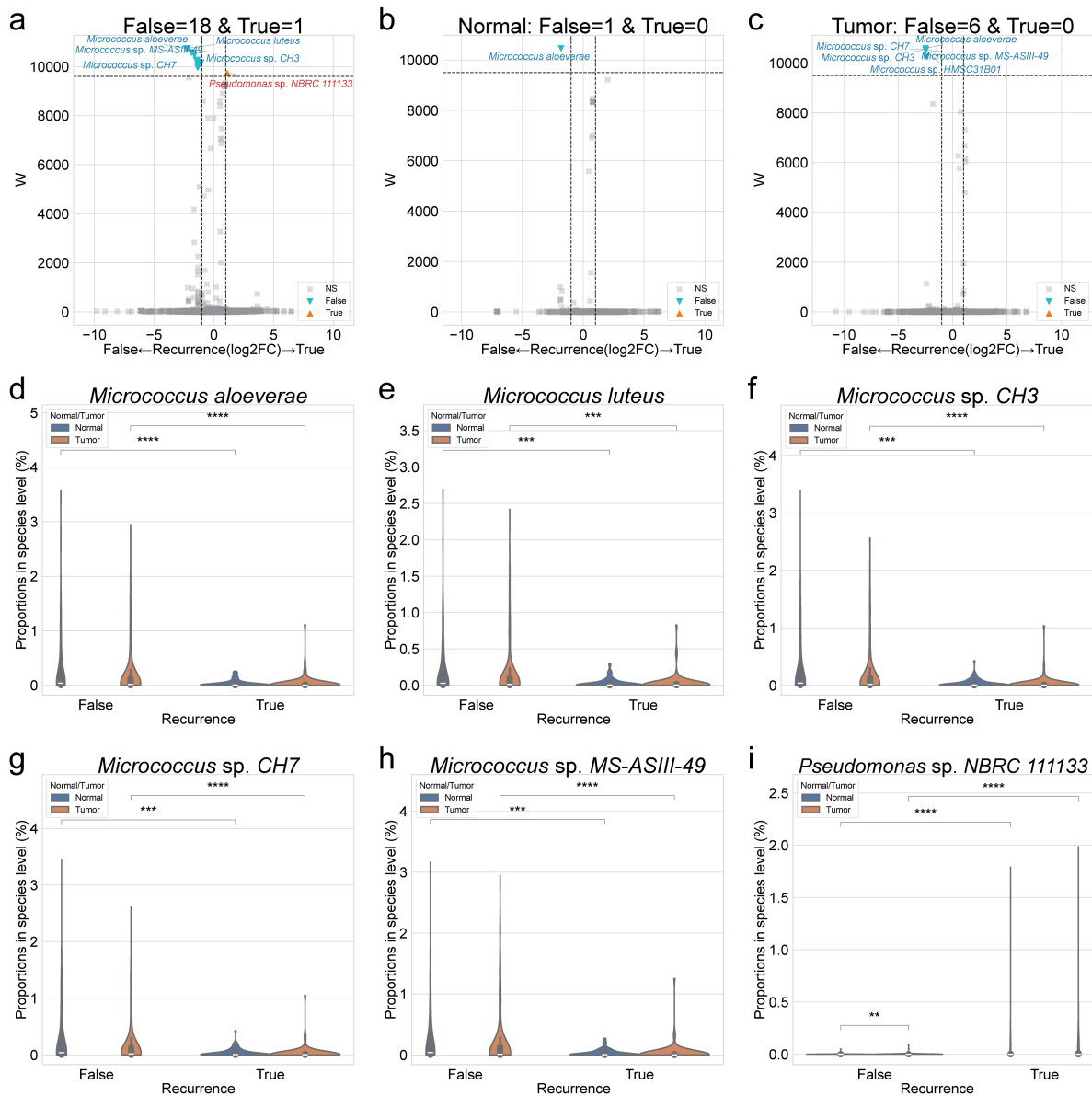


Figure 28: DAT with recurrence in species level.

(a-c) Volcano plots with recurrence. x-axis indicates \log_2 (Fold Change) on recurrence, and y-axis indicates ANCOM significance (W). **(a)** Total **(b)** Normal samples **(c)** Tumor samples. **(d-i)** Violin plots of each taxon proportion with recurrence. **(d)** *Micrococcus aloeverae* **(e)** *Micrococcus luteus* **(f)** *Micrococcus* sp. CH3 **(g)** *Micrococcus* sp. CH7 **(h)** *Micrococcus* sp. MS-ASIII-49 **(i)** *Pseudomonas* sp. NBRC 111133. MWU test: $p < 0.05$ (*), $p < 0.01$ (**), $p < 0.001$ (***)¹, and $p < 0.0001$ (****)

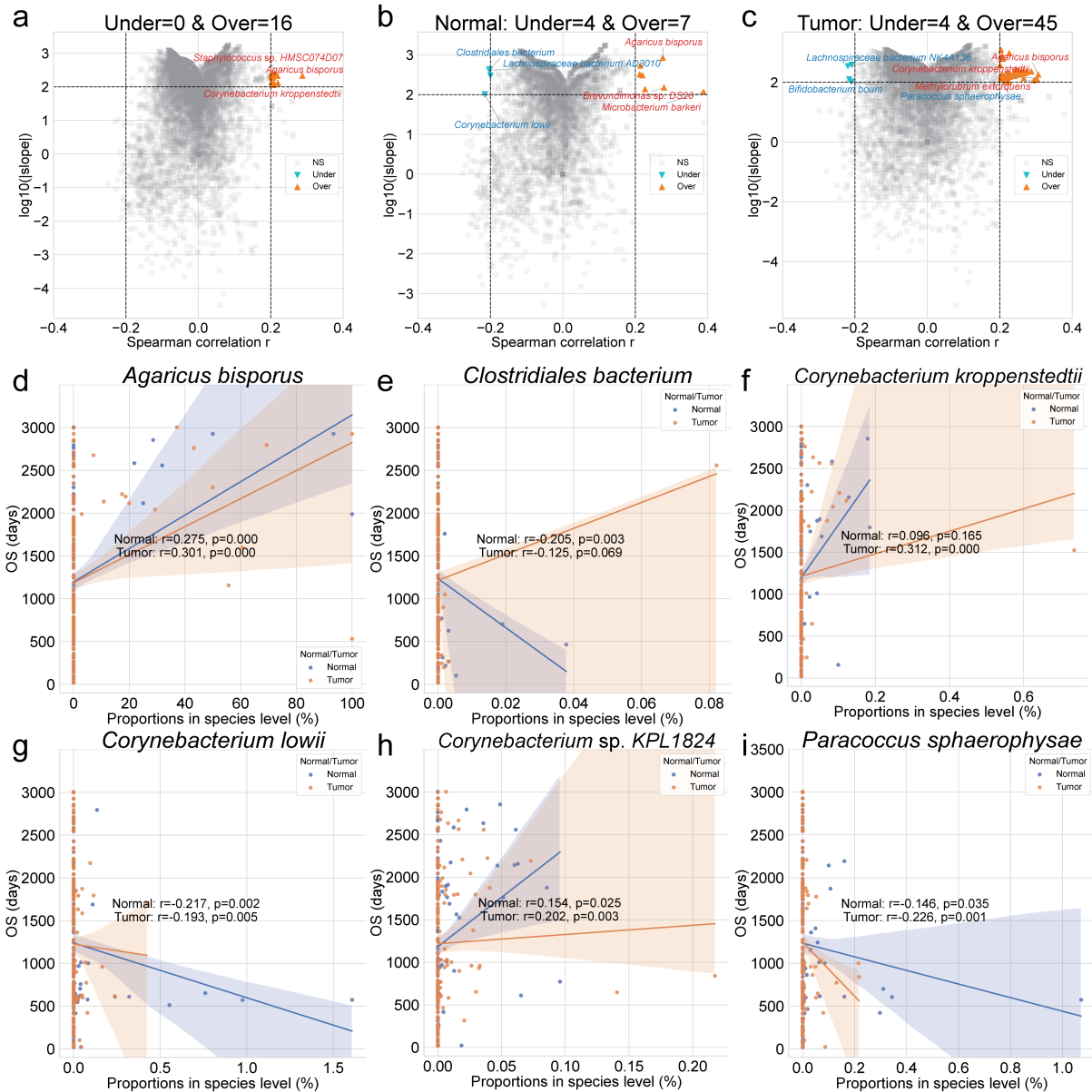


Figure 29: DAT with OS in species level.

(a-c) Volcano plots with OS. x-axis indicates Spearman correlation coefficient (r), and y-axis indicates $\log_{10}(|\text{slope}|)$. **(a)** Total **(b)** Normal samples **(c)** Tumor samples. **(d-li)** Scatter plots of each taxon proportion with OS. **(d)** *Agaricus bisporus* **(e)** *Clostridiales bacterium* **(f)** *Corynebacterium kroppenstedtii* **(g)** *Corynebacterium lowii* **(h)** *Corynebacterium sp. KPL1824* **(i)** *Paracoccus sphaerophysae*. Statistical significance were calculated with Spearman correlation (r and p).

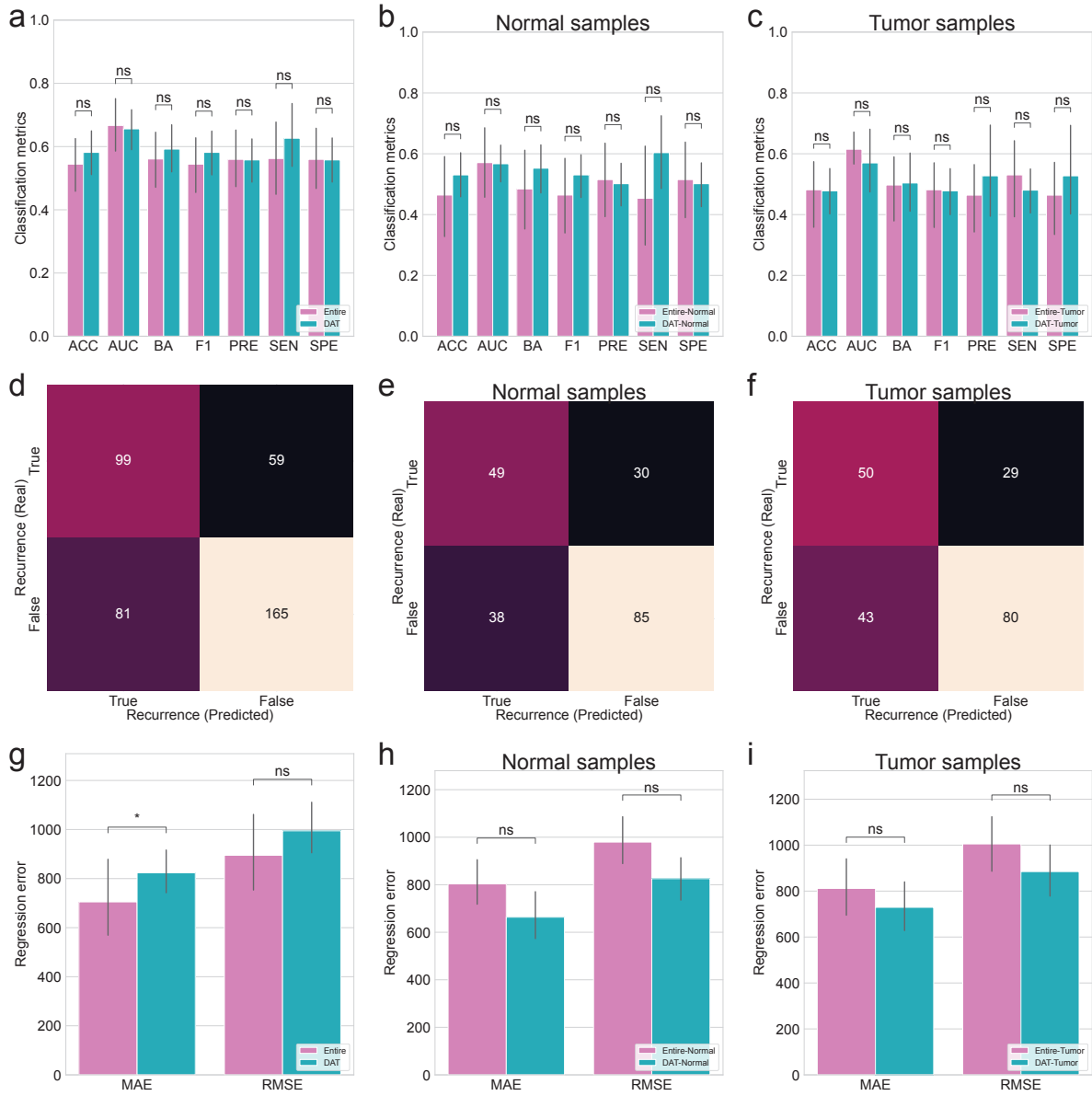


Figure 30: **Random forest classification and regression.**

(a-c) Random forest classification metrics for recurrence. **(a)** Total **(b)** Normal samples **(c)** Tumor samples. **(d-f)** Random forest classification confusion matrices for recurrence. **(d)** Total **(e)** Normal samples **(f)** Tumor samples. **(g-i)** Random forest regression errors for OS. **(g)** Total **(h)** Normal samples **(i)** Tumor samples. MWU test: $p < 0.05$ (*), $p < 0.01$ (**), $p < 0.001$ (***) $p < 0.0001$ (****)

1300 **4.4 Discussion**

1301 **5 Conclusion**

1302 In conclusion, the research described in this doctoral dissertation was conducted to identify significant ...

1303 In the section 2, I show that

1304 References

- 1305 Aagaard, K., Ma, J., Antony, K. M., Ganu, R., Petrosino, J., & Versalovic, J. (2014). The placenta harbors
1306 a unique microbiome. *Science translational medicine*, 6(237), 237ra65–237ra65.
- 1307 Abu-Ghazaleh, N., Chua, W. J., & Gopalan, V. (2021). Intestinal microbiota and its association with
1308 colon cancer and red/processed meat consumption. *Journal of gastroenterology and hepatology*,
1309 36(1), 75–88.
- 1310 Abusleme, L., Hoare, A., Hong, B.-Y., & Diaz, P. I. (2021). Microbial signatures of health, gingivitis,
1311 and periodontitis. *Periodontology 2000*, 86(1), 57–78.
- 1312 Aitchison, J., Barceló-Vidal, C., Martín-Fernández, J. A., & Pawlowsky-Glahn, V. (2000). Logratio
1313 analysis and compositional distance. *Mathematical geology*, 32, 271–275.
- 1314 Aja, E., Mangar, M., Fletcher, H., & Mishra, A. (2021). Filifactor alocis: recent insights and advances.
1315 *Journal of dental research*, 100(8), 790–797.
- 1316 Alelyani, S. (2021). Stable bagging feature selection on medical data. *Journal of Big Data*, 8(1), 11.
- 1317 Altabtbaei, K., Maney, P., Ganesan, S. M., Dabdoub, S. M., Nagaraja, H. N., & Kumar, P. S. (2021). Anna
1318 karenina and the subgingival microbiome associated with periodontitis. *Microbiome*, 9, 1–15.
- 1319 Altingöz, S. M., Kurgan, Ş., Önder, C., Serdar, M. A., Ünlütürk, U., Uyanık, M., ... Günhan, M.
1320 (2021). Salivary and serum oxidative stress biomarkers and advanced glycation end products in
1321 periodontitis patients with or without diabetes: A cross-sectional study. *Journal of periodontology*,
1322 92(9), 1274–1285.
- 1323 Alverdy, J., Hyoju, S., Weigerinck, M., & Gilbert, J. (2017). The gut microbiome and the mechanism of
1324 surgical infection. *Journal of British Surgery*, 104(2), e14–e23.
- 1325 An, S., & Park, S. (2022). Association of physical activity and sedentary behavior with the risk of
1326 colorectal cancer. *Journal of Korean Medical Science*, 37(19).
- 1327 Anderson, M. J. (2014). Permutational multivariate analysis of variance (permanova). *Wiley statsref:
1328 statistics reference online*, 1–15.
- 1329 Aruni, A. W., Mishra, A., Dou, Y., Chioma, O., Hamilton, B. N., & Fletcher, H. M. (2015). Filifactor
1330 alocis—a new emerging periodontal pathogen. *Microbes and infection*, 17(7), 517–530.
- 1331 Aziz, Q., & Thompson, D. G. (1998). Brain-gut axis in health and disease. *Gastroenterology*, 114(3),
1332 559–578.
- 1333 Bai, X., Wei, H., Liu, W., Coker, O. O., Gou, H., Liu, C., ... others (2022). Cigarette smoke promotes
1334 colorectal cancer through modulation of gut microbiota and related metabolites. *Gut*, 71(12),

- 1335 2439–2450.
- 1336 Baldelli, V., Scaldaferrri, F., Putignani, L., & Del Chierico, F. (2021). The role of enterobacteriaceae in
1337 gut microbiota dysbiosis in inflammatory bowel diseases. *Microorganisms*, 9(4), 697.
- 1338 Bardou, M., Rouland, A., Martel, M., Loffroy, R., Barkun, A. N., & Chapelle, N. (2022). Obesity and
1339 colorectal cancer. *Alimentary Pharmacology & Therapeutics*, 56(3), 407–418.
- 1340 Barlow, G. M., Yu, A., & Mathur, R. (2015). Role of the gut microbiome in obesity and diabetes mellitus.
1341 *Nutrition in clinical practice*, 30(6), 787–797.
- 1342 Basavaprabhu, H., Sonu, K., & Prabha, R. (2020). Mechanistic insights into the action of probiotics
1343 against bacterial vaginosis and its mediated preterm birth: An overview. *Microbial pathogenesis*,
1344 141, 104029.
- 1345 Belstrøm, D., Constancias, F., Drautz-Moses, D. I., Schuster, S. C., Veleba, M., Mahé, F., & Givskov, M.
1346 (2021). Periodontitis associates with species-specific gene expression of the oral microbiota. *npj
1347 Biofilms and Microbiomes*, 7(1), 76.
- 1348 Berger, W. H., & Parker, F. L. (1970). Diversity of planktonic foraminifera in deep-sea sediments.
1349 *Science*, 168(3937), 1345–1347.
- 1350 Berghella, V. (2012). Universal cervical length screening for prediction and prevention of preterm birth.
1351 *Obstetrical & gynecological survey*, 67(10), 653–657.
- 1352 Blencowe, H., Cousens, S., Oestergaard, M. Z., Chou, D., Moller, A.-B., Narwal, R., ... others (2012).
1353 National, regional, and worldwide estimates of preterm birth rates in the year 2010 with time trends
1354 since 1990 for selected countries: a systematic analysis and implications. *The lancet*, 379(9832),
1355 2162–2172.
- 1356 Boland, C. R., & Goel, A. (2010). Microsatellite instability in colorectal cancer. *Gastroenterology*,
1357 138(6), 2073–2087.
- 1358 Boleij, A., Hechenbleikner, E. M., Goodwin, A. C., Badani, R., Stein, E. M., Lazarev, M. G., ... others
1359 (2015). The bacteroides fragilis toxin gene is prevalent in the colon mucosa of colorectal cancer
1360 patients. *Clinical Infectious Diseases*, 60(2), 208–215.
- 1361 Bolstad, A., Jensen, H. B., & Bakken, V. (1996). Taxonomy, biology, and periodontal aspects of
1362 fusobacterium nucleatum. *Clinical microbiology reviews*, 9(1), 55–71.
- 1363 Bolyen, E., Rideout, J. R., Dillon, M. R., Bokulich, N. A., Abnet, C. C., Al-Ghalith, G. A., ... others
1364 (2019). Reproducible, interactive, scalable and extensible microbiome data science using qiime 2.
1365 *Nature biotechnology*, 37(8), 852–857.
- 1366 Bombin, A., Yan, S., Bombin, S., Mosley, J. D., & Ferguson, J. F. (2022). Obesity influences composition
1367 of salivary and fecal microbiota and impacts the interactions between bacterial taxa. *Physiological
1368 reports*, 10(7), e15254.
- 1369 Bonnet, M., Buc, E., Sauvanet, P., Darcha, C., Dubois, D., Pereira, B., ... Darfeuille-Michaud, A. (2014).
1370 Colonization of the human gut by e. coli and colorectal cancer risk. *Clinical Cancer Research*,
1371 20(4), 859–867.
- 1372 Breiman, L. (2001). Random forests. *Machine learning*, 45, 5–32.
- 1373 Brennan, C. A., & Garrett, W. S. (2019). Fusobacterium nucleatum—symbiont, opportunist and

- 1374 oncobacterium. *Nature Reviews Microbiology*, 17(3), 156–166.
- 1375 Broom, L. J., & Kogut, M. H. (2018). The role of the gut microbiome in shaping the immune system of
1376 chickens. *Veterinary immunology and immunopathology*, 204, 44–51.
- 1377 Bryll, R., Gutierrez-Osuna, R., & Quek, F. (2003). Attribute bagging: improving accuracy of classifier
1378 ensembles by using random feature subsets. *Pattern recognition*, 36(6), 1291–1302.
- 1379 Bullman, S., Pedamallu, C. S., Sicinska, E., Clancy, T. E., Zhang, X., Cai, D., ... others (2017). Analysis
1380 of fusobacterium persistence and antibiotic response in colorectal cancer. *Science*, 358(6369),
1381 1443–1448.
- 1382 Burt, R. W., Leppert, M. F., Slattery, M. L., Samowitz, W. S., Spirio, L. N., Kerber, R. A., ... others
1383 (2004). Genetic testing and phenotype in a large kindred with attenuated familial adenomatous
1384 polyposis. *Gastroenterology*, 127(2), 444–451.
- 1385 Cai, Y., Li, Y., Xiong, Y., Geng, X., Kang, Y., & Yang, Y. (2024). Diabetic foot exacerbates gut
1386 mycobiome dysbiosis in adult patients with type 2 diabetes mellitus: revealing diagnostic markers.
1387 *Nutrition & Diabetes*, 14(1), 71.
- 1388 Callahan, B. J., McMurdie, P. J., Rosen, M. J., Han, A. W., Johnson, A. J. A., & Holmes, S. P. (2016).
1389 Dada2: High-resolution sample inference from illumina amplicon data. *Nature methods*, 13(7),
1390 581–583.
- 1391 Canakci, V., & Canakci, C. F. (2007). Pain levels in patients during periodontal probing and mechanical
1392 non-surgical therapy. *Clinical oral investigations*, 11, 377–383.
- 1393 Cappellato, M., Baruzzo, G., & Di Camillo, B. (2022). Investigating differential abundance methods in
1394 microbiome data: A benchmark study. *PLoS computational biology*, 18(9), e1010467.
- 1395 Castaner, O., Goday, A., Park, Y.-M., Lee, S.-H., Magkos, F., Shiow, S.-A. T. E., & Schröder, H. (2018).
1396 The gut microbiome profile in obesity: a systematic review. *International journal of endocrinology*,
1397 2018(1), 4095789.
- 1398 Center, M. M., Jemal, A., Smith, R. A., & Ward, E. (2009). Worldwide variations in colorectal cancer.
1399 *CA: a cancer journal for clinicians*, 59(6), 366–378.
- 1400 Centor, R. M. (1991). Signal detectability: the use of roc curves and their analyses. *Medical decision
1401 making*, 11(2), 102–106.
- 1402 Cerqueira, F. M., Photenhauer, A. L., Pollet, R. M., Brown, H. A., & Koropatkin, N. M. (2020). Starch
1403 digestion by gut bacteria: crowdsourcing for carbs. *Trends in Microbiology*, 28(2), 95–108.
- 1404 Champagne, C., McNairn, H., Daneshfar, B., & Shang, J. (2014). A bootstrap method for assessing
1405 classification accuracy and confidence for agricultural land use mapping in canada. *International
1406 Journal of Applied Earth Observation and Geoinformation*, 29, 44–52.
- 1407 Chao, A. (1984). Nonparametric estimation of the number of classes in a population. *Scandinavian
1408 Journal of statistics*, 265–270.
- 1409 Chao, A., & Lee, S.-M. (1992). Estimating the number of classes via sample coverage. *Journal of the
1410 American statistical Association*, 87(417), 210–217.
- 1411 Chapple, I. L., Mealey, B. L., Van Dyke, T. E., Bartold, P. M., Dommisch, H., Eickholz, P., ... others
1412 (2018). Periodontal health and gingival diseases and conditions on an intact and a reduced

- 1413 periodontium: Consensus report of workgroup 1 of the 2017 world workshop on the classification
1414 of periodontal and peri-implant diseases and conditions. *Journal of periodontology*, 89, S74–S84.
- 1415 Chen, T., Marsh, P., & Al-Hebshi, N. (2022). Smdi: an index for measuring subgingival microbial
1416 dysbiosis. *Journal of dental research*, 101(3), 331–338.
- 1417 Chen, T., Yu, W.-H., Izard, J., Baranova, O. V., Lakshmanan, A., & Dewhirst, F. E. (2010). The human
1418 oral microbiome database: a web accessible resource for investigating oral microbe taxonomic and
1419 genomic information. *Database*, 2010.
- 1420 Chen, X., D’Souza, R., & Hong, S.-T. (2013). The role of gut microbiota in the gut-brain axis: current
1421 challenges and perspectives. *Protein & cell*, 4, 403–414.
- 1422 Chen, X., Jansen, L., Guo, F., Hoffmeister, M., Chang-Claude, J., & Brenner, H. (2021). Smoking,
1423 genetic predisposition, and colorectal cancer risk. *Clinical and translational gastroenterology*,
1424 12(3), e00317.
- 1425 Chen, X., Li, H., Guo, F., Hoffmeister, M., & Brenner, H. (2022). Alcohol consumption, polygenic risk
1426 score, and early-and late-onset colorectal cancer risk. *EClinicalMedicine*, 49.
- 1427 Chew, R. J. J., Tan, K. S., Chen, T., Al-Hebshi, N. N., & Goh, C. E. (2024). Quantifying periodontitis-
1428 associated oral dysbiosis in tongue and saliva microbiomes—an integrated data analysis. *Journal
1429 of Periodontology*.
- 1430 Čižmárová, B., Tomečková, V., Hubková, B., Hurajtová, A., Ohlasová, J., & Birková, A. (2022). Salivary
1431 redox homeostasis in human health and disease. *International Journal of Molecular Sciences*,
1432 23(17), 10076.
- 1433 Cullin, N., Antunes, C. A., Straussman, R., Stein-Thoeringer, C. K., & Elinav, E. (2021). Microbiome
1434 and cancer. *Cancer Cell*, 39(10), 1317–1341.
- 1435 Curtius, K., Wright, N. A., & Graham, T. A. (2018). An evolutionary perspective on field cancerization.
1436 *Nature Reviews Cancer*, 18(1), 19–32.
- 1437 Dabke, K., Hendrick, G., Devkota, S., et al. (2019). The gut microbiome and metabolic syndrome. *The
1438 Journal of clinical investigation*, 129(10), 4050–4057.
- 1439 DeSantis, T. Z., Hugenholtz, P., Larsen, N., Rojas, M., Brodie, E. L., Keller, K., … Andersen, G. L.
1440 (2006). Greengenes, a chimera-checked 16s rrna gene database and workbench compatible with
1441 arb. *Applied and environmental microbiology*, 72(7), 5069–5072.
- 1442 Doyle, R., Alber, D., Jones, H., Harris, K., Fitzgerald, F., Peebles, D., & Klein, N. (2014). Term and
1443 preterm labour are associated with distinct microbial community structures in placental membranes
1444 which are independent of mode of delivery. *Placenta*, 35(12), 1099–1101.
- 1445 Fahmy, C. A., Gamal-Eldeen, A. M., El-Hussieny, E. A., Raafat, B. M., Mehanna, N. S., Talaat, R. M., &
1446 Shaaban, M. T. (2019). *Bifidobacterium longum* suppresses murine colorectal cancer through the
1447 modulation of oncomirs and tumor suppressor mirnas. *Nutrition and cancer*, 71(4), 688–700.
- 1448 Faith, D. P. (1992). Conservation evaluation and phylogenetic diversity. *Biological conservation*, 61(1),
1449 1–10.
- 1450 Fettweis, J. M., Serrano, M. G., Brooks, J. P., Edwards, D. J., Girerd, P. H., Parikh, H. I., … others
1451 (2019). The vaginal microbiome and preterm birth. *Nature medicine*, 25(6), 1012–1021.

- 1452 Fisher, R. A., Corbet, A. S., & Williams, C. B. (1943). The relation between the number of species and
1453 the number of individuals in a random sample of an animal population. *The Journal of Animal*
1454 *Ecology*, 42–58.
- 1455 Flanagan, L., Schmid, J., Ebert, M., Soucek, P., Kunicka, T., Liska, V., ... others (2014). Fusobacterium
1456 nucleatum associates with stages of colorectal neoplasia development, colorectal cancer and disease
1457 outcome. *European journal of clinical microbiology & infectious diseases*, 33, 1381–1390.
- 1458 Fortenberry, J. D. (2013). The uses of race and ethnicity in human microbiome research. *Trends in*
1459 *microbiology*, 21(4), 165–166.
- 1460 Francescone, R., Hou, V., & Grivennikov, S. I. (2014). Microbiome, inflammation, and cancer. *The*
1461 *Cancer Journal*, 20(3), 181–189.
- 1462 Friedman, J. H. (2002). Stochastic gradient boosting. *Computational statistics & data analysis*, 38(4),
1463 367–378.
- 1464 Fushiki, T. (2011). Estimation of prediction error by using k-fold cross-validation. *Statistics and*
1465 *Computing*, 21, 137–146.
- 1466 Gambin, D. J., Vitali, F. C., De Carli, J. P., Mazzon, R. R., Gomes, B. P., Duque, T. M., & Trentin, M. S.
1467 (2021). Prevalence of red and orange microbial complexes in endodontic-periodontal lesions: a
1468 systematic review and meta-analysis. *Clinical Oral Investigations*, 1–14.
- 1469 Gao, J., Yin, J., Xu, K., Li, T., & Yin, Y. (2019). What is the impact of diet on nutritional diarrhea
1470 associated with gut microbiota in weaning piglets: a system review. *BioMed research international*,
1471 2019(1), 6916189.
- 1472 Geurts, P., Ernst, D., & Wehenkel, L. (2006). Extremely randomized trees. *Machine learning*, 63, 3–42.
- 1473 Ghanavati, R., Akbari, A., Mohammadi, F., Asadollahi, P., Javadi, A., Talebi, M., & Rohani, M. (2020).
1474 Lactobacillus species inhibitory effect on colorectal cancer progression through modulating the
1475 wnt/β-catenin signaling pathway. *Molecular and Cellular Biochemistry*, 470, 1–13.
- 1476 Ghajogh, B., & Crowley, M. (2019). The theory behind overfitting, cross validation, regularization,
1477 bagging, and boosting: tutorial. *arXiv preprint arXiv:1905.12787*.
- 1478 Ghorbani, E., Avan, A., Ryzhikov, M., Ferns, G., Khazaei, M., & Soleimanpour, S. (2022). Role of
1479 lactobacillus strains in the management of colorectal cancer: An overview of recent advances.
1480 *Nutrition*, 103, 111828.
- 1481 Gilbert, J. A., Blaser, M. J., Caporaso, J. G., Jansson, J. K., Lynch, S. V., & Knight, R. (2018). Current
1482 understanding of the human microbiome. *Nature medicine*, 24(4), 392–400.
- 1483 Gini, C. (1912). Variabilità e mutabilità (variability and mutability). *Tipografia di Paolo Cuppini,*
1484 *Bologna, Italy*, 156.
- 1485 Goldenberg, R. L., Culhane, J. F., Iams, J. D., & Romero, R. (2008). Epidemiology and causes of preterm
1486 birth. *The lancet*, 371(9606), 75–84.
- 1487 Gonçalves, L., Subtil, A., Oliveira, M. R., & de Zea Bermudez, P. (2014). Roc curve estimation: An
1488 overview. *REVSTAT-Statistical journal*, 12(1), 1–20.
- 1489 Good, I. J. (1953). The population frequencies of species and the estimation of population parameters.
1490 *Biometrika*, 40(3-4), 237–264.

- 1491 Goodyear, M. D., Krleza-Jeric, K., & Lemmens, T. (2007). *The declaration of helsinki* (Vol. 335) (No. 1492 7621). British Medical Journal Publishing Group.
- 1493 Haffajee, A., Teles, R., & Socransky, S. (2006). Association of eubacterium nodatum and treponema 1494 denticola with human periodontitis lesions. *Oral microbiology and immunology*, 21(5), 269–282.
- 1495 Hajishengallis, G. (2015). Periodontitis: from microbial immune subversion to systemic inflammation. 1496 *Nature reviews immunology*, 15(1), 30–44.
- 1497 Hamjane, N., Mechita, M. B., Nourouti, N. G., & Barakat, A. (2024). Gut microbiota dysbiosis-associated 1498 obesity and its involvement in cardiovascular diseases and type 2 diabetes. a systematic review. 1499 *Microvascular Research*, 151, 104601.
- 1500 Hamming, R. W. (1950). Error detecting and error correcting codes. *The Bell system technical journal*, 1501 29(2), 147–160.
- 1502 Hampel, H., Frankel, W. L., Martin, E., Arnold, M., Khanduja, K., Kuebler, P., ... others (2008). 1503 Feasibility of screening for lynch syndrome among patients with colorectal cancer. *Journal of 1504 Clinical Oncology*, 26(35), 5783–5788.
- 1505 Han, Y. W. (2015). Fusobacterium nucleatum: a commensal-turned pathogen. *Current opinion in 1506 microbiology*, 23, 141–147.
- 1507 Han, Y. W., & Wang, X. (2013). Mobile microbiome: oral bacteria in extra-oral infections and 1508 inflammation. *Journal of dental research*, 92(6), 485–491.
- 1509 Hand, D. J. (2012). Assessing the performance of classification methods. *International Statistical Review*, 1510 80(3), 400–414.
- 1511 Hartstra, A. V., Bouter, K. E., Bäckhed, F., & Nieuwdorp, M. (2015). Insights into the role of the 1512 microbiome in obesity and type 2 diabetes. *Diabetes care*, 38(1), 159–165.
- 1513 Hashemi Goradel, N., Heidarzadeh, S., Jahangiri, S., Farhood, B., Mortezaee, K., Khanlarkhani, N., & 1514 Negahdari, B. (2019). Fusobacterium nucleatum and colorectal cancer: A mechanistic overview. 1515 *Journal of Cellular Physiology*, 234(3), 2337–2344.
- 1516 Heip, C. (1974). A new index measuring evenness. *Journal of the Marine Biological Association of the 1517 United Kingdom*, 54(3), 555–557.
- 1518 Helmink, B. A., Khan, M. W., Hermann, A., Gopalakrishnan, V., & Wargo, J. A. (2019). The microbiome, 1519 cancer, and cancer therapy. *Nature medicine*, 25(3), 377–388.
- 1520 Hill, M. O. (1973). Diversity and evenness: a unifying notation and its consequences. *Ecology*, 54(2), 1521 427–432.
- 1522 Hiranmayi, K. V., Sirisha, K., Rao, M. R., & Sudhakar, P. (2017). Novel pathogens in periodontal 1523 microbiology. *Journal of Pharmacy and Bioallied Sciences*, 9(3), 155–163.
- 1524 Honda, K., & Littman, D. R. (2012). The microbiome in infectious disease and inflammation. *Annual 1525 review of immunology*, 30(1), 759–795.
- 1526 Honest, H., Forbes, C., Durée, K., Norman, G., Duffy, S., Tsourapas, A., ... others (2009). Screening to 1527 prevent spontaneous preterm birth: systematic reviews of accuracy and effectiveness literature with 1528 economic modelling. *Health Technol Assess*, 13(43), 1–627.
- 1529 Hong, Y. M., Lee, J., Cho, D. H., Jeon, J. H., Kang, J., Kim, M.-G., ... J. K. (2023). Predicting preterm

- 1530 birth using machine learning techniques in oral microbiome. *Scientific Reports*, 13(1), 21105.
- 1531 Hossin, M., & Sulaiman, M. N. (2015). A review on evaluation metrics for data classification evaluations.
1532 *International journal of data mining & knowledge management process*, 5(2), 1.
- 1533 Huang, R.-Y., Lin, C.-D., Lee, M.-S., Yeh, C.-L., Shen, E.-C., Chiang, C.-Y., ... Fu, E. (2007). Mandibular
1534 disto-lingual root: a consideration in periodontal therapy. *Journal of periodontology*, 78(8), 1485–
1535 1490.
- 1536 Iams, J. D., & Berghella, V. (2010). Care for women with prior preterm birth. *American journal of
1537 obstetrics and gynecology*, 203(2), 89–100.
- 1538 Ide, M., & Papapanou, P. N. (2013). Epidemiology of association between maternal periodontal
1539 disease and adverse pregnancy outcomes—systematic review. *Journal of clinical periodontology*,
1540 40, S181–S194.
- 1541 Iniesta, M., Chamorro, C., Ambrosio, N., Marín, M. J., Sanz, M., & Herrera, D. (2023). Subgingival
1542 microbiome in periodontal health, gingivitis and different stages of periodontitis. *Journal of
1543 Clinical Periodontology*, 50(7), 905–920.
- 1544 Inra, J. A., Steyerberg, E. W., Grover, S., McFarland, A., Syngal, S., & Kastrinos, F. (2015). Racial
1545 variation in frequency and phenotypes of apc and mutyh mutations in 6,169 individuals undergoing
1546 genetic testing. *Genetics in Medicine*, 17(10), 815–821.
- 1547 Jaccard, P. (1908). Nouvelles recherches sur la distribution florale. *Bull. Soc. Vaud. Sci. Nat.*, 44,
1548 223–270.
- 1549 Janda, J. M., & Abbott, S. L. (2007). 16s rrna gene sequencing for bacterial identification in the diagnostic
1550 laboratory: pluses, perils, and pitfalls. *Journal of clinical microbiology*, 45(9), 2761–2764.
- 1551 Jiang, W., & Simon, R. (2007). A comparison of bootstrap methods and an adjusted bootstrap approach
1552 for estimating the prediction error in microarray classification. *Statistics in medicine*, 26(29),
1553 5320–5334.
- 1554 John, G. K., & Mullin, G. E. (2016). The gut microbiome and obesity. *Current oncology reports*, 18,
1555 1–7.
- 1556 Johnson, J. S., Spakowicz, D. J., Hong, B.-Y., Petersen, L. M., Demkowicz, P., Chen, L., ... others (2019).
1557 Evaluation of 16s rrna gene sequencing for species and strain-level microbiome analysis. *Nature
1558 communications*, 10(1), 5029.
- 1559 Jorth, P., Turner, K. H., Gumus, P., Nizam, N., Buduneli, N., & Whiteley, M. (2014). Metatranscriptomics
1560 of the human oral microbiome during health and disease. *MBio*, 5(2), 10–1128.
- 1561 Joscelyn, J., & Kasper, L. H. (2014). Digesting the emerging role for the gut microbiome in central
1562 nervous system demyelination. *Multiple Sclerosis Journal*, 20(12), 1553–1559.
- 1563 Kang, Y., Kang, X., Yang, H., Liu, H., Yang, X., Liu, Q., ... others (2022). Lactobacillus acidophilus ame-
1564 liorates obesity in mice through modulation of gut microbiota dysbiosis and intestinal permeability.
1565 *Pharmacological research*, 175, 106020.
- 1566 Karched, M., Bhardwaj, R. G., Qudeimat, M., Al-Khabbaz, A., & Ellepol, A. (2022). Proteomic analysis
1567 of the periodontal pathogen prevotella intermedia secretomes in biofilm and planktonic lifestyles.
1568 *Scientific Reports*, 12(1), 5636.

- 1569 Katz, J., Chegini, N., Shiverick, K., & Lamont, R. (2009). Localization of *p. gingivalis* in preterm delivery
1570 placenta. *Journal of dental research*, 88(6), 575–578.
- 1571 Kau, A. L., Ahern, P. P., Griffin, N. W., Goodman, A. L., & Gordon, J. I. (2011). Human nutrition, the
1572 gut microbiome and the immune system. *Nature*, 474(7351), 327–336.
- 1573 Kelly, B. J., Gross, R., Bittinger, K., Sherrill-Mix, S., Lewis, J. D., Collman, R. G., ... Li, H. (2015).
1574 Power and sample-size estimation for microbiome studies using pairwise distances and permanova.
1575 *Bioinformatics*, 31(15), 2461–2468.
- 1576 Kennedy, J., Alexander, P., Taillie, L. S., & Jaacks, L. M. (2024). Estimated effects of reductions in
1577 processed meat consumption and unprocessed red meat consumption on occurrences of type 2
1578 diabetes, cardiovascular disease, colorectal cancer, and mortality in the usa: a microsimulation
1579 study. *The Lancet Planetary Health*, 8(7), e441–e451.
- 1580 Kim, B.-R., Shin, J., Guevarra, R. B., Lee, J. H., Kim, D. W., Seol, K.-H., ... Isaacson, R. E. (2017).
1581 Deciphering diversity indices for a better understanding of microbial communities. *Journal of
1582 Microbiology and Biotechnology*, 27(12), 2089–2093.
- 1583 Kim, C. H. (2018). Immune regulation by microbiome metabolites. *Immunology*, 154(2), 220–229.
- 1584 Kim, E.-H., Kim, S., Kim, H.-J., Jeong, H.-o., Lee, J., Jang, J., ... others (2020). Prediction of chronic
1585 periodontitis severity using machine learning models based on salivary bacterial copy number.
1586 *Frontiers in Cellular and Infection Microbiology*, 10, 571515.
- 1587 Kim, J.-H. (2009). Estimating classification error rate: Repeated cross-validation, repeated hold-out and
1588 bootstrap. *Computational statistics & data analysis*, 53(11), 3735–3745.
- 1589 Kinane, D. F., Stathopoulou, P. G., & Papapanou, P. N. (2017). Periodontal diseases. *Nature reviews
1590 Disease primers*, 3(1), 1–14.
- 1591 Kindinger, L. M., Bennett, P. R., Lee, Y. S., Marchesi, J. R., Smith, A., Caciato, S., ... MacIntyre,
1592 D. A. (2017). The interaction between vaginal microbiota, cervical length, and vaginal progesterone
1593 treatment for preterm birth risk. *Microbiome*, 5, 1–14.
- 1594 Kogut, M. H., Lee, A., & Santin, E. (2020). Microbiome and pathogen interaction with the immune
1595 system. *Poultry science*, 99(4), 1906–1913.
- 1596 Kostic, A. D., Ojesina, A. I., Pedamallu, C. S., Jung, J., Verhaak, R. G., Getz, G., & Meyerson, M. (2011).
1597 Pathseq: software to identify or discover microbes by deep sequencing of human tissue. *Nature
1598 biotechnology*, 29(5), 393–396.
- 1599 Kotsiantis, S. B., Zaharakis, I. D., & Pintelas, P. E. (2006). Machine learning: a review of classification
1600 and combining techniques. *Artificial Intelligence Review*, 26, 159–190.
- 1601 Kuipers, E. J., Grady, W. M., Lieberman, D., Seufferlein, T., Sung, J. J., Boelens, P. G., ... Watanabe, T.
1602 (2015). Colorectal cancer. *Nature reviews. Disease primers*, 1, 15065.
- 1603 Lafaurie, G. I., Neuta, Y., Ríos, R., Pacheco-Montealegre, M., Pianeta, R., Castillo, D. M., ... oth-
1604 ers (2022). Differences in the subgingival microbiome according to stage of periodontitis: A
1605 comparison of two geographic regions. *PLoS one*, 17(8), e0273523.
- 1606 Lamont, R. J., & Jenkinson, H. F. (2000). Subgingival colonization by *porphyromonas gingivalis*. *Oral
1607 Microbiology and Immunology: Mini-review*, 15(6), 341–349.

- 1608 Lamont, R. J., Koo, H., & Hajishengallis, G. (2018). The oral microbiota: dynamic communities and
1609 host interactions. *Nature reviews microbiology*, 16(12), 745–759.
- 1610 Leitich, H., & Kaider, A. (2003). Fetal fibronectin—how useful is it in the prediction of preterm birth?
1611 *BJOG: An International Journal of Obstetrics & Gynaecology*, 110, 66–70.
- 1612 Le Leu, R. K., Hu, Y., Brown, I. L., Woodman, R. J., & Young, G. P. (2010). Synbiotic intervention of
1613 bifidobacterium lactis and resistant starch protects against colorectal cancer development in rats.
1614 *Carcinogenesis*, 31(2), 246–251.
- 1615 León, R., Silva, N., Ovalle, A., Chaparro, A., Ahumada, A., Gajardo, M., ... Gamonal, J. (2007).
1616 Detection of porphyromonas gingivalis in the amniotic fluid in pregnant women with a diagnosis
1617 of threatened premature labor. *Journal of periodontology*, 78(7), 1249–1255.
- 1618 Li, H., & Durbin, R. (2009). Fast and accurate short read alignment with burrows–wheeler transform.
1619 *bioinformatics*, 25(14), 1754–1760.
- 1620 Li, N., Lu, B., Luo, C., Cai, J., Lu, M., Zhang, Y., ... Dai, M. (2021). Incidence, mortality, survival,
1621 risk factor and screening of colorectal cancer: A comparison among china, europe, and northern
1622 america. *Cancer letters*, 522, 255–268.
- 1623 Li, R., Miao, Z., Liu, Y., Chen, X., Wang, H., Su, J., & Chen, J. (2024). The brain–gut–bone axis in
1624 neurodegenerative diseases: insights, challenges, and future prospects. *Advanced Science*, 11(38),
1625 2307971.
- 1626 Li, W., & Yang, J. (2025). Investigating the anna karenina principle of the breast microbiome. *BMC
1627 microbiology*, 25(1), 1–10.
- 1628 Li, X., Yu, D., Wang, Y., Yuan, H., Ning, X., Rui, B., ... Li, M. (2021). The intestinal dysbiosis of
1629 mothers with gestational diabetes mellitus (gdm) and its impact on the gut microbiota of their
1630 newborns. *Canadian Journal of Infectious Diseases and Medical Microbiology*, 2021(1), 3044534.
- 1631 Li, Y., Qian, F., Cheng, X., Wang, D., Wang, Y., Pan, Y., ... Tian, Y. (2023). Dysbiosis of oral microbiota
1632 and metabolite profiles associated with type 2 diabetes mellitus. *Microbiology spectrum*, 11(1),
1633 e03796–22.
- 1634 Lim, J. W., Park, T., Tong, Y. W., & Yu, Z. (2020). The microbiome driving anaerobic digestion and
1635 microbial analysis. In *Advances in bioenergy* (Vol. 5, pp. 1–61). Elsevier.
- 1636 Lin, H., Eggesbø, M., & Peddada, S. D. (2022). Linear and nonlinear correlation estimators unveil
1637 undescribed taxa interactions in microbiome data. *Nature communications*, 13(1), 4946.
- 1638 Lin, H., & Peddada, S. D. (2020). Analysis of compositions of microbiomes with bias correction. *Nature
1639 communications*, 11(1), 3514.
- 1640 Lin, H., & Peddada, S. D. (2024). Multigroup analysis of compositions of microbiomes with covariate
1641 adjustments and repeated measures. *Nature Methods*, 21(1), 83–91.
- 1642 Listgarten, M. A. (1986). Pathogenesis of periodontitis. *Journal of clinical periodontology*, 13(5),
1643 418–425.
- 1644 Lloyd-Price, J., Abu-Ali, G., & Huttenhower, C. (2016). The healthy human microbiome. *Genome
1645 medicine*, 8, 1–11.
- 1646 López-Aladid, R., Fernández-Barat, L., Alcaraz-Serrano, V., Bueno-Freire, L., Vázquez, N., Pastor-

- 1647 Ibáñez, R., ... Torres, A. (2023). Determining the most accurate 16s rrna hypervariable region for
1648 taxonomic identification from respiratory samples. *Scientific reports*, 13(1), 3974.
- 1649 Love, M. I., Huber, W., & Anders, S. (2014). Moderated estimation of fold change and dispersion for
1650 rna-seq data with deseq2. *Genome biology*, 15, 1–21.
- 1651 Ma, Z. S. (2020). Testing the anna karenina principle in human microbiome-associated diseases. *Iscience*,
1652 23(4).
- 1653 Magnúsdóttir, S., & Thiele, I. (2018). Modeling metabolism of the human gut microbiome. *Current
1654 opinion in biotechnology*, 51, 90–96.
- 1655 Magurran, A. E. (2021). Measuring biological diversity. *Current Biology*, 31(19), R1174–R1177.
- 1656 Mandic, M., Safizadeh, F., Niedermaier, T., Hoffmeister, M., & Brenner, H. (2023). Association of
1657 overweight, obesity, and recent weight loss with colorectal cancer risk. *JAMA network Open*, 6(4),
1658 e239556–e239556.
- 1659 Mann, H. B., & Whitney, D. R. (1947). On a test of whether one of two random variables is stochastically
1660 larger than the other. *The annals of mathematical statistics*, 50–60.
- 1661 Manolis, A. A., Manolis, T. A., Melita, H., & Manolis, A. S. (2022). Gut microbiota and cardiovascular
1662 disease: symbiosis versus dysbiosis. *Current Medicinal Chemistry*, 29(23), 4050–4077.
- 1663 Martin, C. R., Osadchiy, V., Kalani, A., & Mayer, E. A. (2018). The brain-gut-microbiome axis. *Cellular
1664 and molecular gastroenterology and hepatology*, 6(2), 133–148.
- 1665 Maulud, D., & Abdulazeez, A. M. (2020). A review on linear regression comprehensive in machine
1666 learning. *Journal of Applied Science and Technology Trends*, 1(2), 140–147.
- 1667 Mayer, E. A., Tillisch, K., Gupta, A., et al. (2015). Gut/brain axis and the microbiota. *The Journal of
1668 clinical investigation*, 125(3), 926–938.
- 1669 Melguizo-Rodríguez, L., Costela-Ruiz, V. J., Manzano-Moreno, F. J., Ruiz, C., & Illescas-Montes, R.
1670 (2020). Salivary biomarkers and their application in the diagnosis and monitoring of the most
1671 common oral pathologies. *International journal of molecular sciences*, 21(14), 5173.
- 1672 Merrill, L. C., & Mangano, K. M. (2023). Racial and ethnic differences in studies of the gut microbiome
1673 and osteoporosis. *Current Osteoporosis Reports*, 21(5), 578–591.
- 1674 Miller, C. S., Ding, X., Dawson III, D. R., & Ebersole, J. L. (2021). Salivary biomarkers for discriminating
1675 periodontitis in the presence of diabetes. *Journal of clinical periodontology*, 48(2), 216–225.
- 1676 Morita, T., Yamazaki, Y., Mita, A., Takada, K., Seto, M., Nishinoue, N., ... Maeno, M. (2010). A cohort
1677 study on the association between periodontal disease and the development of metabolic syndrome.
1678 *Journal of periodontology*, 81(4), 512–519.
- 1679 Na, H. S., Kim, S. Y., Han, H., Kim, H.-J., Lee, J.-Y., Lee, J.-H., & Chung, J. (2020). Identification of
1680 potential oral microbial biomarkers for the diagnosis of periodontitis. *Journal of clinical medicine*,
1681 9(5), 1549.
- 1682 Nemoto, T., Shiba, T., Komatsu, K., Watanabe, T., Shimogishi, M., Shibasaki, M., ... others (2021).
1683 Discrimination of bacterial community structures among healthy, gingivitis, and periodontitis
1684 statuses through integrated metatranscriptomic and network analyses. *Msystems*, 6(6), e00886–21.
- 1685 Nesbitt, M. J., Reynolds, M. A., Shiau, H., Choe, K., Simonsick, E. M., & Ferrucci, L. (2010). Association

- of periodontitis and metabolic syndrome in the baltimore longitudinal study of aging. *Aging clinical and experimental research*, 22, 238–242.
- Network, C. G. A., et al. (2012). Comprehensive molecular characterization of human colon and rectal cancer. *Nature*, 487(7407), 330.
- Nibali, L., Sousa, V., Davrandi, M., Spratt, D., Alyahya, Q., Dopico, J., & Donos, N. (2020). Differences in the periodontal microbiome of successfully treated and persistent aggressive periodontitis. *Journal of Clinical Periodontology*, 47(8), 980–990.
- Novaković, J. D., Veljović, A., Ilić, S. S., Papić, Ž., & Tomović, M. (2017). Evaluation of classification models in machine learning. *Theory and Applications of Mathematics & Computer Science*, 7(1), 39.
- Obuchowski, N. A., & Bullen, J. A. (2018). Receiver operating characteristic (roc) curves: review of methods with applications in diagnostic medicine. *Physics in Medicine & Biology*, 63(7), 07TR01.
- Ochiai, A. (1957). Zoogeographic studies on the soleoid fishes found in japan and its neighbouring regions. *Bulletin of Japanese Society of Scientific Fisheries*, 22, 526–530.
- Offenbacher, S., Katz, V., Fertik, G., Collins, J., Boyd, D., Maynor, G., ... Beck, J. (1996). Periodontal infection as a possible risk factor for preterm low birth weight. *Journal of periodontology*, 67, 1103–1113.
- Ojesina, A. I., Pedamallu, C. S., Kostic, A., Jung, J., Auclair, D., Lohr, J., ... Meyerson, M. (2013). High throughput sequencing-based pathogen discovery in multiple myeloma. *Blood*, 122(21), 5322.
- Omondiagbe, D. A., Veeramani, S., & Sidhu, A. S. (2019). Machine learning classification techniques for breast cancer diagnosis. In *Iop conference series: materials science and engineering* (Vol. 495, p. 012033).
- O'Sullivan, D. E., Sutherland, R. L., Town, S., Chow, K., Fan, J., Forbes, N., ... Brenner, D. R. (2022). Risk factors for early-onset colorectal cancer: a systematic review and meta-analysis. *Clinical gastroenterology and hepatology*, 20(6), 1229–1240.
- Paganini, D., & Zimmermann, M. B. (2017). The effects of iron fortification and supplementation on the gut microbiome and diarrhea in infants and children: a review. *The American journal of clinical nutrition*, 106, 1688S–1693S.
- Pan, A. Y. (2021). Statistical analysis of microbiome data: the challenge of sparsity. *Current Opinion in Endocrine and Metabolic Research*, 19, 35–40.
- Papapanou, P. N., Sanz, M., Buduneli, N., Dietrich, T., Feres, M., Fine, D. H., ... others (2018). Periodontitis: Consensus report of workgroup 2 of the 2017 world workshop on the classification of periodontal and peri-implant diseases and conditions. *Journal of periodontology*, 89, S173–S182.
- Parizadeh, M., & Arrieta, M.-C. (2023). The global human gut microbiome: genes, lifestyles, and diet. *Trends in Molecular Medicine*.
- Park, J., Park, S. H., Lee, D., Lee, J. E., Lee, D., Na, K. J., ... Im, H.-J. (2024). Detecting cancer microbiota using unmapped rna reads on spatial transcriptomics. *Cancer Research*, 84(6_Supplement), 4881–4881.
- Payne, M. S., Newnham, J. P., Doherty, D. A., Furfarro, L. L., Pendal, N. L., Loh, D. E., & Keelan, J. A.

- 1725 (2021). A specific bacterial dna signature in the vagina of australian women in midpregnancy
1726 predicts high risk of spontaneous preterm birth (the predict1000 study). *American journal of*
1727 *obstetrics and gynecology*, 224(2), 206–e1.
- 1728 Peirce, J. M., & Alviña, K. (2019). The role of inflammation and the gut microbiome in depression and
1729 anxiety. *Journal of neuroscience research*, 97(10), 1223–1241.
- 1730 Peltomaki, P. (2003). Role of dna mismatch repair defects in the pathogenesis of human cancer. *Journal*
1731 *of clinical oncology*, 21(6), 1174–1179.
- 1732 Pezzino, S., Sofia, M., Greco, L. P., Litrico, G., Filippello, G., Sarvà, I., ... Latteri, S. (2023). Microbiome
1733 dysbiosis: a pathological mechanism at the intersection of obesity and glaucoma. *International*
1734 *Journal of Molecular Sciences*, 24(2), 1166.
- 1735 Pollard, T. J., Johnson, A. E., Raffa, J. D., & Mark, R. G. (2018). tableone: An open source python
1736 package for producing summary statistics for research papers. *JAMIA open*, 1(1), 26–31.
- 1737 Premaraj, T. S., Vella, R., Chung, J., Lin, Q., Hunter, P., Underwood, K., ... Zhou, Y. (2020). Ethnic
1738 variation of oral microbiota in children. *Scientific reports*, 10(1), 14788.
- 1739 Raut, J. R., Schöttker, B., Hollecze, B., Guo, F., Bhardwaj, M., Miah, K., ... Brenner, H. (2021).
1740 A microrna panel compared to environmental and polygenic scores for colorectal cancer risk
1741 prediction. *Nature Communications*, 12(1), 4811.
- 1742 Rebersek, M. (2021). Gut microbiome and its role in colorectal cancer. *BMC cancer*, 21(1), 1325.
- 1743 Redanz, U., Redanz, S., Treerat, P., Prakasam, S., Lin, L.-J., Merritt, J., & Kreth, J. (2021). Differential
1744 response of oral mucosal and gingival cells to corynebacterium durum, streptococcus sanguinis, and
1745 porphyromonas gingivalis multispecies biofilms. *Frontiers in cellular and infection microbiology*,
1746 11, 686479.
- 1747 Relvas, M., Regueira-Iglesias, A., Balsa-Castro, C., Salazar, F., Pacheco, J., Cabral, C., ... Tomás, I.
1748 (2021). Relationship between dental and periodontal health status and the salivary microbiome:
1749 bacterial diversity, co-occurrence networks and predictive models. *Scientific reports*, 11(1), 929.
- 1750 Renson, A., Jones, H. E., Beghini, F., Segata, N., Zolnik, C. P., Usyk, M., ... others (2019). Sociodemo-
1751 graphic variation in the oral microbiome. *Annals of epidemiology*, 35, 73–80.
- 1752 Renvert, S., & Persson, G. (2002). A systematic review on the use of residual probing depth, bleeding on
1753 probing and furcation status following initial periodontal therapy to predict further attachment and
1754 tooth loss. *Journal of clinical periodontology*, 29, 82–89.
- 1755 Rideout, J. R., Caporaso, G., Bolyen, E., McDonald, D., Baeza, Y. V., Alastuey, J. C., ... Sharma, K.
1756 (2018, December). *biocore/scikit-bio: scikit-bio 0.5.5: More compositional methods added*. Zenodo.
1757 Retrieved from <https://doi.org/10.5281/zenodo.2254379> doi: 10.5281/zenodo.2254379
- 1758 Rôças, I. N., Siqueira Jr, J. F., Santos, K. R., Coelho, A. M., & de Janeiro, R. (2001). “red com-
1759 plex”(bacteroides forsythus, porphyromonas gingivalis, and treponema denticola) in endodontic
1760 infections: a molecular approach. *Oral Surgery, Oral Medicine, Oral Pathology, Oral Radiology,*
1761 *and Endodontology*, 91(4), 468–471.
- 1762 Romero, R., Dey, S. K., & Fisher, S. J. (2014). Preterm labor: one syndrome, many causes. *Science*,
1763 345(6198), 760–765.

- 1764 Romero, R., Hassan, S. S., Gajer, P., Tarca, A. L., Fadrosh, D. W., Nikita, L., ... others (2014). The
1765 composition and stability of the vaginal microbiota of normal pregnant women is different from
1766 that of non-pregnant women. *Microbiome*, 2, 1–19.
- 1767 Rosan, B., & Lamont, R. J. (2000). Dental plaque formation. *Microbes and infection*, 2(13), 1599–1607.
- 1768 Rubio, C. A., Lang-Schwarz, C., & Vieth, M. (2022). Further study on field cancerization in the human
1769 colon. *Anticancer Research*, 42(12), 5891–5895.
- 1770 Schwabe, R. F., & Jobin, C. (2013). The microbiome and cancer. *Nature Reviews Cancer*, 13(11),
1771 800–812.
- 1772 Segata, N., Izard, J., Waldron, L., Gevers, D., Miropolsky, L., Garrett, W. S., & Huttenhower, C. (2011).
1773 Metagenomic biomarker discovery and explanation. *Genome biology*, 12, 1–18.
- 1774 Sen, P. C., Hajra, M., & Ghosh, M. (2020). Supervised classification algorithms in machine learning: A
1775 survey and review. In *Emerging technology in modelling and graphics: Proceedings of iem graph
1776 2018* (pp. 99–111).
- 1777 Sepich-Poore, G. D., Zitvogel, L., Straussman, R., Hasty, J., Wargo, J. A., & Knight, R. (2021). The
1778 microbiome and human cancer. *Science*, 371(6536), eabc4552.
- 1779 Sharma, S., & Tripathi, P. (2019). Gut microbiome and type 2 diabetes: where we are and where to go?
1780 *The Journal of nutritional biochemistry*, 63, 101–108.
- 1781 Shi, N., Li, N., Duan, X., & Niu, H. (2017). Interaction between the gut microbiome and mucosal
1782 immune system. *Military Medical Research*, 4, 1–7.
- 1783 Simpson, E. (1949). Measurement of diversity. *Nature*, 163.
- 1784 Sokal, R. R., & Sneath, P. H. (1963). Principles of numerical taxonomy.
- 1785 Song, M., Chan, A. T., & Sun, J. (2020). Influence of the gut microbiome, diet, and environment on risk
1786 of colorectal cancer. *Gastroenterology*, 158(2), 322–340.
- 1787 Söreide, K., Janssen, E., Söiland, H., Körner, H., & Baak, J. (2006). Microsatellite instability in colorectal
1788 cancer. *Journal of British Surgery*, 93(4), 395–406.
- 1789 Sørensen, T. (1948). A method of establishing groups of equal amplitude in plant sociology based on
1790 similarity of species content and its application to analyses of the vegetation on danish commons.
1791 *Biologiske skrifter*, 5, 1–34.
- 1792 Sotiriadis, A., Papatheodorou, S., Kavvadias, A., & Makrydimas, G. (2010). Transvaginal cervical
1793 length measurement for prediction of preterm birth in women with threatened preterm labor: a
1794 meta-analysis. *Ultrasound in Obstetrics and Gynecology: The Official Journal of the International
1795 Society of Ultrasound in Obstetrics and Gynecology*, 35(1), 54–64.
- 1796 Spss, I., et al. (2011). Ibm spss statistics for windows, version 20.0. *New York: IBM Corp*, 440, 394.
- 1797 Stafford, G., Roy, S., Honma, K., & Sharma, A. (2012). Sialic acid, periodontal pathogens and tannerella
1798 forsythia: stick around and enjoy the feast! *Molecular Oral Microbiology*, 27(1), 11–22.
- 1799 Stout, M. J., Conlon, B., Landeau, M., Lee, I., Bower, C., Zhao, Q., ... Mysorekar, I. U. (2013).
1800 Identification of intracellular bacteria in the basal plate of the human placenta in term and preterm
1801 gestations. *American journal of obstetrics and gynecology*, 208(3), 226–e1.
- 1802 Strong, W. (2002). Assessing species abundance unevenness within and between plant communities.

- 1803 *Community Ecology*, 3(2), 237–246.
- 1804 Sultan, S., El-Mowafy, M., Elgaml, A., Ahmed, T. A., Hassan, H., & Mottawea, W. (2021). Metabolic
1805 influences of gut microbiota dysbiosis on inflammatory bowel disease. *Frontiers in physiology*, 12,
1806 715506.
- 1807 Suzuki, N., Nakano, Y., Yoneda, M., Hirofumi, T., & Hanioka, T. (2022). The effects of cigarette
1808 smoking on the salivary and tongue microbiome. *Clinical and Experimental Dental Research*, 8(1),
1809 449–456.
- 1810 Swidsinski, A., Khilkin, M., Kerjaschki, D., Schreiber, S., Ortner, M., Weber, J., & Lochs, H. (1998).
1811 Association between intraepithelial escherichia coli and colorectal cancer. *Gastroenterology*,
1812 115(2), 281–286.
- 1813 Swift, D., Cresswell, K., Johnson, R., Stilianoudakis, S., & Wei, X. (2023). A review of normalization
1814 and differential abundance methods for microbiome counts data. *Wiley Interdisciplinary Reviews: Computational Statistics*, 15(1), e1586.
- 1815 Tanner, A. C., Kent Jr, R., Kanasi, E., Lu, S. C., Paster, B. J., Sonis, S. T., ... Van Dyke, T. E. (2007).
1816 Clinical characteristics and microbiota of progressing slight chronic periodontitis in adults. *Journal of clinical periodontology*, 34(11), 917–930.
- 1817 Tanner, A. C., Paster, B. J., Lu, S. C., Kanasi, E., Kent Jr, R., Van Dyke, T., & Sonis, S. T. (2006).
1818 Subgingival and tongue microbiota during early periodontitis. *Journal of dental research*, 85(4),
1819 318–323.
- 1820 Tejeda, M., Farrell, J., Zhu, C., Haines, J. L., Wang, L.-S., Schellenberg, G. D., ... others (2021). Multiple
1821 viruses detected in human dna are associated with alzheimer disease risk. *Alzheimer's & Dementia*,
1822 17, e054585.
- 1823 Teles, F., Wang, Y., Hajishengallis, G., Hasturk, H., & Marchesan, J. T. (2021). Impact of systemic
1824 factors in shaping the periodontal microbiome. *Periodontology 2000*, 85(1), 126–160.
- 1825 Thaiss, C. A., Zmora, N., Levy, M., & Elinav, E. (2016). The microbiome and innate immunity. *Nature*,
1826 535(7610), 65–74.
- 1827 Tian, R., Liu, H., Feng, S., Wang, H., Wang, Y., Wang, Y., ... Zhang, S. (2021). Gut microbiota dysbiosis
1828 in stable coronary artery disease combined with type 2 diabetes mellitus influences cardiovascular
1829 prognosis. *Nutrition, Metabolism and Cardiovascular Diseases*, 31(5), 1454–1466.
- 1830 Tilg, H., Kaser, A., et al. (2011). Gut microbiome, obesity, and metabolic dysfunction. *The Journal of
1831 clinical investigation*, 121(6), 2126–2132.
- 1832 Tonetti, M. S., Greenwell, H., & Kornman, K. S. (2018). Staging and grading of periodontitis: Framework
1833 and proposal of a new classification and case definition. *Journal of periodontology*, 89, S159–S172.
- 1834 Tringe, S. G., & Hugenholtz, P. (2008). A renaissance for the pioneering 16s rRNA gene. *Current opinion
1835 in microbiology*, 11(5), 442–446.
- 1836 Tucker, C. M., Cadotte, M. W., Carvalho, S. B., Davies, T. J., Ferrier, S., Fritz, S. A., ... others (2017). A
1837 guide to phylogenetic metrics for conservation, community ecology and macroecology. *Biological
1838 Reviews*, 92(2), 698–715.
- 1839 Ulger Toprak, N., Yagci, A., Gulluoglu, B., Akin, M., Demirkalem, P., Celenk, T., & Soyletir, G. (2006).

- 1842 A possible role of bacteroides fragilis enterotoxin in the aetiology of colorectal cancer. *Clinical*
1843 *microbiology and infection*, 12(8), 782–786.
- 1844 Ursell, L. K., Metcalf, J. L., Parfrey, L. W., & Knight, R. (2012). Defining the human microbiome.
1845 *Nutrition reviews*, 70(suppl_1), S38–S44.
- 1846 Utzschneider, K. M., Kratz, M., Damman, C. J., & Hullarg, M. (2016). Mechanisms linking the gut
1847 microbiome and glucose metabolism. *The Journal of Clinical Endocrinology & Metabolism*,
1848 101(4), 1445–1454.
- 1849 Vander Haar, E. L., So, J., Gyamfi-Bannerman, C., & Han, Y. W. (2018). Fusobacterium nucleatum and
1850 adverse pregnancy outcomes: epidemiological and mechanistic evidence. *Anaerobe*, 50, 55–59.
- 1851 Van der Maaten, L., & Hinton, G. (2008). Visualizing data using t-sne. *Journal of machine learning*
1852 *research*, 9(11).
- 1853 Vasen, H. F., Mecklin, J.-P., Khan, P. M., & Lynch, H. T. (1991). The international collaborative group
1854 on hereditary non-polyposis colorectal cancer (icg-hnpcc). *Diseases of the Colon & Rectum*, 34(5),
1855 424–425.
- 1856 Vilar, E., & Gruber, S. B. (2010). Microsatellite instability in colorectal cancer—the stable evidence.
1857 *Nature reviews Clinical oncology*, 7(3), 153–162.
- 1858 Walker, M. A., Pedamallu, C. S., Ojesina, A. I., Bullman, S., Sharpe, T., Whelan, C. W., & Meyerson, M.
1859 (2018). Gatk pathseq: a customizable computational tool for the discovery and identification of
1860 microbial sequences in libraries from eukaryotic hosts. *Bioinformatics*, 34(24), 4287–4289.
- 1861 Weaver, W. (1963). *The mathematical theory of communication*. University of Illinois Press.
- 1862 Whiteside, S. A., Razvi, H., Dave, S., Reid, G., & Burton, J. P. (2015). The microbiome of the urinary
1863 tract—a role beyond infection. *Nature Reviews Urology*, 12(2), 81–90.
- 1864 Witkin, S. (2019). Vaginal microbiome studies in pregnancy must also analyse host factors. *BJOG: An*
1865 *International Journal of Obstetrics & Gynaecology*, 126(3), 359–359.
- 1866 Wong, T.-T., & Yeh, P.-Y. (2019). Reliable accuracy estimates from k-fold cross validation. *IEEE*
1867 *Transactions on Knowledge and Data Engineering*, 32(8), 1586–1594.
- 1868 Wyss, C., Moter, A., Choi, B.-K., Dewhirst, F., Xue, Y., Schüpbach, P., ... Guggenheim, B. (2004).
1869 Treponema putidum sp. nov., a medium-sized proteolytic spirochaete isolated from lesions of
1870 human periodontitis and acute necrotizing ulcerative gingivitis. *International journal of systematic*
1871 *and evolutionary microbiology*, 54(4), 1117–1122.
- 1872 Xia, Y. (2023). Statistical normalization methods in microbiome data with application to microbiome
1873 cancer research. *Gut Microbes*, 15(2), 2244139.
- 1874 Yaman, E., & Subasi, A. (2019). Comparison of bagging and boosting ensemble machine learning methods
1875 for automated emg signal classification. *BioMed research international*, 2019(1), 9152506.
- 1876 Yang, I., Claussen, H., Arthur, R. A., Hertzberg, V. S., Geurs, N., Corwin, E. J., & Dunlop, A. L. (2022).
1877 Subgingival microbiome in pregnancy and a potential relationship to early term birth. *Frontiers in*
1878 *cellular and infection microbiology*, 12, 873683.
- 1879 Yildiz, B., Bilbao, J. I., & Sproul, A. B. (2017). A review and analysis of regression and machine learning
1880 models on commercial building electricity load forecasting. *Renewable and Sustainable Energy*

- 1881 *Reviews*, 73, 1104–1122.
- 1882 Yoshimura, F., Murakami, Y., Nishikawa, K., Hasegawa, Y., & Kawaminami, S. (2009). Surface
1883 components of *porphyromonas gingivalis*. *Journal of periodontal research*, 44(1), 1–12.
- 1884 Zhang, C.-Z., Cheng, X.-Q., Li, J.-Y., Zhang, P., Yi, P., Xu, X., & Zhou, X.-D. (2016). Saliva in the
1885 diagnosis of diseases. *International journal of oral science*, 8(3), 133–137.
- 1886 Zhou, X., Wang, L., Xiao, J., Sun, J., Yu, L., Zhang, H., ... others (2022). Alcohol consumption,
1887 dna methylation and colorectal cancer risk: Results from pooled cohort studies and mendelian
1888 randomization analysis. *International journal of cancer*, 151(1), 83–94.
- 1889 Zhu, W., & Lee, S.-W. (2016). Surface interactions between two of the main periodontal pathogens:
1890 *Porphyromonas gingivalis* and *tannerella forsythia*. *Journal of periodontal & implant science*,
1891 46(1), 2–9.
- 1892 Zhu, X., Han, Y., Du, J., Liu, R., Jin, K., & Yi, W. (2017). Microbiota-gut-brain axis and the central
1893 nervous system. *Oncotarget*, 8(32), 53829.
- 1894 Zhuang, Y., Wang, H., Jiang, D., Li, Y., Feng, L., Tian, C., ... others (2021). Multi gene mutation
1895 signatures in colorectal cancer patients: predict for the diagnosis, pathological classification, staging
1896 and prognosis. *BMC cancer*, 21, 1–16.

Acknowledgments

1898 I would like to disclose my earnest appreciation for my advisor, Professor **Semin Lee**, who provided
 1899 solicitous supervision and cherished opportunities throughout the course of my research. His advice and
 1900 consultation encouraged me to become as a researcher and to receive all humility and gentleness. I am also
 1901 grateful to all of my committee members, Professor **Taejoon Kwon**, Professor **Eunhee Kim**, Professor
 1902 **Kyemyung Park**, and Professor **Min Hyuk Lim**, for their meaningful mentions and suggestions.

1903 I extend my deepest gratitude to my Lord, **the Flying Spaghetti Monster**, His Noodly Appendage
 1904 has guided me through the twist and turns of this academic journey. His presence, ever comforting and
 1905 mysterious, has been a source of strength and humor during both highs and lows. In moments of doubt, I
 1906 found solace in the belief that you were there, gently reminding me to keep faith in the process. His Holy
 1907 Noodle has nourished my mind, and for that, I am truly overwhelmed. May His Holy Noodle continue to
 1908 guide me in all my future endeavors. *R’Amen.*

1909 I would like to extend my heartfelt gratitude to Professor **You Mi Hong** for her invaluable guidance
 1910 and insightful advice on PTB study. Her expertise in maternal and fetal health, along with her deep under-
 1911 standing of statistical and clinical interpretations, greatly contributed to refining the analytical framework
 1912 of this study. Her constructive feedback and thoughtful discussions provided critical perspectives that
 1913 enhanced the robustness and relevance of the research findings. I sincerely appreciate her generosity
 1914 in sharing her knowledge and effort, as well as her encouragement throughout my Ph.D. journey. Her
 1915 support has been instrumental in strengthening this work, and I am truly grateful for her contributions.

1916 I also would like to express my sincere gratitude for Professor **Jun Hyeok Lim** for his invaluable
 1917 guidance and insightful advice on lung cancer study. His expertise in cancer genomics and data interpreta-
 1918 tion provided essential perspectives that greatly enriched the analytical approach of my Ph.D. journey. His
 1919 constructive feedback and thoughtful discussion helped refine methodologies and enhance the scientific
 1920 rigor of the research. I deeply appreciate his willingness to share his knowledge and expertise, which has
 1921 been instrumental in shaping key aspects of this work. His support and encouragement have been truly
 1922 inspiring, and I am grateful for the opportunity to have benefited from his mentorship.

1923 I would like to extend my heartfelt gratitude to my colleagues of the **Computational Biology Lab @**
 1924 **UNIST**, whose collaboration, friendship, brotherhood, and support have been an invaluable part of my
 1925 journey. Your willingness to share insights, engage in thoughtful discussions, and offer encouragement
 1926 during the challenging moments of research has significantly shaped my academic experience. The
 1927 camaraderie in Computational Biology Lab made even the most demanding days more enjoyable, and I
 1928 am deeply grateful for the collaborative environment we created together. I appreciate you for standing
 1929 by my side throughout this Ph.D. journey.

1930 I would like to express my heartfelt gratitude to **my family**, whose unwavering support has been the
 1931 foundation of everything I have achieved. Your love, encouragement, and belief in me have sustained me
 1932 through every challenge, and I could not have come this far without you. From your words of wisdom to
 1933 your patience and understanding, each of you has played a vital role in helping me navigate this journey.
 1934 The strength and comfort I have drawn from our family bond have been my greatest source of resilience.

1935 Your presence, both near and far, has filled my life with warmth and motivation. I am deeply grateful for
1936 your unconditional love and for always being there when I needed you the most. Thank you for being my
1937 constant source of strength and inspiration.

1938 I am incredibly pleased to my friends, especially my GSHS alumni (**이망특**), for their unwavering
1939 support and encouragement throughout this journey. The bonds we formed back in our school days have
1940 only grown stronger over the years, and I am fortunate to have had such loyal and understanding friends
1941 by my side. Your constant words of motivation, and even moments of levity during stressful times have
1942 helped keep me grounded. Whether it was a late-night conversations, a shared laugh, or a simple message
1943 of reassurance, you all have played a vital role in keeping me focused and motivated. I am relieved for the
1944 ways you celebrated each small achievement with me and how you patiently listened to my worries. The
1945 memories of our shared past provided me with comfort and a sense of stability when the road ahead felt
1946 uncertain. I could not have reached this point without the love and friendship that you all have generously
1947 given. Each of your, in your unique way, has contributed to this dissertation, even if indirectly, and for
1948 that, I am forever beholden. I look forward to continuing our friendship as we all grow in our individual
1949 paths, knowing that the support we share is something truly special.

1950 I would like to express my deepest recognition to **my girlfriend (expected)** for her unwavering
1951 support, patience, and companionship throughout my Ph.D. journey. Her presence has been a constant
1952 source of comfort and motivation, helping me navigate the challenges of research and writing with
1953 renewed energy. Through moments of frustration and accomplishment alike, her encouragement has
1954 reminded me of the importance of balance and perseverance. Her kindness, understanding, and belief
1955 in me have been invaluable, making even the most difficult days feel lighter. I am truly grateful for her
1956 support and for sharing this journey with me, and I look forward to all the moments we will continue to
1957 experience together.

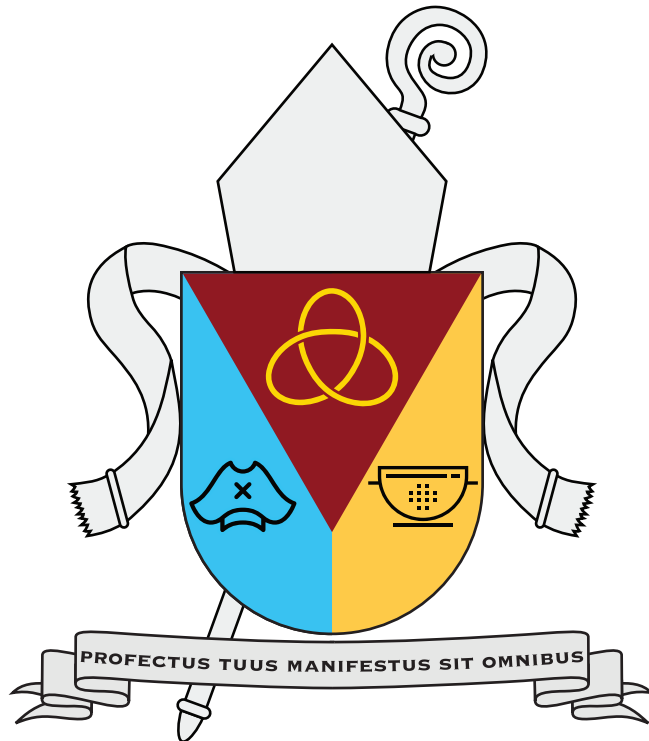
1958 I would like to express my sincere gratitude to the amazing members of my animal protection groups,
1959 DRDR (**두루두루**) and UNIMALS (**유니멀스**), whose dedication and compassion have been a constant
1960 source of motivation. Your unwavering commitment to improving the lives of animals has inspired me
1961 throughout this journey. I am also thankful for the beautiful cats we have cared for, whose presence
1962 brought both joy and purpose to our allegiance. Their playful spirits and gentle companionship served as
1963 daily reminders of why we continue to fight for animal rights. The bond we share, both with each other
1964 and with the animals we protect, has enriched my life in countless ways. I appreciate you all again for
1965 your support, dedication, and for being part of this meaningful cause.

1966 I would like to express my deepest gratitude to **everyone** I have had the honor of meeting throughout
1967 this journey. Your kindness, encouragement, and support have carried me through both the challenging
1968 and rewarding moments of my life. Whether through a kind word, thoughtful advice, or simply being
1969 there when I needed it most, your presence has made all the difference. I am incredibly fortunate to have
1970 received such generosity and warmth from those around me, and I do not take it for granted. Every act
1971 of kindness, no matter how big or small, has been a source of strength and motivation for me. To all
1972 my friends, colleagues, mentors, and beloved ones, thank you for your unwavering support. I am truly
1973 grateful for each of you, and your kindness has left an indelible mark on my journey.

1974 My Lord, *the Flying Spaghetti Monster*,
1975 give us grace to accept with serenity the things that cannot be changed,
1976 courage to change the things that should be changed,
1977 and the wisdom to distinguish the one from the other.

1978
1979 Glory be to *the Meatball*, to *the Sauce*, and to *the Holy Noodle*.
1980 As it was in the beginning, is now, and ever shall be.

1981 *R'Amen.*



May your progress be evident to all

